Addis Ababa University

Addis Ababa Institute of Technology

School of Mechanical and Industrial Engineering

Characterizing Tensile and Flexural Properties of Synthetic Fibers-Reinforced Epoxy Composite for Foot Prosthetic Application

By: Galana Abay
ID NO.:-GSR/9971/12

A Thesis Submitted to School of Graduate Studies of Addis Ababa University in Partial Fulfillment of the Requirements for Degree of Masters of Science in Mechanical Engineering (Mechanical Design).

Advisor: Dr. Samuel Tesfaye

September, 2021

ADDIS ABABA UNIVERSITY

ADDIS ABABA INSTITUTE OF TECHNOLOGY (AAiT)

SCHOOL OF MECHANICAL AND INDUSTRIAL ENGINEERING

MSc final thesis approval

Submitted By:

Galana Abay	_____	_____
Student Name	*Signature*	*Date*

Recommended By:

Samuel Tesfaye (PhD)	_____	_____
Advisor	*Signature*	*Date*

Examined By:

Desalegn Wogaso (PhD)	_____	_____
Internal Examiner	*Signature*	*Date*
Haileleoul Sahle (PhD)	_____	_____
External Examiner	*Signature*	*Date*

Approved By:

Araya A. (PhD)	_____	_____
Chair	*Signature*	*Date*

Endorsed by:

Yilma Tadesse (PhD)	_____	_____
Dean	*Signature*	*Date*
Ermiyas Tesfaye (PhD)	_____	_____
Associate Director,	*Signature*	*Date*
Post graduate program		

Declaration

I hereby declare that the work which is being presented in this thesis entitled "Characterizing tensile and flexural properties of synthetic fibers-reinforced epoxy composite for foot prosthetic application'' is original work of my own, has not been presented for a degree of any other university/institutions and all the resource of materials used for this thesis have been fully acknowledged.

Galana Abay

Signature: _____

Date:-_____

This thesis has been submitted for examination and signed by:

Advisor: _____Signature _____Date_____

Acknowledgement

Firstly, I would like to express my deep gratitude to my advisor Dr. Samuel Tesfaye for his valuable advices and guidance during my thesis work. Secondly, I wish to express my special thanks to prosthetic and orthotic center (POC) officials and workers for their contributions in data collection. Lastly, I would like to acknowledge and appreciate all staff members of SMIE, my friends and families who directly or indirectly played a valuable roles and contribution towards the success completion of this thesis.

Abstract

Materials has direct and critical impact on the performance of prosthetic foot. The aim of this thesis is to characterize the tensile and flexural properties of the four stacking sequences of E-glass and hybrid (E-glass/carbon) epoxy composite for prosthetic foot using powerful FEA software (ANSYS 19.2) for selecting stacking sequence that yields high strength without experimental cost. Additionally, to compare the design and strength performance of prosthetic foot model for two materials (Homo-polymer-polypropylene and selected composite) by numerical simulation. This starts from determining the elastic property of lamina to modeling of testing samples according to their standards for each stacking configuration using ANSYS workbench and verifying the numerical result with analytical MATLAB solution.

The result shows that the ROM and Halpin-Tsai predicts longitudinal and transversal properties of the lamina with an acceptable range of errors from (1.66%-3.04%) and (0.5%-3.02%) respectively compared to experimental result of [34]. In pure E-glass/epoxy and hybrid/epoxy laminate the ultimate tensile strength is increased from 777.44MPa to1475.5MPa and 1865MPa to 1935MPa respectively. Similarly, in flexural testing the ultimate flexural strength of hybrid composite is increased from 1299.2Mpa -1934.3MPa due effect of stacking sequence. Among the all stacking configuration the SS-3 ($[0_c/90/45]_s$) results higher tensile and flexural strength and selected for prosthetic foot. The failure loads of laminate in each stacking sequence verified the numerical results with an error less than 2% and 3% for tensile and flexural loading respectively. The composite prosthetic model has higher performance than Homo-polymer-polypropylene model. The model of prosthetic foot from Homo-polymer-polypropylene is not operating under the material stress limits. The deformation resistance, energy storage capacity, safety factor and stiffness of composite foot is increased by 18.9%, 53.2%, 56.2% and 18.8% respectively compared to HPP prosthetic foot. Its weight and is reduced by 30.62%. Finally, this composite is suggested for prosthetic producers (Prosthetic and orthotic center).

Keywords: - Prosthetic Foot, Homo polymer poly propylene, Composite Laminate, Stacking Sequence, Property Characterization, Tensile Strength, Flexural Strength, Numerical Simulation, Energy Storage.

Table of Contents

List of Figures

List of Tables

List of Abbreviations and Acronyms

POC	Prosthetic and Orthotic center
HPP	Homo polymer poly propylene
ASTM	American society of testing materials
FEA	Finite element analysis
PWD	People living with disability
MATLAB	Matrix laboratory
SR	Strength ratio
FI	Failure index
FPF	First ply failure load
LPF	Last ply failure load
UD	Unidirectional
CLT	Classical lamination theory
PFA	Progressive failure analysis
ACP	Anys composite prep Post
SS	Stacking sequence
3D	Three dimensional
FRP	Fiber Reinforced Plastics
FEM	Finite Element Method
ROM	Rule of mixture
SS-1	Stacking sequence of [0/90/45/45/90/0]
SS-2	Stacking sequence of [45/0/90/90/0/45]
SS-3	Stacking sequence of [0c/90/45/45/90/0c]
SS-4	Stacking sequence of [45c/0/90/90/0/45c]

CHAPTER ONE
INTRODUCTION

1.1 Background of the Study

Prosthetic limbs are artificial devices which substitutes missing body parts (limbs) of the amputee. A person may face amputation due to disease or accidents. According to 2007 census in Ethiopia the number of people living with disability (PWDs) constitutes to be 864,218 among 31.18% have leg, hand and body movement difficulties and the total population with physical disabilities is estimated to be 36,940 out of which 5% of people with disabilities requiring Prosthesis & Orthosis device and physiotherapy [1]. As study at Tikur Anbessa Hospital shows, for 12 months from May 1-April 31, 2001- 2002 E.C 110 amputations were recorded [2]. The amputee's limbs are hence replaced by prosthetic limbs which are designed to meet the performance level of natural human limbs equally providing comfort to the amputee. Prosthetic limbs allow amputees to continue their day to day life. According to observational study in Germany national hospital, a total of 55,595 amputations of the lower limb in 2015 were identified [3]. Lower extremity prosthesis provides replacement of lower limbs at varying levels of amputation. Among lower extremity prosthesis the Prosthetic foot helps the amputee to walk independently adapting amputee's gait.

Prosthetic foot is designed in such a way that they provide comfort to the amputee without compromising the degree of performance. The performance this prosthetic foot depends on the selection of prosthetic material and its property. But this is often overlooked because clinicians aren’t necessarily trained in metallurgy or materials science and strength. The homo polymer polypropylene material is the older material used for the prosthetic foot. It is the most widely used polypropylene material in industry having the approximate market share 65-75% [4]. This material is applicable for ankle foot orthosis, dynamic ankle-foot orthosis, definitive prosthetic sockets, frame sockets and knee ankle foot orthosis [5]. It’s also applicable for shape-retaining orthosis components, e.g. paralysis orthoses, antibacterial effect, reinforced with 617R11PP Thermo-prepreg and it is easy to dye with Otto bock thermos-papers [6]. This material is lower in its strength, energy storage, safety factor and weight when they are applied for such application [7]. Similarly, the prosthetic orthotic center in Ethiopia are still using this material.

Composite materials well suited for the application of prosthetic foot due it's possible to obtain lightweight, strong under tension and bending, flexible, capable of resisting stress, durable (to resist fracture under impact planes), cost effective and easy to apply [8]. This composite material is applicable in most researches for the application of prosthetic foot running blades for the athletics rather than for normal amputees [9]. The synthetic fibers-reinforced epoxy composite materials are used for such application due to possibility of obtaining Light weight and good mechanical property. But, the composite material needs to characterize its property to identify the configuration of the laminas in the laminate that yields strong properties. This requires experimental testing machine which is time consuming and expensive. The mechanical property characterization of composite with the experimental method has a long time history. The mechanical properties of Carbon Fiber, Glass Fiber and blend of Glass Fiber and Carbon Fiber was experimentally analyzed [10]. The short carbon fiber blend (5-15%) reinforced with Poly-Methyl-Metha-Acrylate (PMMA) and Silicone rubber (SR) was studied [11]. The experimental program (i.e. tensile, flexural and fatigue test) was conducted to decide best composite among two systems of stacking sequence [12]. But, this characterization need to done through FEA for the selection best configuration of laminate for intended application. This requires to analyses properties of lamina and laminate with failure analysis of laminate that determine the final load carrying capability and strength of the composite.

In this thesis the tensile and flexural properties of pure E-glass/epoxy and hybrid glass carbon/epoxy laminate with four stacking configuration are simulated and its results are validated theoretically with MATLAB results in terms of their ultimate failure load. As this material is for prosthetic foot blade the thickness and number of layer in each laminate is kept constant (2.5mm thickness and 6 layer) respectively. The effect of stacking sequences on orders of plies failure, on tensile and flexural strength of glass/epoxy and hybrid composite is analyzed and compared for the selecting the best configuration for this prosthetic foot application. The selected configuration of the composite applied for the model of single blade of prosthetic foot and simulated to compare their performances with HPP prosthetic foot model available in POC and recommending to them.

1.2 Problem statement

Composite materials are now a days very interesting for the application of prosthetic foot because of it's possible to obtain light weight, low cost and strong properties by characterizing the mechanical properties of composite material. The mechanical properties (i.e. high tensile strength and high flexural strength) of this composite are needed for the design and manufacturing of prosthetic foot for amputed limbs [13]. The properties of this composite materials depends mainly on orientation of fibers, stacking sequences and types of reinforcement. The stacking sequence is one of the major parameters that determine the tensile and flexural strength of the synthetic fiber reinforced epoxy composite [14]. It's mandatory to know the strength of composite for selecting the material for specific application in prosthetic foot. The selection of best configuration of laminates having highest tensile and flexural strength in experimental method is costive and time consuming [15].

According to the observation in prosthetic and orthotics center (POC) in Ethiopia, for longer time, they are using plastic material (homo-polymer polypropylene) for manufacturing of prosthetic foot. Even though, this material was plastic of choice for many years for such application. It has limitations, its lower in strength, energy storage (strain energy), safety factor, stiffness, deformation resistance and weight compared to composite material when it's applied for prosthetic device. Additionally, its thermo-forming can negatively affect the performance of a device and affected by thermal history and it becomes brittle in cold weather [7]. According to observation and collected data in POC, there is customer feedback as the foot is less comfortable and it requires maintenance within 3-5months. This made the center to takes more time for the maintenance. This problem arises from low stiffness and strength of the HPP material and it becomes permanently deform and lost its energy storing capacity to feel discomfort on the amputees.

As a result the development of new composite material is in need to minimize those limitation in production of prosthetic foot. Most researches is carried out on the application composite for prosthetic foot running blades for the athletics rather than for normal amputees [9]. In POC, the E-glass fiber, carbon fiber and epoxy matrix is imported and available in small amount for trial as it is expected to be used instead of homo-polymer polypropylene material for the prosthetic devices. But, there is lack of characterizing the mechanical properties of composite for selecting best

stacking configuration for specific prosthetic foot application due to the lack of mechanical testing machines.

So, the main focus of this thesis is to characterize the tensile and flexural properties of the four stacking sequences of E-glass and hybrid (E-glass/carbon) epoxy composite for prosthetic foot using powerful FEA software (ANSYS 19.2).This is done by applying micro-mechanics approach for determining the elastic and strength property of lamina, then applying progressive failure analysis based on Tsai-Wu failure theory in ANSYS 19.2 work bench and validating the numerical result with analytical MATLAB solution. This helps to select the stacking sequence that yields high tensile and flexural strength of composite for specific application without further experimental costs and time. The selected composite material (SS-3) is applied for the model of single blade of prosthetic foot that replaces the four blades of prosthetic foot made from HPP with higher performance, in terms of the its stiffness, strength, safety, weight, and energy storage ability. This material provide high strength, safety factor, energy storage capacity (strain energy) and stiffness than the model HPP prosthetic foot with lower weight.

1.3 Research Question

In order to solve the above stated problem from material property characterization for the selection of stacking configuration of the composite to the specific application this composite to prosthetic foot the following research question need to be answered.

1. What is the elastic property of lamina and how the laminate property is characterized theoretically using MATLAB for numerical validation of ANSYS result.
2. What is the tensile and flexural properties of the composite for each stacking configuration of laminate and which configuration is best in its strength for this specific prosthetic foot.
3. What is effect of stacking sequence on the orders of plies failure, tensile and flexural properties of pure E-glass/epoxy and glass-carbon hybrid /epoxy composite?
4. What are the numerical results comparison of two material model of current HPP and composite prosthetic foot?

1.4 Objectives

1.4.1 General objective

To characterize tensile and flexural properties of synthetic fiber epoxy composite for prosthetic foot application using finite element method.

1.4.2 Specific objectives

1. To analyze elastic property of lamina and theoretical characterization of the laminate property using MATLAB for numerical validation of ANSYS laminate failure load result.
2. To characterize tensile and flexural properties of the composite for each stacking configuration of laminate and identify best configuration laminate in its strength for this specific prosthetic foot.
3. To analyze the effect of stacking sequences of lamina on; the orders of ply failure, tensile and flexural properties of pure E-glass/epoxy and glass-carbon hybrid /epoxy composite?
4. To compare the numerical results of two material model of current HPP and composite prosthetic foot. Additionally, to calculate and compare their stiffness, weight and material cost

1.5 The Research Method and Methodology

Methods and methodologies employed to achieve the objectives are:

a) Literature review and Data collection

Literature review of relevant material on the classification, advantage, mechanical properties, mechanical property characterization of composite, application of composites and HPP for prosthetic foot is done. The review is based on the available literatures collected from scientific journal, books and websites. In addition to secondary data from previous research, the actual primary data is collected from prosthetic and orthotic center (POC) available in Paulo's Hospital. The relevant data including individual properties of fibers (carbon and E-glass) and matrix (epoxy) for prosthetic foot and other relevant scientific finding used in the paper is collected through literature review. The material properties of HPP is taken from online source of SIMONA products.

b) Modeling and analysis

Based on collected data,

- Theoretical elastic properties of lamina that are input for numerical analysis is analytically solved by using micromechanics approach and empirical approach.
- Theoretical analysis of laminate for property characterization by ply discount method using classical lamination theory and Tsai-Wu failure criteria is carried out for numerical validation of failure load with MATLAB script.
- Modeling of tensile and flexural testing samples according to ASTM standard for each stacking configuration of E-glass/epoxy and hybrid (E-glass/carbon)/epoxy composite in ANSYS 19.2 workbench.
- Tensile and three-point bending tests in ANSYS 19.2 for each sample of composite laminate is carried out according to progressive failure analyses then the stress-strain graphs, load-deflection graphs that it helps extract their ultimate ply failure load and strength is prepared.
- Comparison and analysis of tensile and flexural propitiates of each stacking configuration of the composite and selection of high strength stacking sequence for prosthetic foot model.
- Modeling and analysis of the two models of prosthetic foot made from HPP and selected composite.
- Calculating weight and stiffness for the two model of prosthetic foot.

c) Result, discussion, conclusion, recommendation and future work

The results of the analysis is discussed and concluded based on the analysis method. The recommendations is given after concluding the result. Finally; based on the limitations and scope of the thesis, future work is forwarded for further studies. The overall work follow the research methodology is shown in figure 1.1

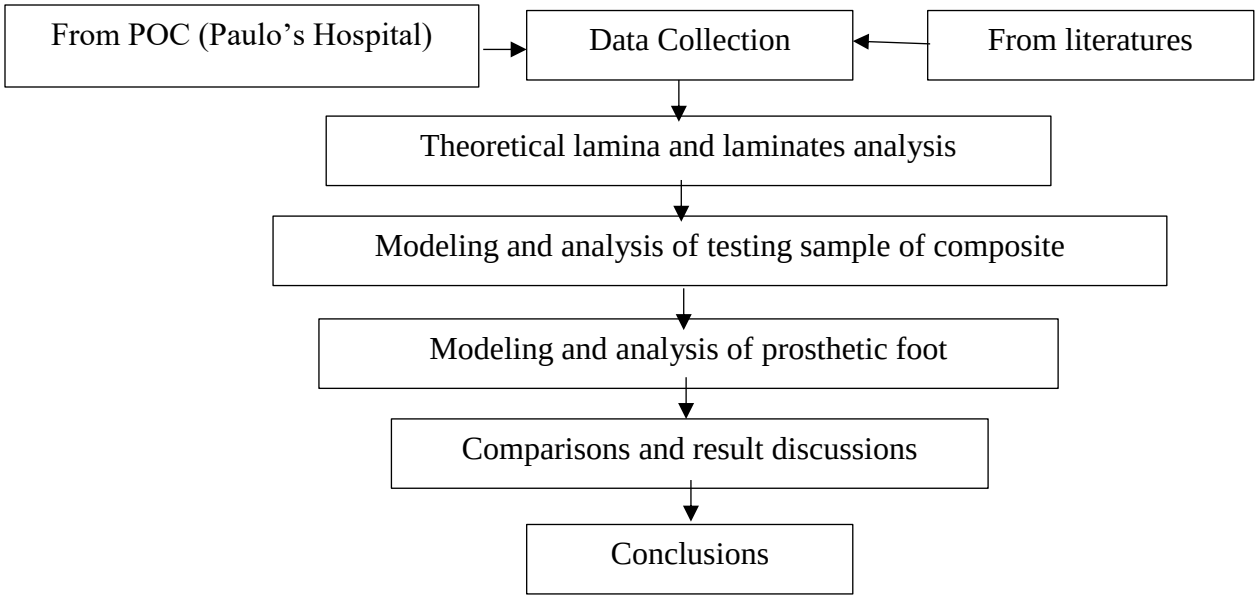

Figure 1. 1 The general work flow of the research methodology

1.6 Significance of the study

The outcome of this research benefits:

a) The prosthetics producers

- This research suggests higher tensile and flexural strength hybrid glass-carbon/epoxy composite applicable for prosthetic foot instead of homo-polymer-polypropylene material.
- To follow the same numerical procedures to select best configuration of laminate for specific application of any prosthetic device without experimental cost and further testing machines.
- The research benefits the Ethiopian prosthetic and orthotic center as they are still using HPP for prosthetic devices. This research suggests, a single blade prosthetic foot model of 2.5mm thickness from a hybrid glass-carbon/epoxy composite instead of current four blades of HPP with more strength, higher safety, higher energy storage, lower weight and stiffness prosthetic foot.

b) The other researcher

- Contributing a body of knowledge in analysis of the composite material for specific application from theoretical lamina and laminate failure analysis to numerical testing of composite sample in ANSYS Software package.

- Contributing a body of knowledge on analysis prosthetic foot for further performance in terms their weight reduction, increasing energy storage, stiffness and safety of prosthetic foot.
- As the experimental method is quite expensive, it initiates the researcher for the further study on numerical strength prediction of composite for specific application.
- Initiating the researcher on the performance improvement of prosthetic foot and reducing its cost for lower income countries.

1.7 Scope of the study

This thesis is intended to characterize tensile and flexural properties of composite material for prosthetic foot with strong and light weight prosthetics by theoretical and numerical simulation. The effect of stacking sequences on orders of ply failure, tensile and flexural properties and selection of stacking configuration for prosthetic foot. Additionally, the numerical analysis and comparison of the two prosthetic model from composite and HPP is aimed for analysis.

1.8 Limitation

The study has some limitation. The prototype of prosthetic foot doesn't manufactured in this study. Numerical impact analysis of composite is not studied as experimental investigations is not conducted and important data of composite is not extracted for this numerical simulation. Therefore, this work mainly focuses on tensile and flexural properties characterization of the composite for specific prosthetic foot.

1.9 Organization of thesis

This thesis work is organized in five chapters.

The first chapter is introduction; in which brief discussion is devoted from background on mechanical property characterization of composite and application of composite and HPP for prosthetic foot. The problem statement, the research question addressed, general and specific objective of the thesis, methodology of the research with significance, scope and limitation in the study is included under this chapter.

The second chapter is literature review; the chapter presents literature review on classification, properties and advantage of composite for prosthetic foot, application of HPP and composite for prosthetic foot, mechanical properties of composite and mechanical property characterization of composite for prosthetic foot.

The third chapter deals with the theoretical analysis of elastic property lamina by micromechanics and empirical approach. The laminate analysis for numerical validation by classical lamination theory with MATLAB script discussed in this chapter.

The fourth chapter is the steps used in ANSYS Workbench software for the analysis of required result. The modeling, mesh generation, loading and boundary conditions of composite for tensile, flexural and prosthetic foot model simulation are briefly discussed. The theoretical calculation of stiffness, weight, material cost for prosthetic foot is also under this chapter.

The fifth chapter discusses the results obtained from ANSYS Workbench software. The result for the effect of stacking configuration on order of plies failure and strength of composite laminate is described. The theoretical results and validation of numerical analysis and comparison of the two model of prosthetic foot. Results.

The sixth chapter is devoted to discuss conclusions and recommendation drawn from the results analyses and also the future work of the study for further research.

CHAPTER TWO
LITERATURE REVIEW

2.1 Composite material

A composite material is an engineered structural material consisting of two or more constituents combined at macroscopic level and not soluble in each other [16]. One constituent is called the reinforcing phase and the one in which it is embedded is called the matrix. It is formation of two or more constituent materials having significantly different physical or chemical properties when combined together produces a material which possesses unique characteristics different from the constituent elements [17]. After the age of revolution, plastic and composite material has been widely spread for manufacturing medical devices such as the orthosis and prosthesis [18]. Since middle of 20^{th} century, composite materials are one of the hot research topic in the modern technology due their promising characteristics for numerous application in industrial field.

2.1.1 Properties and advantages of composite material for prosthetic foot

The property of composite is the combined properties of reinforcement and matrix which are not available in nature. This made the composite to have high fracture toughness at high strength levels, a property impossible to obtain with a single material. The matrix plays an important role in transferring the load to the fibers and evenly distribute stress concentration. The overall properties of the composites depend on the geometry, orientation and percentage of reinforcing material.

The composite materials have several advantages compared to traditional materials [19]. The composite are lighter in weight. Fiber reinforced composite are typically 30-40% lighter than steel parts of equal strength. It has lower manufacturing complexity and 80% less manufacturing tools cost than comparable metal parts. They have incomparable damage (dent) resistance than steel, aluminum and thermoplastic panels. They do not embrittle when exposed to cold temperatures nor will they melt in the presence of extreme heat as do thermoplastics. The FRP are superior corrosion, wear and inherent chemical resistance when exposed to moisture which makes them well suited for prosthetic applications. They have better internal damping, design flexibility and cost effective.

2.1.2 Classification and manufacturing Techniques of composite Material

a) Classification of composite materials

The composite materials are classified according to their constituents as shown in figure 2.1.

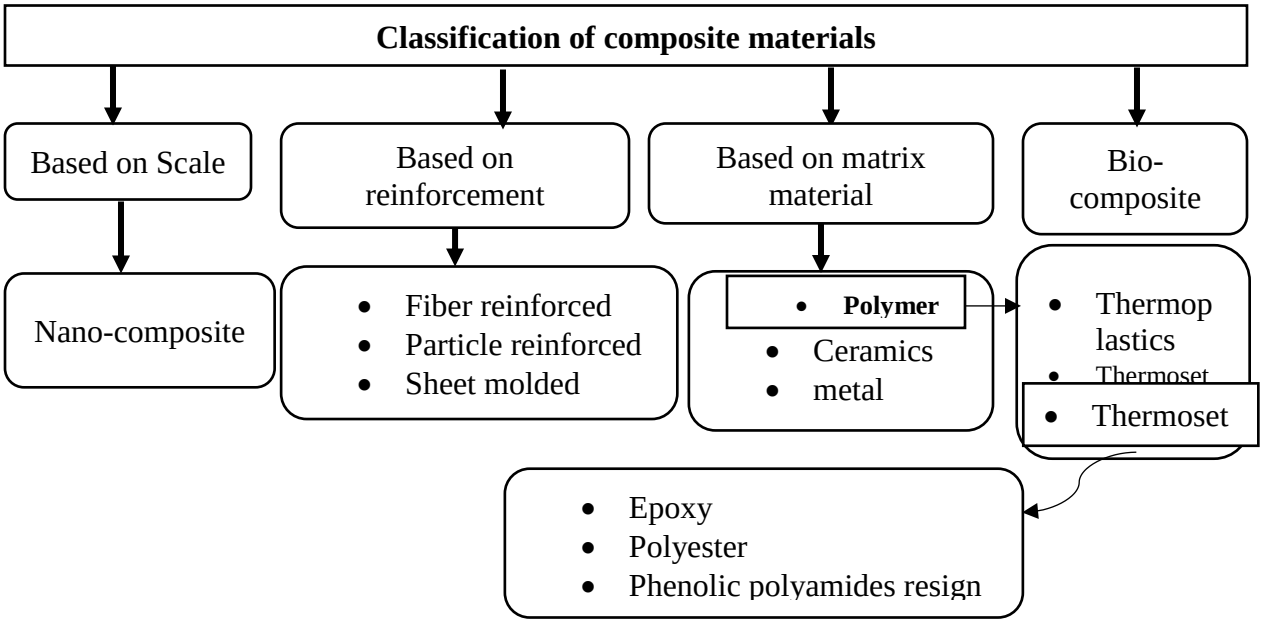

Figure 2. 1 Classification of composite materials [20]

Most commonly used matrix materials are Polymers and it's an ideal materials as they can be processed easily, possess lightweight, and desirable mechanical properties. This is due to the processing of polymer matrix composites need not involve high pressure and high temperature. Also, the equipment's required for manufacturing polymer matrix composites are simpler. Thermosets and thermoplastics are the two main types of polymer matrix. Thermosets have qualities such as a well-bonded three-dimensional molecular structure after curing, decompose instead of melting on hardening and simply by changing the basic composition of the resin, possible to alter the conditions suitably for curing and determine its other characteristics. They can be retained in a partially cured condition too over prolonged periods of time, rendering Thermosets very flexible. Thus, they are most suited as matrix bases for advanced conditions fiber reinforced composites [21].

The two types of polymer composite are fiber (FRP) and particle (PRP) reinforced polymer. FRP composite are composed of fibers and matrix. Fibers are reinforcement and the main source of

strength while the matrix binds the fibers together and transferring stress between fibers. The most common synthetic fibers for prosthetic application are E-glass and carbon fiber. Similarly epoxy is common matrix materials as it has higher adhesion, less shrinkage and lower cost [21].

b) Manufacturing Techniques of composite material

There are variety of techniques to manufacture the composite. This manufacturing techniques are selected based on the type of fiber or matrix used. Some of the manufacturing techniques are categorized as shown in figure 2.2.

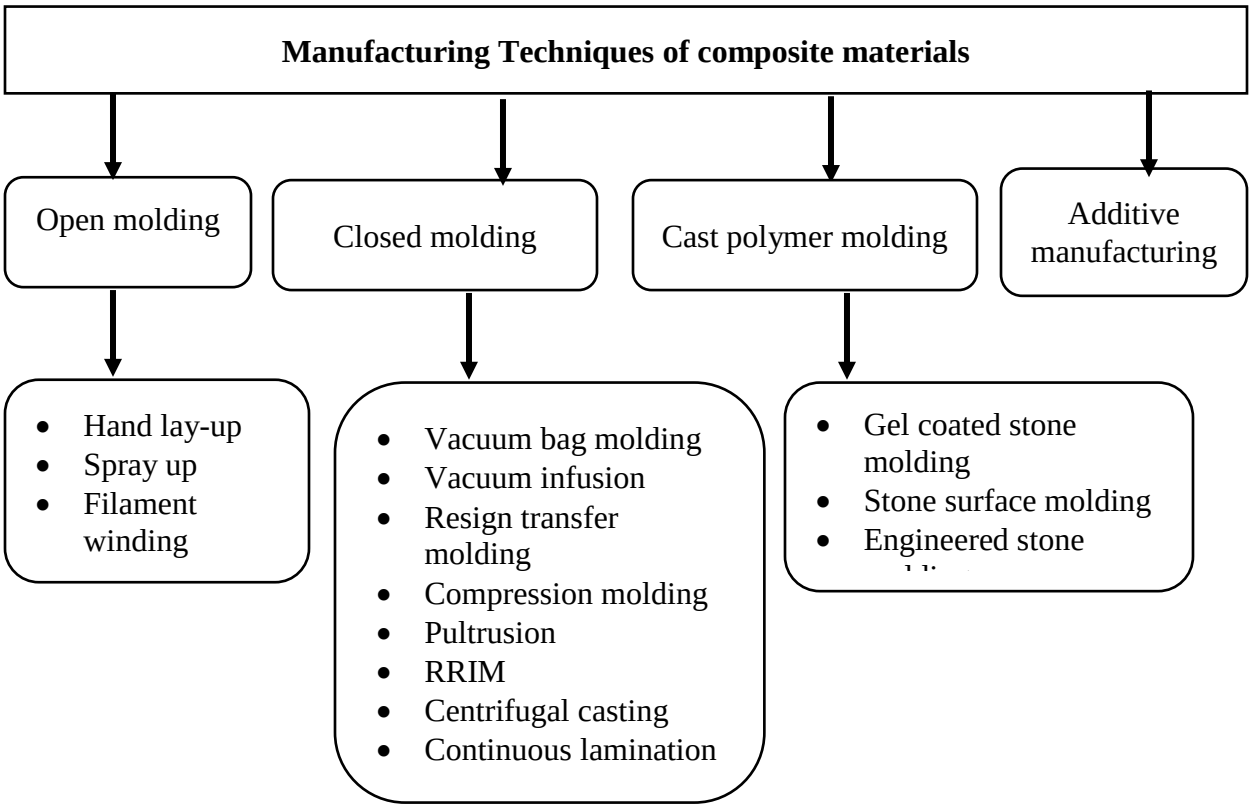

Figure 2. 2 Composite manufacturing Techniques [22]

In hand lay-up techniques the material is exposed to air for getting harder while in closed molding curing takes place inside the molding and used for large volume production as it can be automated. In cast polymer molding there is no fiber reinforcement in it and used to meet specific requirement for intended application [23]. Additive manufacturing is advanced manufacturing techniques in which the composite structures are made layer by layer with the use of computer aided designing

process without mold. The most common and widely used manufacturing techniques is hand lay-up techniques. This happened due to the least amount equipment is required for manufacturing process.

2.2 Application of HPP and composite for foot prosthetics

In prosthetics and orthotics, materials have a direct and critical impact on a device's performance, but this is often overlooked because clinicians aren't necessarily trained in metallurgy or materials science. Knowledge of materials affects what types of forming techniques are used and can ultimately make a critical difference in component selection, structural strength, and functional optimization. Plastics are categorized into four main groups: thermoplastics, elastomers, and thermosets and polymer compounds. Thermoplastics are either amorphous or semi-crystalline. Typically, semi-crystalline resins includes polyamide (PA) and polypropylene (PP) [7].

Polypropylene (pp) was discovered in 1954 and gained a strong popularity very quickly due to the fact that PP has the lowest density among commodity plastics. Polypropylene is the main output of propylene among other derivatives with two-thirds consumption rate. PP is the lightest type of plastics with a density of 0.90 g/cm3. There are three different types of polypropylene. Homo-polymer (HPP), impact copolymer (ICP) and random copolymer (RCP). Homo-polymer polypropylene (HPP) is a type of pp containing only propylene monomer in a semi-crystalline solid form. It is the most widely used polypropylene material in industry having the approximate market share 65-75% [4].

Homo-polymer polypropylene is available in sheet form of different size, thickness and molding temperatures ranging from 180-220 $°c$. This material is applicable for ankle foot orthosis – AFOs, dynamic ankle-foot orthosis – DAFOs, definitive prosthetic sockets, frame sockets and knee ankle foot orthosis – KAFOs [5]. This material is applicable for shape-retaining orthosis components, e.g. paralysis orthoses, dynamic AFOs, antibacterial effect, Can be reinforced with 617R11PP Thermo-prepreg PP easy to dye with Otto bock thermos-papers [6]. HPP- has been the plastic of choice for many years because it's easy to shape using heat and vacuum-forming devices, it mills well, it's lightweight and inexpensive, and it's relatively nontoxic to work with, but it has limitations isn't as strong as composites like carbon fiber and provides little energy return. The researchers quantified the material weaknesses in posterior leaf-spring AFOs made of

polypropylene and polyethylene, when plantar flexed from 0° to 10° in a testing machine, lost stiffness and became permanently deformed after about 90,000 cycles. Thermoplastic devices may begin to cold flow and early models sometimes failed as a result. Thermoforming can negatively affect the performance of a device if it's molded incorrectly or at too high a temperature. It's also affected by thermal history; heating and cooling times and temperatures have profound and lasting effects on strength and stiffness. In addition to those already mentioned, it becomes brittle in cold weather [7].

As a result the development of new composite material is in need to minimize those limitation in production of prosthetic and orthotics device. The new composite materials properties depends on several parameters; especially those fiber reinforced depends mainly on orientation and stacking sequence lamina. Composite materials well suited for the application of prosthetic foot application due it's possible to obtain lightweight, strong under tension and bending, flexible capable of resisting stress, durable (to resist fracture under impact planes), cost effective and easy to apply [8].

2.3 Mechanical Property of composite for foot prosthetics

Mechanical properties of Carbon Fiber, Kevlar and Glass Fiber was studied and compared [8]. Authors analyzed that Kevlar is the lightest material compared with Carbon Fiber and Fiber Glass and is also very expensive. It gives excellent fracture resistance under fracture loading and can also absorb high loads of stress and torque. However, Kevlar is weak in maintaining structure under load and is about five times weak under compression than under tension. Tensile strength of Kevlar is 103.42MPa whereas its compressive strength is 20.68MPa. Kevlar gives excellent chemical resistance. It is difficult to saturate Kevlar with resin. Hence to overcome this Author blend Kevlar with carbon fiber producing a quasi-isotropic hybrid by arranging composite fibers in mat/knit form. This places fibers in three dimensional or multiplane manner. This hybrid blend improved drawbacks of Kevlar desirably providing lightness, stiffness as well as torque and impact resistance. He also studied properties of Fiber Glass. It was found that Fiber Glass is easy to saturate with resin. It is also possible to obtain it in different quality and forms. It is highly durable and flexible. Its fiber strength is twice stronger under tension than under compression. Its tensile strength is 68.94MPa whereas its compressive strength is 34.47MPa. The material is also cost

efficient. But the high flexibility of the material makes it difficult to regain its original shape after the toe off and hence doesn't provide enough momentum. Authors then studied blend of Fiber Glass with Carbon Fiber which achieved better properties.

The fatigue and tensile characteristics of carbon fiber for prosthetic foot using different types of reinforcements were studied [24]. They conducted tensile and fatigue tests using ANSYS-11 and compared the values with the theoretical results. They compared properties of 5 different reinforcements with epoxy resin i.e. glass fibers, Perlon fiber, (carbon + glass) fiber, carbon fiber, (carbon + glass) fibers+SiO2 particles. The result shows that the mechanical properties of the carbon fiber can be improved by changing the type of reinforcement. The scientists concluded that (epoxy + carbon reinforcement) composite gives better mechanical properties i.e. improved fatigue strength due to high value of Young's modulus and also higher factor of safety is obtained whereas Perlon reinforcement gave lowest values in all properties.

The short carbon fiber blend (5-15%) reinforced with Poly-Methyl-Metha-Acrylate (PMMA) and Silicone rubber (SR) was studied [11]. Authors experimented these two materials so as to improve flexural strength of carbon fiber. They prepared different polymer blends by changing the concentration ratio of (PMMA: SR) from 90:10, 80:20, 70:30, 60:40 to 50:50. These blends also support dorsiflexion movement of ankle foot. The result of the test for flexural strength concluded that flexural strength of polymer blends increases as reinforcement with carbon fiber increases from 5-15%. (PMMA: SR) (80:20) reinforced with 15% carbon fiber improved the flexural strength by approximately 17%, giving the highest value of all. The author concluded that polymer blends reinforced with short carbon fiber will not only increase flexural strength of material but also the flexural modulus, reducing the cost.

The comparative study analysis of material properties of carbon fiber, Kevlar and glass fiber and conclude as orientation of fibers decides the properties of material hence the mechanical properties of Carbon Fibers as well as Glass Fiber can be improved by adapting the sandwich structure of orientation of fiber laminates, the type of reinforcement also determines the material properties [25]. It is observed that orientation of fibers decides the properties of material hence the mechanical properties of Carbon Fibers as well as Glass Fiber can be improved by adapting the sandwich structure of orientation of fiber laminates. Blending of Carbon Fiber with Poly-Methyl Metha

Acrylate (PMMA) and Silicone rubber (SR) increases its flexural strength by almost 17%. The type of reinforcement also determines the material properties. Hence blending of Carbon Fiber with Glass Fiber will not only improve its mechanical properties but also reduce its cost and increase its durability. Hybrid blend of Carbon Fiber with Kevlar also shows excellent improvement in mechanical properties as lightweight, stiffness, high tensile as well as compressive strength, desired flexibility and also cost efficient.

The experiment was conducted using two systems of stacking sequence (2 Perlon fiber + 1 Carbon fiber + 2 Perlon fiber + 1 Carbon fiber + 2 Perlon fiber) and (2 Perlon fiber + 1 Carbon fiber + 1 Perlon fiber + 2 Carbon fiber + 1 Perlon fiber + 1 Carbon fiber + 2 Perlon fiber) to decide best composite and optimal shape of the Syme prosthesis cut-out [12].To achieve this aim tensile test, Three Point Bending Flexural Test and fatigue test was conducted. The results showed that by increasing number of carbon and perlon fiber layers, the strength is increased, system two showed better results where it leads to decrease the maximum stress, maximum deflection and Von Mises stress by 37.7%, 97.6 %, and 25% respectively as compared to polypropylene socket. The results indicate that the elliptical shape of socket cut-out is recommended to be used in manufacturing the prostheses, where the maximum stress, maximum deflection, and Von Mises stress were reduced by 50%, 30 %, and 44% respectively as compared to the socket with $\theta = 210°$ Cut-Out (Old socket).

The research has been conducted to prove an engineered interface can improve the mechanical properties of epoxy/glass composites simultaneously inducing a piezo-resistive response [26]. E-glass fibers were coated with graphene oxide (GO) by electrophoretic deposition, while reduced graphene oxide (rGO) coated fibers were obtained by subsequent chemical reduction. The fiber-matrix interfacial shear strength (measured by the single-fiber fragmentation test) increased for both GO and rGO coated fibers. Unidirectional composites with a high content of both uncoated and coated fibers were produced and mechanically tested under various configurations (three-point bending, short beam shear and mode-I fracture toughness, creep). Mechanical test (three-point bending, short beam shear and mode-I fracture toughness) on high fiber volume fraction composites revealed that GO coted fibers lead to an increase of elastic modulus, stress at break and inter-laminar shear strength, while composites with rGO coated fibers perform similarly to composites with uncoated fibers.

The experimental investigation on three laminated composite groups (Only perlon reinforcement, 3Perlon +2carbon fiber +3perlon and 3Perlon + 2 glass fiber + 3perlon) layers to find their mechanical properties (modulus of elasticity, tensile and yield strength) that have been used to design and manufacture a socket for partial foot prosthesis using ANSYS model [27]. The socket composite material was tested for tensile and fatigue properties; then, its results were used in the ANSYS model. The result shows that the calculated factor of safety for the prosthesis that has been made from a selected composite material with the following layers (3 Perlon+2 carbon fiber+3 Perlon) is 1.037 which is safe for design prosthetic applications. ANSYS model used the boundary condition from the measured contact pressure between the socket and the patient's stump. The Mat-Scan (F-socket) pressure sensor utilized these interface pressure measurements. This helps to analyze the prosthetics before manufacturing and more prosthetic designs to be modelled and manufactured as Prosthetics and orthotics are usually custom-made for each patient according to its specific requirements.

The influence of different resin on physio-mechanical properties of hybrid fiber reinforced polymer composites was studied [28]. Composites for prosthetic limb were manufactured with constant 5 wt% glass fiber hybridized with varied jute and grewia-optiva loading (2.5 wt%, 5 wt% and 7.5 wt% each) reinforced based epoxy, vinyl ester and polyester matrix. Results show that the strength and hardness get improved as the ratio of natural fiber increases. The highest tensile, flexural, were obtained for epoxy-based hybrid composite at 7.5 wt%, vinyl ester based hybrid composite at 5 wt% samples E3, V2, E3 and E2 respectively. In addition, both Impact energy and hardness were observed to be maximum for epoxy based hybrid composites at 7.5 wt% and 5 wt% respectively. Results also reveal that 5 wt% glass fiber (fixed), 10 wt% natural fiber with epoxy is the best composition among fabricated samples followed by the vinyl ester composite of the same composition.

2.4 Mechanical Property characterization of composite for foot prosthetics

The mechanical properties of Carbon Fiber, Glass Fiber and blend of Glass Fiber and Carbon Fiber for the application of prosthetic foot was experimentally analyzed considering the orientation of the fiber laminate [10]. By applying bending moment, it was found that properly laminated Carbon fiber with continuous and straight fibers was thrice stiffer than Glass Fiber; whereas Glass Fiber

structure was five times stiffer than Glass Fiber- Carbon Fiber mix without spending any effort on straightening and orienting the fibers in correct direction. This concludes that if Glass Fiber is correctly used will give excellent result. He put forward an orientation scheme for each layer of fiber which will result in improved tensile and compressive strengths.

Mechanical properties and response of unidirectional E-glass composite lamina for aerospace application in term of tensile, compression and thermal responses were quantified using ABAQUS finite element commercial software [29]. The ultimate load failures, tensile strength and other properties of laminated plates are determined from stress and strain curves. In the analysis of their e-glass unidirectional composite, FEA simulation is higher than the values obtained from the experiment due to the influence that the experimental process may discover an environmental or human error such as trapped air in the specimen, improper binding for each layer of specimen during experiment and unsuitable temperature for cured process.

The stress analyses of carbon fiber reinforced polymer composite laminates with and without cut-outs was investigated by analytical and finite element approaches [30]. The MATLAB code is developed for analytical method using CLT and composite failure theory. MSC.NASTRAN finite element code is used for finite element analysis and failure load of composite laminates are predicted using four failure criteria's. It's observed that, the stress and strain values are in are in good agreement for analytical and numerical results. The Tsai-Wu failure criteria is the most appropriate failure criteria as it gives very close result to the experimental failure load.

Flexural properties of symmetric carbon and glass fiber reinforced epoxy composite laminates was investigated using experimental and numerical analysis for various stacking sequence to find effect of hybridization [31]. In FEA the ANSYS software was employed to predict the flexural properties based on maximum shear stress criteria and a rule of how to arrange the carbon and glass fibers in the hybrid composite was developed. The result shows that, When the flexural strengths the full carbon and full glass composites are the same, the glass/epoxy plies should be placed on the outside of the hybrid composite; While, the flexural strength of the full carbon composite is greater carbon/epoxy plies should be placed on the outside of the hybrid composite to obtain positive hybrid effect. The hybrid composite has the highest flexural strength when it contains half carbon/epoxy plies and half glass/epoxy plies.

The effect of the combination of polyester matrix and GFs in two forms (WGF and CSM) at different plies numbers with and without a gelcoat on the mechanical and hygroscopic properties was studied by [32]. The results showed that using the same thickness, the mechanical properties, especially in terms of bending and buckling, are influenced by the layers' number. While the second part this study was devoted a case of application of this new formulation and original structure design in the sports domain (running blade prosthesis). Three different running blades "Flex-foot Cheetah" were manufactured to be experimentally and numerically (ANSYS ACP software) characterized to simulate real conditions. The results showed a good agreement between the experimental and numerical values in terms of total displacement, which is around 50 mm, the produced blade has been tested in quasi-static and dynamic compression, and results showed that the relaxation behavior depends on the structure design and the used materials.

2.5 Application of finite element analysis software for composite

Any engineering problems can be solved by analytical, numerical and experimental method. The analytical method is based on classical approach to give accurate result's but, only applicable in simple problems. While, the experimental method is the actual measurement that is applicable only on physical prototype and it's time consuming and needs expensive setup due to more prototype must be tested to believe on the results. Due to this difficulties, the numerical methods are developed based on mathematical approach to approximate the results that are applicable to real life complicated problems without experimental costs but, it needs analytical or experimental method for verification of the result. Among the numerical methods the FE method is very popular method based upon discretization of component into finite number of blocks (elements) and applicable for linear, nonlinear, thermal, dynamics, buckling and fatigue analysis [33]. There are many software packages available to industries that use FEA. A list of some of these commercial packages can be seen in table 2.1

Table 2. 1 List of some commercial available FEA software's [33]

Software Codes	Company Name	Notes	
ANSYS	ANSYS.Inc.canonbargs.PA	General purpose work station	Codes built in pre and post processor for composite analysis
ABAQUS	Hibbit, karlsson and Sorenson Inc.	Non-linear and dynamic analysis	
ALGOR	Algor.Inc.pittsburgh.PA	PC and work station	
COSMOL	Structural research and analysis corp.	General purpose FEA	
NASTRAN/ DYTRAN	MSC. Software corp.	General purpose FEA on mainframe, built in separate pre and post processor	
PATRAN	MSC. Software corp.	Built in Pre and post processor	
Hyper Mesh	Altair.Engineering.Inc		

Out of the packages listed above, ANSYS were selected due to:-

- It's easily availability and wide usage in industries and research areas.
- The Pre-post processor Codes built in one, makes it easier for composite analysis.
- The workbench (user interface) in ANSYS is easy to use and user friendly.
- The composite failure criteria's are defined and simplify failure analysis process.
- It's easy to define the stacking sequence and the property of new composite materials.

The summary of important literature review and identified gaps are shown in table 2.2.

Table 2. 2 Summary of literature reviews

Author	**Title**	**Method and application**	**Gaps**	**Finding and solution**
J. M. Khare et al.(2020)	Influence of different resins on Physico Mechanical properties of hybrid fiber reinforced polymer composites used in human prosthetics	-Conventional hand layup process -for prosthetic application	Conventionally, natural fibers are not used for prosthesis and influence of different resign on physio mechanical properties of hybrid composite	Use natural and synthetic fibers to fabricate a prosthetic limb and 5 wt% glass fiber (fixed), 10 wt% natural fiber with epoxy is the best composition among fabricated samples followed by the vinyl ester composite of the same composition.
Wafa Ouarhim et al.(2020)	Characterization and numerical simulation of laminated glass	-Hand-layup process, numerically by ANSYS	To explore different types of deformations (buckling, bending,	-Using the same thickness, bending and buckling, are influenced by the Layers' number.

	fiber–polyester composites for a prosthetic running blade	-for sport application	and relaxation) on the properties of laminated composites based on polyester as the matrix and glass fiber in two forms: woven and chopped Strand mat.	-Relaxation behavior depends on the structure design and the used materials.
Aif M. Abbas et al.(2020)	Effects of Composite Material Layers on the Mechanical Properties for Partial Foot Prosthetic Socket	-Vacuum pressure system -for partial foot amputees	Experimental investigation on three laminated composite group layer on mechanical property to design and manufacture a socket for partial foot prosthesis using ANSYS model.	The calculated factor of safety for the prosthesis that has been made from a selected composite material with the following layers (3 Perlon+2 carbon fiber+3 Perlon) is 1.037 which is safe for design prosthetic applications.
Haroon Mahmood et al.(2018)	Mechanical properties of glass-epoxy composites with graphene coated fibers	By electrophoretic deposition and subsequent chemical rxn- for coating fibers -for proving, no identified application	To prove an engineered interface can improve the mechanical properties of epoxy/glass composites simultaneously inducing a piezo-resistive response.	Graphene oxide (GO) coted fibers lead to an increase of elastic modulus, stress at break and interlaminar shear strength, while composites with Reduced GO (rGO) coated fibers perform similarly to composites with uncoated fibers.
Aif M. Abbas et al.(2020)	Fatigue Characteristics and Numerical Modelling Prosthetic for Chopart Amputation.	-Using mold and vacuum device to avoid poor lamination -for manufacturing a Syme prosthesis	-Optimal shape of the Syme prosthesis cut-out -Deciding the type of composite material and number of layers to be used in the manufacturing a Syme prosthesis of high strength as compared to the conventions polypropylene type.	-Increasing number of carbon and perlon fiber layers, the strength is increased, as compared to polypropylene socket. -The elliptical shape of socket cut-out is recommended as compared to the socket with $\theta = 210°$ Cut-Out (Old socket).

CHAPTER-THREE
THEORETICAL ANALYSIS OF LAMINA AND LAMINATE

3.1 Lamina property analysis

Lamina is thin layer of composite material with the thickness less than 0.5mm and stacked together in thickness direction to produce a laminate as shown in figure 3.1 [34]. The behavior of a composite lamina, which forms the basic building block of composite laminates and structures, is a function of the constituent properties and geometric characteristics, such as fiber volume ratio and geometric parameters. One objective of micromechanics is to obtain functional relationships for average elastic properties of the composite.

The properties of composite material is predicted by various approach (mechanics of materials, numerical, self-consistent field, bounding (Variational approach), semi empirical and experimental). The mechanics of materials approach is based on simplifying assumptions of either uniform strain or uniform stress in the constituents. The mechanics of materials predictions are adequate for longitudinal properties such as Young's modulus E_1 and major Poisson's ratio v_{12} of a unidirectional continuous-fiber composite. On the other hand, the mechanics of materials approach not accurately predict the transverse and shear properties, that is, transverse modulus E, and shear modulus GI, of such unidirectional materials. Semi-empirical relationships have been developed to circumvent the difficulties with the theoretical approaches above and to facilitate computation." The so-called Hulpin-Tsuirelution ships have a consistent form for all properties and represent an attempt at judicious interpolation between the series and parallel models used in the mechanics of materials approach or between the upper and lower bounds of the variational approach [35, p. 61]

Stiffness of lamina is important to determine property of laminate and unlike homogeneous isotropic material, in composite material the stiffness lamina varies from point to point. Accounting this variation makes any kind of mechanical modeling of the lamina very complicated. The macro mechanical analysis of lamina simplify this complexity by considering average value and lamina to be homogeneous [34].

So, it's important to calculate the stiffness of the individual lamina to model the composite in ANSYS workbench. This stiffness mainly depends on factors Volume fraction of the matrix and fiber, type of reinforcement used, continuous or discontinuous fiber used and orientation of fibers with respect to a common reference axis. There are several methods to evaluate the mechanical properties of composite materials such as experimental, analytical and computational methods. Computational modeling and analysis method is developed drastically in these few years. Finite element method (FEM) is the one of the numerical method which is more powerful in its application in real world problems by commercial software's and can be used to calculate elastic properties [36].

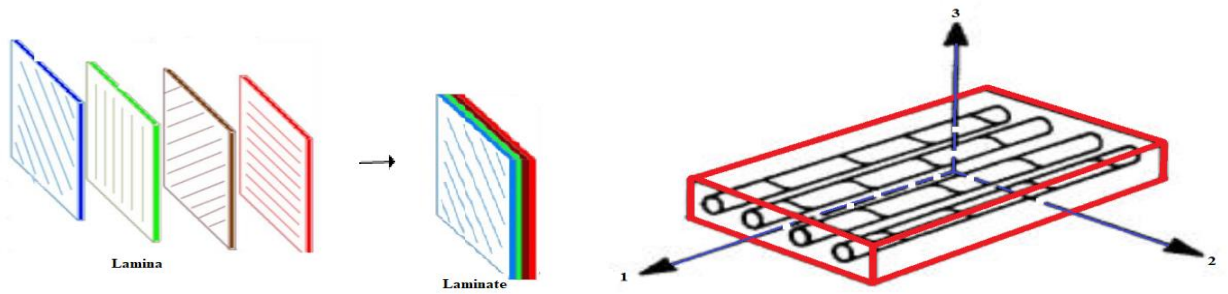

a) b)

Figure 3. 1 a) Schematic diagram of lamina and laminate, b) unidirectional lamina [37, p. 71]

The experimental method to evaluate the mechanical property of composite is costive and time consuming. Analytical method uses various mathematical expressions to predict the elastic constants such as stiffness and strength of composite material. Different methods used evaluate the elastic properties of the composite material are Rule of mixture, Halpin-Tsai, Nielsen and Chamis method. Here, two different theoretical models are used to calculate the ply properties, they are micro-mechanics approach (rule of mixture) and semi-Empirical approach (Halpin/Tsai model). The results from both models are compared and verified.

3.1.1 Micro Mechanics Approach (Rule of mixture)

The rule of mixture is the simplest and correct approximation to determine the elastic property of UD composite material [36]. It estimates the bulk properties, young's modulus and shear modulus, of composite material that is used to describe the deformation of homogeneous and isotropic material based on the contribution of the constituent of the composite. This approach does not take

into account the curvatures of the fibers within the section and the distribution of the fibers along the thickness [21]. Homogenized material characteristics of fibers immersed in resin can be found by using characteristics of the fiber and the resin, and volumetric contribution of these [38].

Based on rule of mixture, for two component composite lamina (i.e. fiber and matrix), a composite property,P_C can be estimated by:

$$P_C = P_f V_f + P_m V_m \quad ---------- \quad (3.1)$$

Where, V_f, V_m = fiber and matrix volume fraction respectively

P_f, P_m = property of fiber and matrix respectively

Assuming the composite is void free,

$$V_f + V_m = 1 \quad ---------- \quad (3.2)$$

To apply the rule of mixture for a single ply, the individual properties of fiber and matrix is needed. In Table 3.1, material characteristics of E-glass, carbon and epoxy resin are given. This material property is taken from [35]. For effective reinforcement of the matrix, the fiber volume fraction V_f in the composite must be greater than a critical value $V_{f_{cr}}$ [39].

$$\varepsilon_{fu} = \frac{\sigma_{1Tf}}{E_{1f}} = 0.047 \text{ and } \varepsilon_{mu} = \frac{\sigma_{mT}}{E_m} = 0.024$$

$$\sigma_{fmu} = E_{1f} \text{ x } \varepsilon_{mu=1752MPa}$$

Table 3. 1 Elastic properties of matrix and fiber materials shown in appendix-1

Fibers material property							
Fibers	Density, ρ ($^{g}/_{cm^3}$)	$E_{1f} = E_{2f}$(GPa)	$G_{12f} = G_{23f}$(GPa)	v_{12f}		σ_{1Tf}(MPa)	
E-glass fiber	2.6	73	30	0.23		3450	
Carbon fiber	1.75	235	27	0.2		3700	
Matrix material properties							
Matrix	Density, ρ ($^{g}/_{cm^3}$)	E_m(GPa)	G_m(GPa)	v_m	σ_{mT}(MPa)	σ_{mC}(MPa)	τ_m(MPa)
Epoxy resin	1.17	3.4	1.26	0.36	80	104	40

Where,

- E,G,v – represents modulus of elasticity, shear modulus and Poisson's ratio respectively
- Subscript 1,2 shows longitudinal and transversal direction
- Subscript f and m is to represent fiber and matrix
- ε_{fu} and ε_{mu} are failure strain of fibers and matrix respectively.

- σ_{fmu}=fiber stress at matrix failure strain.

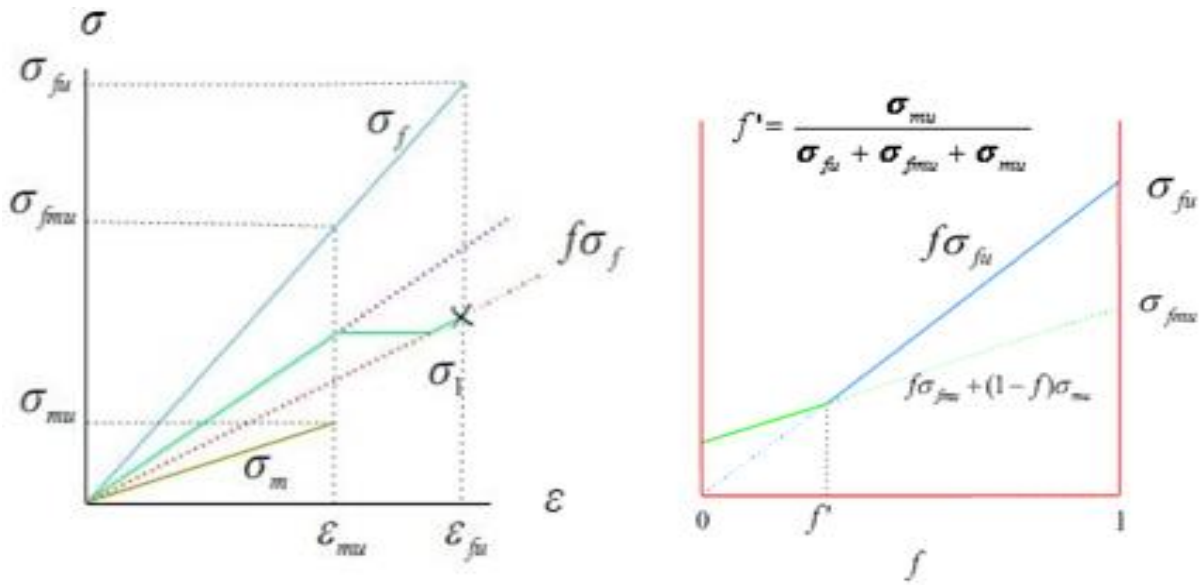

Figure 3. 2 longitudinal tensile loading of unidirectional lamina [source: [35]]

According to [35] this matrix has the lower failure (**u**ltimate) strain ($\varepsilon_{fu} > \varepsilon_{mu}$) the critical fiber volume fraction is given by:

$$V_{f_{cr}} = \frac{\sigma_{mT}}{\sigma_{1Tf} + \sigma_{fmu} + \sigma_{mT}} x100\% = 1.50\%$$

In practical case, the fiber volume fractions fall in the range 30% to 70% (i.e. $>V_{f_{cr}}$) and since it is usually the case that $\sigma_{mT} << \sigma_{1Tf}$, it is evident from above graphs that the fiber strength is dominant in determining the axial strength of continues fiber composites. The E-glass fiber volume fraction is taken from [35] is, $V_f = 0.55$. This value satisfy the requirement for effective reinforcement of matrix. From equation (3.2) epoxy matrix volume fraction is

$$V_m = 1 - V_f = 0.45$$

Applying the rule of mixture (ROM) the longitudinal, transversal and shear properties can be calculated by the (equation 3.3-3.8) given below.

Longitudinal properties of lamina,

- Longitudinal Elastic modulus,

$$E_1 = E_{1f}V_f + E_m(1 - V_f) \quad ---------- (3.3)$$

- Major Poisson's ratio,

$$v_{12} = v_{12f}V_f + v_m V_m \quad ---------- (3.4)$$

Transversal properties of lamina,

- Transversal Elastic modulus,

$$E_2 = \frac{E_m E_{1f}}{E_m V_f + E_f V_m} \quad ---------- (3.5)$$

- Transversal Poisson's ratio, v_{23} ,according to improved rule of mixture for accounting initial imperfections [40] is given by

$$v_{23} = k\left(v_{12f}V_f + v_m V_m\right) \quad ---------- (3.6)$$

$$\text{where, k} = 1.095 + 0.27(0.8 - \text{V}_\text{f})$$

Shear properties,

$$G_{12} = \frac{G_{12f}G_m}{G_m V_f + G_{12f}(1 - V_f)} \quad ---------- (3.7)$$

$$G_{23} = \frac{E_2}{2(1 + v_{23})} \quad ----------(3.8)$$

Using equation (3.3-3.8) the elastic mechanical properties of ply is given in table 3.2 below.

Table 3. 2 Elastic properties of E-glass/epoxy lamina by ROM

Elastic mechanical property	Units	Calculated result
Longitudinal Elastic modulus, E_1	GPa	41.6800
Transversal Elastic modulus, E_2	GPa	7.1486
Major Poisson's ratio, v_{12}	-	0.2885
Transversal Poisson's ratio, v_{23}	-	0.3354
In plane shear modulus, G_{12}	GPa	2.6633
Out of plane shear modulus, G_{23}	GPa	2.7740

3.1.2 Semi-Empirical Approach (Halpin-Tsai model)

The Halpin-Tsai equation developed as a semi-empirical model to produce more complicated results on transverse Young's modulus and longitudinal shear modulus [41] considering the geometry of the reinforcing fiber. The equation is good enough whenever the fiber volume fraction is less than 100%. According to [36, 42] of Halpin/Tsai model the equations for longitudinal modulus, transverse modulus and shear modulus are shown in (Equation 3.9-3.14).

- **The transverse properties,**

$$E_2 = \frac{E_m(1 + \xi\eta V_f)}{(1 - \eta V_f)} \text{ – – – – – – – – – – – – – – – – } (3.9)$$

$$\eta = \frac{\left(\frac{E_{2f}}{E_m}\right) - 1}{\left(\frac{E_{2f}}{E_m}\right) + \xi} \text{ – – – – – – – – – – – – – – – – – – } (3.10)$$

- **The shear modulus,**

$$G_{12} = \frac{G_m(1 + \xi\eta V_f)}{(1 - \eta V_f)} \text{ – – – – – – – – – – – – } (3.11)$$

$$\text{Where, } \eta = \frac{\left(\frac{G_{12f}}{G_m}\right) - 1}{\left(\frac{G_{12f}}{G_m}\right) + \xi} \text{ – – – – – – – – – – – – – – – } (3.12)$$

- **Poisson's ratio is**

$$v_{23} = \frac{v_m(1 + \xi\eta V_f)}{(1 - \eta V_f)} \text{ – – – – – – – – – } (3.13)$$

$$\text{Where, } \eta = \frac{\left(\frac{v_f}{v_m}\right) - 1}{\left(\frac{v_f}{v_m}\right) + \xi} \text{ – – – – – – – – } (3.14)$$

ξ is an empirical factor, which measures fiber reinforcement of the composite material that depends on the loading and boundary condition of the fiber geometry. Experimental results fall within a band of $1 < \xi < 2$. Usually, it is assumed that $\xi = 1$ for fiber for hexagonal arrays and circular fiber for calculating shear modulus, transversal modulus and Poisson's ratio [6, 8]. While for longitudinal properties E_1 and v_{12} are expressed in the same way as rule of mixture (i.e. Equation 3.3 and 3.4).From the equation (3.9-3.14) calculated values are shown in table 3.3.

Table 3. 3 Elastic properties of E-glass/epoxy lamina by Halpin-Tsai

Elastic mechanical property	Units	Calculated result
Transversal Elastic modulus, E_2	GPa	10.2000
In plane shear modulus, G_{12}	GPa	3.8377
Out of plane shear modulus, G_{23}	GPa	3.9581
Out of plane Poisson's ratio , v_{23}	-	0.5026

The ROM are correctly predict for longitudinal properties, Young's modulus E_1 and major Poisson's ratio v_{12} with error of 1.66% and 3.04% respectively. But, it under estimates the transversal properties, Transversal Elastic modulus, E_2, Transversal Poisson's ratio, v_{23} , shear modulus, G_{12}, $G_{23}$with an error greater than 20% which is un-acceptable.. While, Halpin-Tsai correctly predict the transversal properties with an acceptable error as shown in table 3.4.The longitudinal elastic properties of ROM and transversal elastic properties of H-T are used for tensile and flexural testing of laminated composite for foot prosthetic application in power full software ANSYS 19.2.

Table 3. 4 The comparison of ROM and H-T with experimental result [35]

Elastic mechanical property	**Units**	**Rule of mixture(RoM)**	**Halpin-Tsai(H-T)**	**Experimental** [35]	**Error (%)**	
					RoM	**H-T**
Longitudinal Elastic modulus, E_1	GPa	**41.6800**	41.6800	41.0000	1.66	1.66
Transversal Elastic modulus, E_2	GPa	-	**10.2000**	10.4000	31.3	1.96
Major Poisson's ratio, v_{12}	-	**0.2885**	0.2885	0.28	3.04	3.04
Transversal Poisson's ratio, v_{23}	-	-	0.5026	0.5	-	0.52
In plane shear modulus, G_{12}	GPa	-	**3.8377**	4.3	-	10.8
Out of plane shear modulus, G_{23}	GPa	-	**3.3491**	3.5	-	3.02

3.1.3. The strength of unidirectional E-glass/epoxy composite lamina

The longitudinal tensile and compressive strength, transversal tensile and compressive strength as well as shear strength of lamina is mandatory and input FEA. This strength necessary to put the stress and strain limit when tensile and flexural testing of composite laminate is carried out in ASNSYS workbench by progressive damage analysis. Analytical models are developed to calculate fairly accurately strength lamina [43].

a) Longitudinal strength

Since, the ultimate tensile strain of the matrix is lower than that of the fiber, the composite will fail when its longitudinal strain reaches the ultimate tensile strain of the matrix.

$$\varepsilon_{fu} = \frac{\sigma_{1Tf}}{\mathrm{E_{1f}}} = 0.047 \; and \; \varepsilon_{mu} = \frac{\sigma_{mT}}{\mathrm{E_m}} = 0.024$$

$$\sigma_{fmu} = \mathrm{E_{1f}}\, x\, \varepsilon_{mu=1752Mpa}$$

- The longitudinal tensile strength from [36],

$$\sigma_{1t} = \mathrm{V_f}\sigma_{fmu} + \mathrm{V_m}\sigma_{mT=}1000MPa$$

- The longitudinal compressive strength is predicted by a simple equation given by [43]

$$\sigma_{1c} = G_{12}(1 + 4.76\, x)^{-0.69} \qquad (3.15)$$

Where,$x = \frac{G_{12}\alpha_\sigma}{\tau_{12}}$ = 3.268 and $\alpha_\sigma$is standard deviation of fiber misalignment, calculated from available experimental data [6] which is 0.06764 radian.

Using equation (3.15) above for $G_{12} = 3.8377Mpa$ [Table 3.3, Halphin -Tsai value]

$$\sigma_{1c} = 3.8377(1 + 4.76(3.268))^{-0.69} = 553.34MPa$$

b) Transversal strength

Transverse tensile failure of a unidirectional lamina occurs when a transverse crack propagates along the fiber direction, splitting the lamina.

$$\sigma_{2t} = \sigma_{mt}C_v\left(1 - V_f^{\frac{1}{3}}\right)\frac{\mathrm{E_2}}{\mathrm{E_m}} \qquad (3.16)$$

Where, $C_v = 1 - \sqrt{\frac{4V_v}{\pi(1-V_f)}}$ =1 for void free lamina and $\mathrm{E_2}$-transversal modulus of elasticity (Table 3.3 Halphin-Tsai result)

$$\sigma_{2t} = 80\left(1 - 0.55^{\frac{1}{3}}\right)\frac{10.2}{3.4} = 43.36MPa$$

- Transversal compressive strength,

An empirical formula for estimating the transverse compressive strength is given by [43].

$$\sigma_{2c} = \sigma_{mc} C_v \left[1 + \left(V_f - \sqrt{V_f}\right)\left(1 - \frac{\mathrm{E_m}}{\mathrm{E_{2f}}}\right)\right] \qquad (3.17)$$

$$\sigma_{2c} = 104\left[1 + \left(0.55 - \sqrt{0.55}\right)\left(1 - \frac{3.4}{73}\right)\right] = 85MPa$$

Since, empirical formulas are not accurate, experimental values are often required and obtained from [6].

c) In plane shear strength

The empirical formula that is useful to estimate shear strength is given by [43].

$$\tau_{12} = \tau_m C_v \left[1 + \left(V_f - \sqrt{V_f}\right)\left(1 - \frac{\mathrm{G_m}}{\mathrm{G_{12}}}\right)\right] \qquad (3.18)$$

$$\tau_{12} = 40\left[1 + \left(0.55 - \sqrt{0.55}\right)\left(1 - \frac{1.26}{30}\right)\right] = 33MPa$$

Table 3. 5 The comparison of analytical and experimental [35] value of lamina.

Strength of lamina	**Units**	**Analytical prediction**	**Experimental** [35]	**Error (%)**
Longitudinal tensile strength, σ_{1t}	MPa	1000	1140	12.3
Transversal tensile strength, σ_{2t}	MPa	43.36	39	11.2
Longitudinal compressive strength, σ_{1c}	MPa	553.34	620	10.8
Transversal compressive strength, σ_{2c}	MPa	85	128	33.6
In plane shear strength, τ_{12}	MPa	33	89	62.9
Out of plane shear strength, τ_{23}	MPa	-	49	-

The model over estimate transversal compressive and shear strength of lamina as shown in table 3.5 above. The reasons for the discrepancy between predictions and experimental data are many, and research is very active in this area. The experimental value is taken as input for numerical analysis.

3.2 Theoretical Laminate analysis (Macro-mechanics approach)

The laminate analysis has been carried out by macro-mechanical analysis. Tensile and bending loads are applied on the laminates for predicting tensile and flexural strength of composite for the un-symmetric angle ply laminates of the required stacking sequence. Based on the applied load the stress and strain in global and local axis for each ply is found. The classical lamination theory (CLT) develops the relation between those applied loads with stress and strain based on the assumption that each lamina is orthotropic and homogeneous. The knowledge of the stresses and strains in the laminate is used in Tsai-Wu failure theories to identify whether the plies at the given applied load are failed or not. The last ply failure load is taken as ultimate failure load and used to calculate the ultimate tensile and flexural stress (strength. The first MATLAB code has been written for analyzing stress and strain for each ply in laminate and the second MATLAB code written for predicting the failures in a plies.

3.2.1 Mechanical properties of lamina for theoretical laminate analysis

Mechanical properties of lamina is required for laminate analysis. The elastic and strength properties for limiting stress and strain from lamina analysis are used for this purpose and shown in Table 3.6 below.

Table 3. 6 Mechanical properties of E-glass/Epoxy lamina

Elastic mechanical property of lamina	**Units**	**E-Glass/Epoxy**
Longitudinal Elastic modulus, E_1	GPa	41.0000
Transversal Elastic modulus, E_2	GPa	10.4000
Major Poisson's ratio, v_{12}	-	0.28
Transversal Poisson's ratio, v_{23}	-	0.5
In plane shear modulus, G_{12}	GPa	4.3
Strength limit of lamina		
Longitudinal tensile strength, σ_{1t}	MPa	1140
Transversal tensile strength, σ_{2t}	MPa	39
Longitudinal compressive strength, σ_{1c}	MPa	620
Transversal compressive strength, σ_{2c}	MPa	128
In plane shear strength, τ_{12}	MPa	89

3.2.2. Theoretical mechanical property characterization of laminate

In order to verify FEA simulation the theoretical laminate analysis was being used. The stress analysis by CLT and failure analysis by Tsai-Wu failure theory is need to done to determine the tensile and flexural properties for each stacking sequence. The MATLAB code has been written for stress and failure analysis.

3.2.2.1 Stress and failure analysis

a) Stress and strain analysis

The classical lamination theory are used to develop the relationship between tensile and flexural loading with stress and strain based on the assumption that the each lamina is orthotropic. The subscripts 1, 2, and 3 (figure 3.3) represent principal fiber direction, in-plane direction perpendicular to the fibers, and out-of-plane direction perpendicular to the fibers. These numbers also represent the principal axes of the orthotropic material behavior. Since, the unidirectional falls under orthotropic material the lamina is thin (thickness=2.5mm) the plane stress formula is being used. Therefore, the principal stress in out of plane direction, σ_3,are taken as zero.

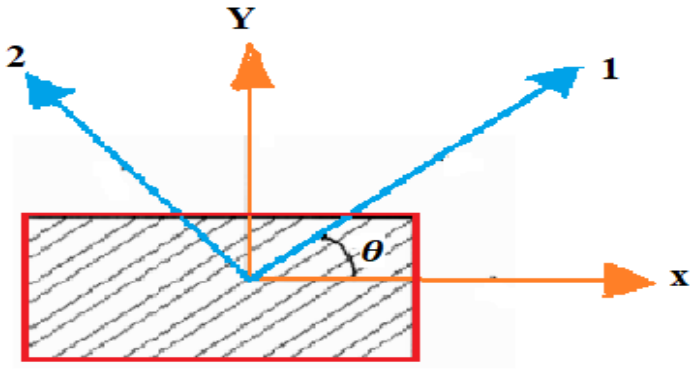

Figure 3. 3 Global and local axis of angle ply lamina

The reduced stiffness matrix [Q], which are related to the Compliance coefficients as Stiffness coefficients in terms of engineering or technical constants (E_1, E_2, ν_{12}, G_{12}) for each ply is shown in Equation (3.19) below.

$$[Q] = \begin{bmatrix} Q_{11} & Q_{12} & Q_{16} \\ Q_{12} & Q_{22} & Q_{26} \\ Q_{16} & Q_{26} & Q_{66} \end{bmatrix} - - - - - (3.19)$$

Where,$Q_{11} = \frac{E_1}{1-v_{21}v_{12}}$,$Q_{12} = \frac{v_{12}E_2}{1-v_{21}v_{12}}$ $Q_{22} = \frac{E_2}{1-v_{21}v_{12}}$ and $Q_{66} = G_{12}$

For angle ply laminate the transformed reduced stiffness matrix $[\bar{Q}]$ for each ply using the reduced matrix [Q] of Eq.3.19 is determined by Eq. (3.20) and (3.21) below.

$$\bar{Q}_{11} = Q_{11}c^4 + Q_{22}s^4 + 2(Q_{12} + 2Q_{66})c^2s^2$$
$$\bar{Q}_{12} = (Q_{11}c^4 + Q_{22}s^4 - 4Q_{66})c^2 + Q_{12}(c^4 + s^4)$$
$$\bar{Q}_{16} = (Q_{11} - Q_{12} - 2Q_{66})c^3s - (Q_{22} - Q_{12} - 2Q_{66})s^3c$$
$$\bar{Q}_{22} = Q_{11}s^4 + Q_{22}c^4 + 2(Q_{12} + 2Q_{66})c^2s^2 \quad ----------(3.20)$$
$$\bar{Q}_{26} = (Q_{11} - Q_{12} - 2Q_{66})s^3c - (Q_{22} - Q_{12} - 2Q_{66})c^3s$$
$$\bar{Q}_{66} = (Q_{11} + Q_{12} - 2Q_{12} - 2Q_{66})s^2c^2 + Q_{66}(c^4 + s^4)$$
$$where, c = cos\theta \; and \; s = sin\theta$$

Elements reduced transformed stiffness matrix, $[\bar{Q}]_\theta$ for each angle ply is only the function of reduced stiffness matrix, [Q].

$$[\bar{Q}]_\theta = \begin{bmatrix} \overline{Q_{11}} & \overline{Q_{12}} & \overline{Q_{16}} \\ \overline{Q_{12}} & \overline{Q_{22}} & \overline{Q_{26}} \\ \overline{Q_{16}} & \overline{Q_{26}} & \overline{Q_{66}} \end{bmatrix} ----- [3.21]$$

The top, middle and bottom location of each plies in the laminate is determined in the laminate.

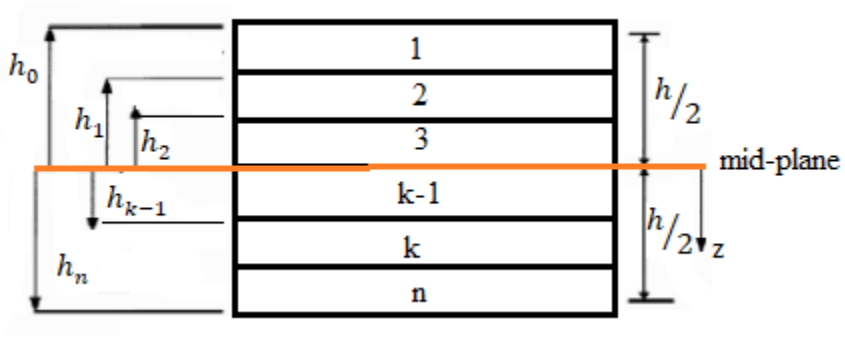

Figure 3. 4 Plies locations in the laminates

The three stiffness matrices [A], [B] and [D] are called the extensional, coupling, and bending stiffness matrices, respectively and determined by (Eq.3.22).

$$A_{ij} = \sum_{k=1}^{3} [\overline{Q_{ij}}]_k (h_k - h_{k-1}), B_{ij} = \frac{1}{2}\sum_{k=1}^{3} [\overline{Q_{ij}}]_k (h_k{}^2 - h_{k-1}{}^2), B_{ij} = \frac{1}{3}\sum_{k=1}^{3} [\overline{Q_{ij}}]_k (h_k{}^3 - h_{k-1}{}^3) ----(3.22)$$

The applied forces and bending moments can be written in terms of the mid-plane strains and curvatures. This mid plane strain and curvatures are determined by six simultaneous equation

given in Eq. (3.23).In tensile loading in x-direction,N_x, applied to the laminate of different stacking sequence for characterizing the tensile properties and for flexural testing only bending load , M_x,is applied for verification of finite element result.

$$\begin{bmatrix} N_x \\ N_y \\ N_{xy} \\ M_x \\ M_y \\ M_{xy} \end{bmatrix} = \begin{bmatrix} A_{11} & A_{12} & A_{16} & B_{11} & B_{12} & B_{16} \\ A_{12} & A_{22} & A_{26} & B_{12} & B_{22} & B_{26} \\ A_{16} & A_{26} & A_{66} & B_{16} & B_{26} & B_{66} \\ B_{11} & B_{12} & B_{16} & D_{11} & D_{12} & D_{16} \\ B_{12} & B_{22} & B_{26} & D_{12} & D_{22} & D_{26} \\ B_{16} & B_{26} & B_{66} & D_{16} & D_{26} & D_{66} \end{bmatrix} \begin{bmatrix} {\varepsilon_x}^0 \\ {\varepsilon_y}^0 \\ {\gamma_{xy}}^0 \\ k_x \\ k_y \\ k_{xy} \end{bmatrix} ------(3.23)$$

Finally using the mid-plane strain curvatures values, the global stress and strain in each plies are determined by the Eq.3.24 and 3.25.

$$\begin{Bmatrix} \varepsilon_x \\ \varepsilon_y \\ \gamma_{xy} \end{Bmatrix} = \begin{Bmatrix} {\varepsilon_x}^0 \\ {\varepsilon_y}^0 \\ {\gamma_{xy}}^0 \end{Bmatrix} + z \begin{Bmatrix} k_x \\ k_y \\ k_{xy} \end{Bmatrix} ------(3.24)$$

$$\begin{bmatrix} \sigma_x \\ \sigma_y \\ \tau_{xy} \end{bmatrix} = \begin{bmatrix} \overline{Q_{11}} & \overline{Q_{12}} & \overline{Q_{16}} \\ \overline{Q_{12}} & \overline{Q_{22}} & \overline{Q_{26}} \\ \overline{Q_{16}} & \overline{Q_{26}} & \overline{Q_{66}} \end{bmatrix} \begin{Bmatrix} \varepsilon_x \\ \varepsilon_y \\ \gamma_{xy} \end{Bmatrix} ------(3.25)$$

The local strain and stress are determined by Eq.3.26 based on transformation matrix below.

$$[T] = \begin{bmatrix} c^2 & s^2 & 2sc \\ s^2 & c^2 & -2sc \\ -sc & cs & c^2 - s^2 \end{bmatrix} and\ [R] = \begin{bmatrix} 1 & 0 & 0 \\ 0 & 1 & 0 \\ 0 & 0 & 2 \end{bmatrix}$$

$$\text{local strains,} \begin{bmatrix} \varepsilon_1 \\ \varepsilon_2 \\ \gamma_{12} \end{bmatrix} = [\mathrm{R}][\mathrm{T}][\mathrm{R}]^{-1} \begin{bmatrix} \varepsilon_x \\ \varepsilon_y \\ \gamma_{xy} \end{bmatrix} \text{ and local stresses,} \begin{bmatrix} \sigma_1 \\ \sigma_2 \\ \tau_{12} \end{bmatrix} = [\mathrm{T}]^{-1} \begin{bmatrix} \sigma_x \\ \sigma_y \\ \tau_{xy} \end{bmatrix} ----(3.26)$$

b) Failure analysis

There are different failure criteria's to predict failure of Fiber Reinforced Polymer (FRP) composite materials. Among them, Tsai-Wu failure criteria which was the traditional failure criteria developed in the 1960s and 70s is used for analysis of this composite. Because, it still continues to rule and applicable in the industries. Additionally, due to its interactive behaviors, it interacts with stress and strain of composite obtained by CLT to characterize the tensile and flexural properties of those composite.

This failure criterion is based on total strain energy failure theory where failure is assumed to occur if the following condition is satisfied in the lamina [44]: That means, when failure index (FI) is greater than one.

$$H_1\sigma_{11} + H_2\sigma_{22} + H_{11}{\sigma_{11}}^2 + H_{22}{\sigma_{22}}^2 + H_{66}{\tau_{12}}^2 + 2H_1\sigma_{11}\sigma_{22} \geq 1 - - - - - (3.27)$$

Where, $H_1 = \frac{1}{\sigma_{1t}} - \frac{1}{\sigma_{1C}};\ H_{11} = \frac{1}{\sigma_{1t}\,\sigma_{1C}}; H_2 = \frac{1}{\sigma_{2t}} - \frac{1}{\sigma_{2C}}; H_{22} = \frac{1}{\sigma_{2t}\,\sigma_{2C}}; H_{66} = \frac{1}{\tau_{12}}; H_{12} = -[H_{11}H_{22}]^{\frac{1}{2}}$

3.2.2.2 MATLAB Code for verification of finite element simulation

The MATLAB codes are developed using Classical Lamination Theory and Tsai-Wu failure criteria for determining local stress-strains and failures. The cases considered for theoretical solution in MATLAB to verify finite elements results are in table 3.7.

Table 3. 7 Stacking sequences for tensile and flexural property characterization

Cases	**Stacking sequences**	**Representation symbol**	**Description**
Case 1	[0 90 45 45 90 0]	**SS-1**	All layers are E-glass/Epoxy
Case 2	[45 0 90 90 0 45]	**SS-2**	
Case 3	[0 c 90 45 45 90 0c]	**SS-3**	Carbon/Epoxy layer's at end's
Case 4	[45 c 0 90 90 0 45c]	**SS-4**	

a) MATLAB code for Stress and Strain Analysis

The MATLAB code for stress and strain analysis are shown in appendix-2

b) MATLAB code for Tsai-Wu failure analysis

The code for failure analysis has been written in appendix-3. This code takes the mechanical properties of each lamina as input along with the ply orientation. Once the loading matrix (either tensile or flexural loading) is applied the program tells us if the laminate will fail or not. This code is written by [45] and modified for this analysis.

CHAPTER-FOUR

FINITE ELEMENT MODELING AND ANALYSIS

4.1 Analysis method description by ANSYS workbench

The tensile and flexural test simulation to characterize the mechanical properties of the composite under different stacking sequence was done underframe work of finite element package ANSYS 19.2 Workbench. Its powerful software used all over the world in industries and also in academic purposes. The analyses was done for composite material by modeling/importing the geometry, defining material property, applying (tensile or flexural) load step by step and boundary condition to investigate the failure of plies in laminate to determine ultimate failure load of composite and subsequently to generate the stress, strain and deflections.

The objective of this analysis and simulation is to characterize the tensile and flexural properties of different stacking sequence of E-glass/epoxy and Hybrid composite for prosthetic foot without experimental cost to select best stacking sequence that will be compared and verified by analytical classical lamination theory. Within ANSYS work bench there are shell and solid elements that can be used to model composite lay ups. There are a variety of specific elements associated with each element type. Specific element selection depends upon application and the type of results that must be calculated [46].

4.1.1 Geometry and Dimension of Specimen

As per American Society for Testing & Materials (ASTM) test method D3039-00 [34] for determination of tensile properties of isotropic and orthotropic fiber reinforced composite materials [47] was selected for tensile tests. As it is shown in figure 4.1, 20 mm wide, 220 mm long and 2.5 mm thick by 100 mm gage length was used for tensile simulation. According to ASTM D790 [48] the specimen dimension for composite for flexural simulation is prepared as shown in figure 4.2 below.

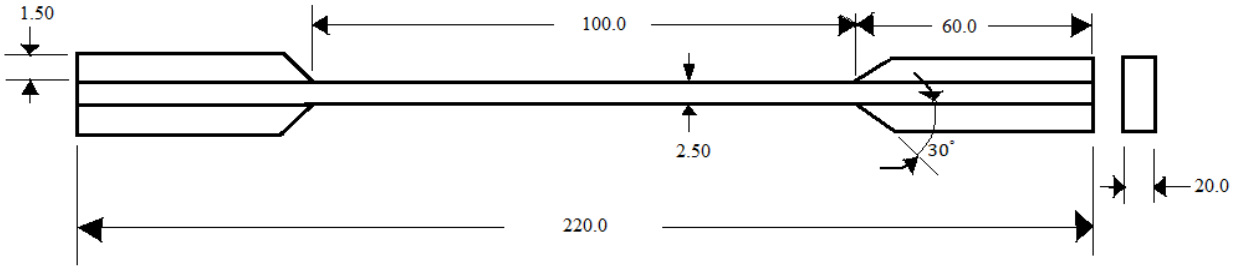

Figure 4. 1Tensile test simulation geometry

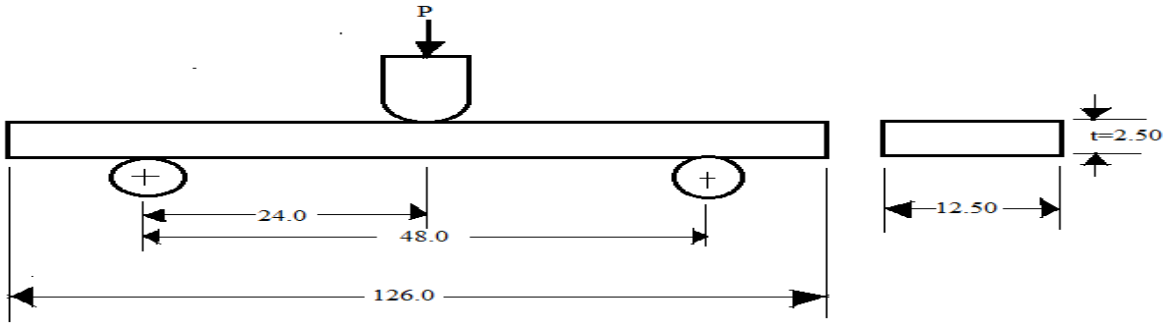

Figure 4. 2 Flexural test simulation geometry

4.1.2 Material Constants input for ANSYS

The orthotropic elastic properties of lamina are needed for laminate analysis through ANSYS workbench. This properties are used for both analytical and numerical simulation shown in table 3.6. Since, this property is not available in ANSYS Engineering data library, new material property 'UD E-GLASS/EPOXY' is created as shown in figure 4.3 below. The material properties of UD-Carbon/epoxy to see effect of addition of a layer of carbon on laminate is already available in ANSYS Engineering data library.

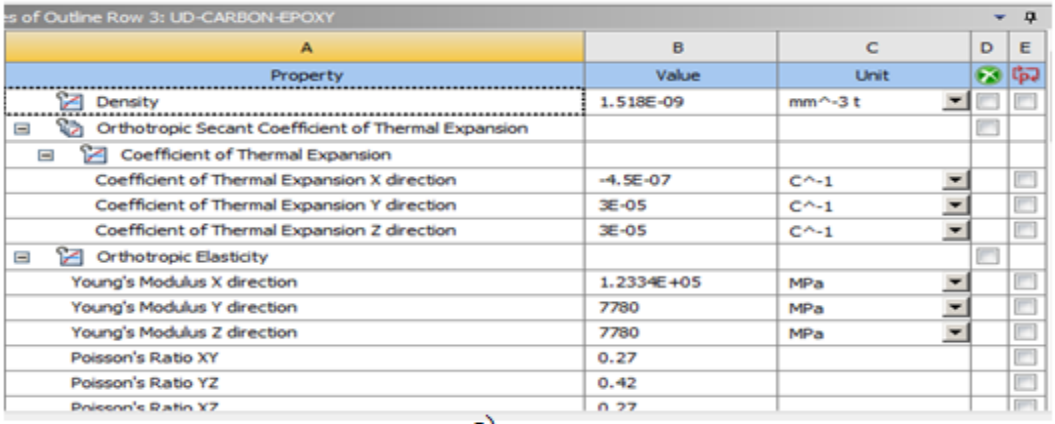

Property	Value	Unit
Density	1.518E-09	mm^-3 t
Orthotropic Secant Coefficient of Thermal Expansion		
Coefficient of Thermal Expansion		
Coefficient of Thermal Expansion X direction	-4.5E-07	C^-1
Coefficient of Thermal Expansion Y direction	3E-05	C^-1
Coefficient of Thermal Expansion Z direction	3E-05	C^-1
Orthotropic Elasticity		
Young's Modulus X direction	1.2334E+05	MPa
Young's Modulus Y direction	7780	MPa
Young's Modulus Z direction	7780	MPa
Poisson's Ratio XY	0.27	
Poisson's Ratio YZ	0.42	

a)

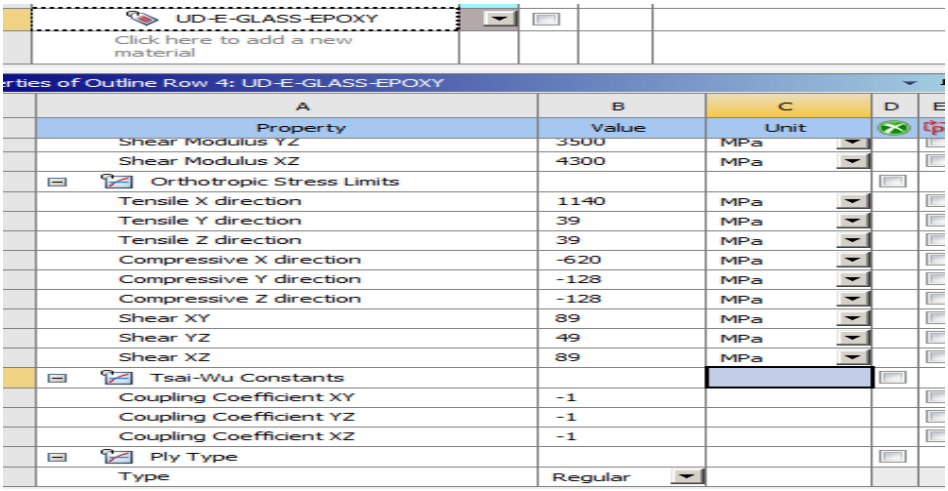

Property	Value	Unit
Shear Modulus YZ	3500	MPa
Shear Modulus XZ	4300	MPa
Orthotropic Stress Limits		
Tensile X direction	1140	MPa
Tensile Y direction	39	MPa
Tensile Z direction	39	MPa
Compressive X direction	-620	MPa
Compressive Y direction	-128	MPa
Compressive Z direction	-128	MPa
Shear XY	89	MPa
Shear YZ	49	MPa
Shear XZ	89	MPa
Tsai-Wu Constants		
Coupling Coefficient XY	-1	
Coupling Coefficient YZ	-1	
Coupling Coefficient XZ	-1	
Ply Type		
Type	Regular	

b)

Figure 4. 3 Orthotropic property a) Carbon and b) E-glass -Epoxy in Ansys Engineering Data

4.1.3 Stacking Squences for testing simulation

Total of four stacking squences are considered for charactering the mechanical properties under tensile and flexural testing as shown in chapter-3 of table 3.7.The first two cases are E-glass/Epoxy composite and the remaining are hydrid composite (carbon-E-glass/epoxy) in order to analyse the effect of addition carbon layer on bottom and top of laminate for prosthetic foot in terms of its mechanical property.

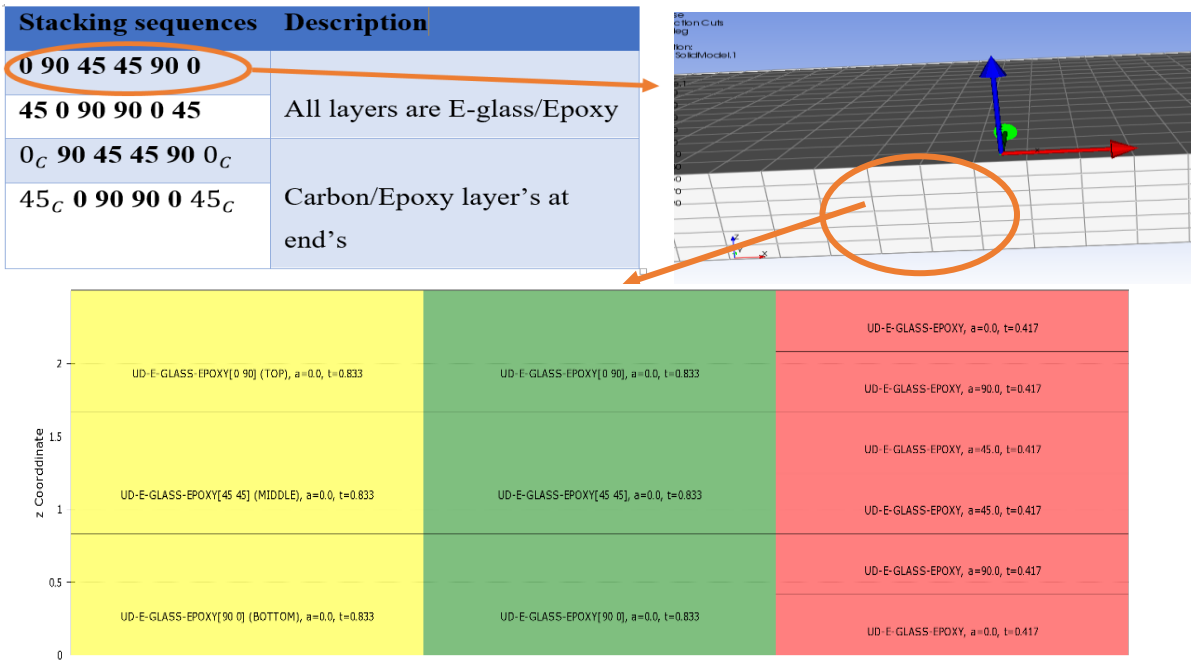

Figure 4. 4 Composite lay-up in ANSYS workbench for testing simulation

4.2 Tensile test simulation using ANSYS 19.2 workbench

Tensile testing is a fundamental material science testing in which the results from the test are commonly used for selecting the material for specific application. Under this topic composite material for foot prosthetic application is simulated in ANSYS Workbench for selecting the stacking sequence that yields high tensile strength without experimental cost. This starts from modeling specimen geometry to stress and failure analysis of composite layers in ACP tools. The general process tensile simulation in work bench are shown in figure 4.5.

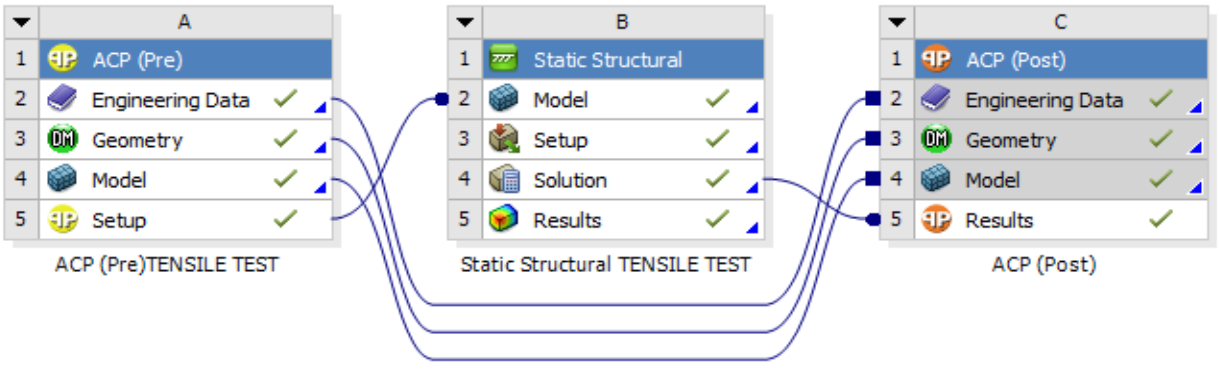

Figure 4. 5 The process of tensile test simulation

4.2.1 Creating the geometry, defining the model and mesh in ACP (Pre)

After new material property is created in engineering data as shown in figure 4.3, geometry of tensile specimen is need to be modeled. This is created in SOLIDWORK software and saved as .STEP file to be imported to ANSYS ACP (pre) geometry. The surface is created from imported 3D geometry by using concept (figure 4.6 (a)). In a model, the geometry is discretized into required number of element. The more fine the mesh more accurate result but it needs more computation time. A convergence study was performed to determine the appropriate finite element mesh to be used in static structural analysis of testing specimen. Meshes were developed, with decreasing of element size and the equivalent stress for these testing samples models. The total deformation stabiles at optimizing element size equal to 1mm with total number of 4323 nodes and 4084 elements for optimum mesh as shown in figure 4.6 b).The mesh convergence analysis graph is shown in appendix 6.

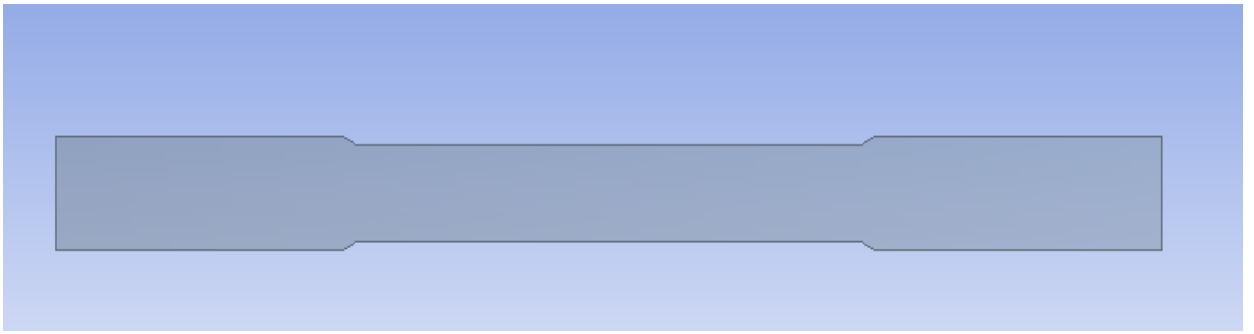

a)

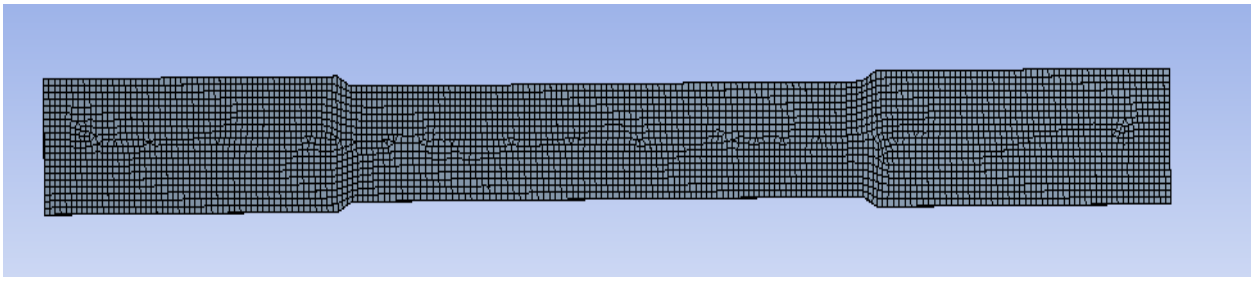

b)

Figure 4. 6 Tensile simulation specimen a) geometry b) Element mesh

4.2.2 Defining the stacking sequence, applying load and boundary conditions

According to [49] the stacking sequence of lamina in the laminate are defined by using ‘Rosset’ and ‘Orientated Selection Set’. The Rosset is used define reference coordinate system and oriented

selected set is used to set lay-up direction in ACP (pre)-setup. The stacking sequence for each testing cases are defined in this set-up as shown in figure 4.7.

The composite data (solid or shell data) in ACP (pre)-setup is dragged into the model of static structural for the application of load and boundary condition. The fixed BC is applied at one end of the specimen and displacement BC that allows the specimen to deform in global x-direction only is applied on the face of composite specimen. The load is applied at the other end of the specimen with type force in global x direction at different magnitudes until last ply failure load, which is ultimate load capacity of the composite as shown in figure 4.8.

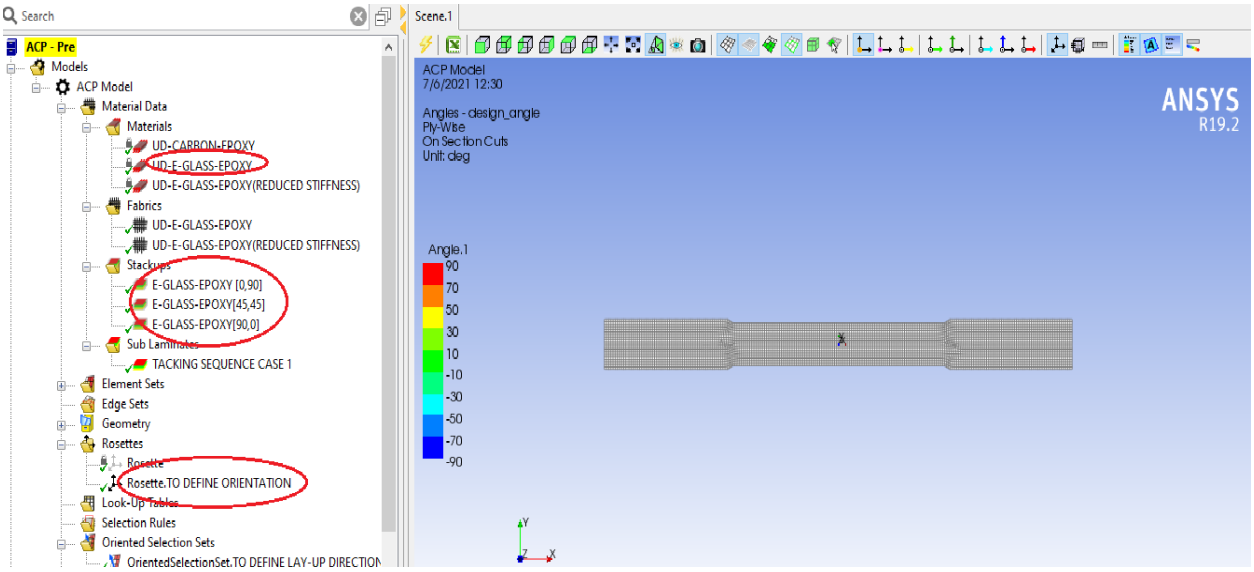

Figure 4. 7 Defining lay-up sequence in ACP (pre)-setup

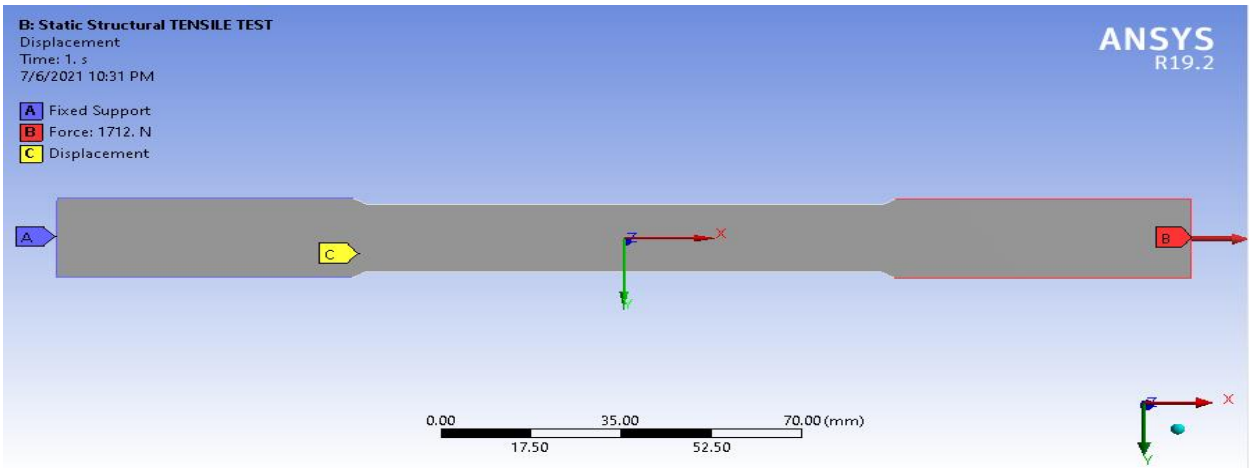

Figure 4. 8 Applied load and boundary condition in tensile test simulation

4.2.3 Defining the failure criteria and apply progressive failure analysis

In ANSYS Workbench different failure is provided in composite failure tool. The Tsai-Wu failure criteria is 'on' in order to check plies failure at each load increment as shown in figure 4.9. According to this criteria, there is failure in ply or entire laminate, if the 'inverse reverse factor' or failure index (FI) is greater than or equal to one. The failure of composite structures is not a sudden occurrence, but with a gradual damage process due to the mechanical behavior of composite structures [50].Therefore, the progressive failure analysis (PFA) adapted to analyze the mechanical behavior of composite specimens for the study of its progressive failures and strength. The whole process of the progressive damage method consists of stress analysis, failure analysis and material property degradation [51]. This procedure is interactive cycle of local failure, stress extraction, and application of failure criteria, material property degradation, and final failure determination.

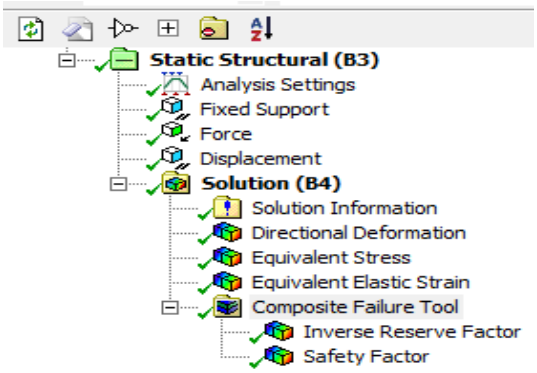

Details of "Composite Failure Tool"

Defined By	Direct Input
Reinforced Ply Criteria	
Maximum Strain	Off
Maximum Stress	Off
Tsai-Wu	On
Tsai-Hill	Off
Hoffman	Off
Hashin	Off
Puck	Off
LaRC	Off
Cuntze	Off

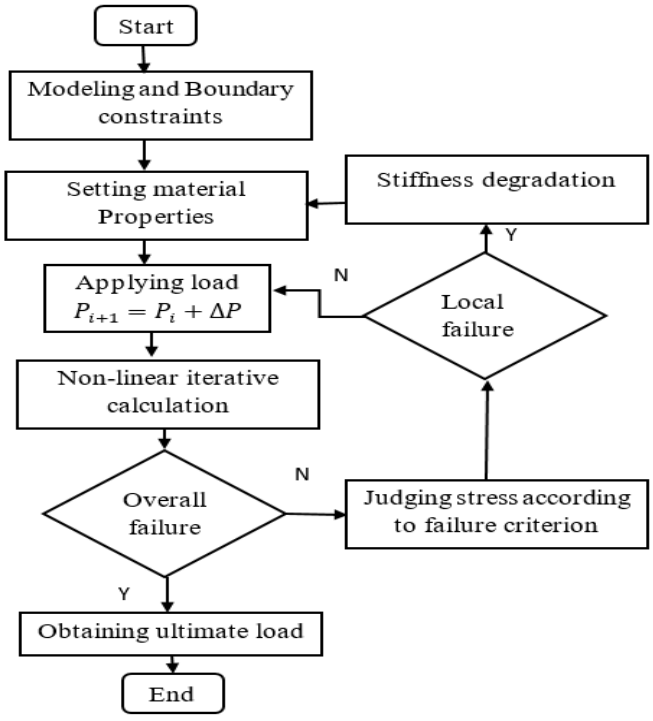

a) b)

Figure 4. 9 a) Failure criteria and b) Progressive failure analysis procedure [50].

Once the model of the finite element occurred local failure when calculating, the stiffness of the element in the failure area would be degraded according to the established material property degradation modes, and then the model would be rebalanced under the same load conditions.

Otherwise, the method would assign a load increment to continue the calculation. This calculation procedure is repeated until the ultimate failure of the structure occurs, and then the ultimate load of the structure is obtained [50] and [52]. The flowchart of the progressive failure method is exhibited in Figure 4.9 b).

The stiffness of failed plies are degrade to reduce the stress in the failure area. According [37] the stiffness of failed ply is degraded to non-zero small value (25%) of the original young's poisons ratio and shear modulus, r_1=0.99, $r_2 = r_{12}$= 0.00000001 as shown Eq.4.1 below.

$$E_1{}^f = r_1 E_1$$
$$E_2{}^f = r_2 E_2 \quad ---------(4.1)$$
$$G_{12}{}^f = r_{12} G_{12}$$
$$v_{12}{}^f = r_1 v_{12}$$

4.2.4 Solving and generating the results in static structural or ACP (Post)

The stress, strain, deformation and FI in each ply or the entire laminate is solved in static structural according to progressive failure analysis at each load step. The detail results can be seen in ACP (Post) after dragging the data's and solutions from ACP (Pre) and static structural. The simulation was set run for the four lay-up configurations shown in figure 4.4 above that are proposed for the prosthetic foot. In this simulation, stress, strain, deformation at each loading step until ultimate failure load is recorded in tabular form to draw stress vs strain and load vs deformation graph of all stacking sequences.

In this simulation, the six layer composite lamina with the four stacking sequence was created composite specimen for tensile testing. The composite laminate is divided into three partition for analysis purpose. The strength ratio (SR) and failure index (FI) used to identify ply failure. The SR is the ratio of ultimate stress (load) to applied stress (load) and FI is vice versa. The FI$\geq$ 1 or SR$\leq$ 1 shows a failure. The ply failure load is obtained by multiplying applied load to SR.

4.3 Three point bending test simulation using ANSYS 19.2 workbench

Three point bending testing is important to understand the flexural Stress, and flexural Strain of the composite materials. The flexural property results from the test are commonly used for selecting the material for specific application. Under this topic, the flexural property of composite

laminate obtained by simulating the composite in ANSYS Workbench for different stacking sequences. This starts from modeling of specimen geometry surface, pusher and supporting member in SOLIDWORK modeling software. The model is imported to ANSYS ACP for stress and failure analysis of composite layers. The general process of the simulation in Workbench discussed below.

4.3.1 Defining material property and modeling geometry of test sample

The ACP Pre is dragged and the material property of E-glass-reinforced epoxy composite is added for sample to be tested and rigid structural steel for pusher and fixed support in engineering data (shown in figure 4.10.a). The testing sample, pusher and supports are assembled in SOLIDWORK and saved as (.STEP) file for importing into ANSYS geometry. Then, the geometry is opened to import the saved file and suppress the solid parts to be convert to the surface in material modular.

4.3.2. Assigning the material and meshing surfaces

A rigid structural steel is assigned for pusher and support member while E-glass epoxy lamina is for composite sample surface. The size meshing is necessary for dividing the sample in to required number of elements for applying convergence analysis and the total number of element for the sample is 4513 (figure 4.10.b) and other the three member is 3281.

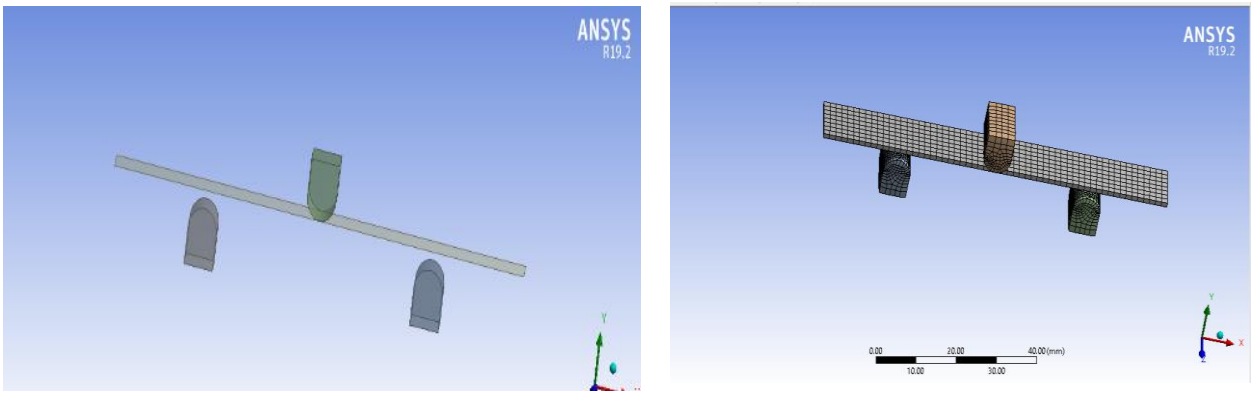

a) b)

Figure 4. 10 Flexural test simulation a) imported geometry b) Meshed model

4.3.3. Defining the Stacking sequence of laminate for testing

The stack up are created according to the required stacking sequence with a thickness of each lamina 0.41666mm and the testing sample is selected by setting the element.(i.e. Composite element).The Rosset and element orientation set is created to define reference coordinate and laying up direction respectively (Figure 4.11.a). The model (figure 4.11.b) is grouped in to TOP, MIDDLE AND BOTTOM partition and for structural analysis the solid element is created.

4.3.4. Combining the composite specimen and supporting members

The composite specimen in ACP (Pre) and the supporting members (pusher and support) in mechanical models are combined in static structural (shown in figure 4.12). Drag the setup of ACP (pre) and mechanical model of pusher and support member to the static structural model then the model of static structure is opened to select the contact and target body.

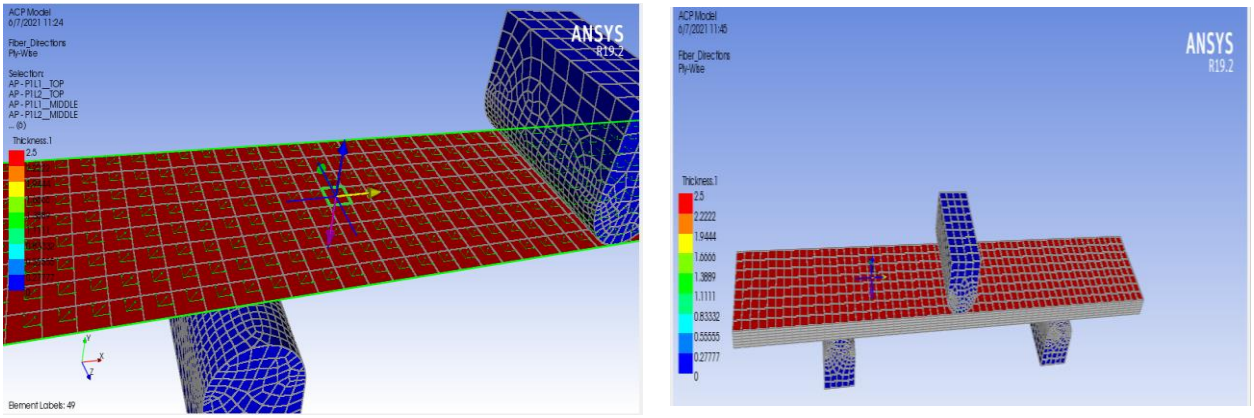

a) b)

Figure 4. 11 a). Reference and orientation of fibers b). Modeled composite beam

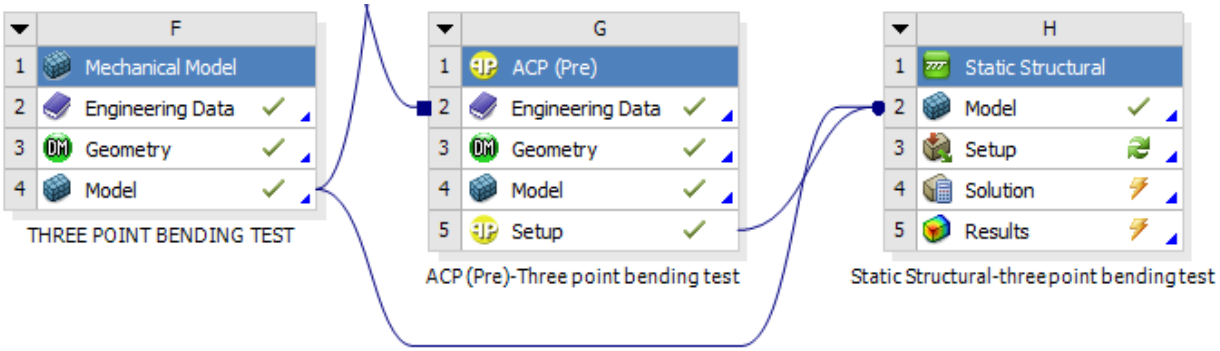

Figure 4. 12 Combining of specimen and supporting members.

4.3.5 Applying a load and setting boundary condition

The top faces of the two support member is fixed and the sample is allowed to displace only in y-direction. Then the bottom face of the pusher is allowed to displace by -3mm and back to its original position (shown in figure 4.13).

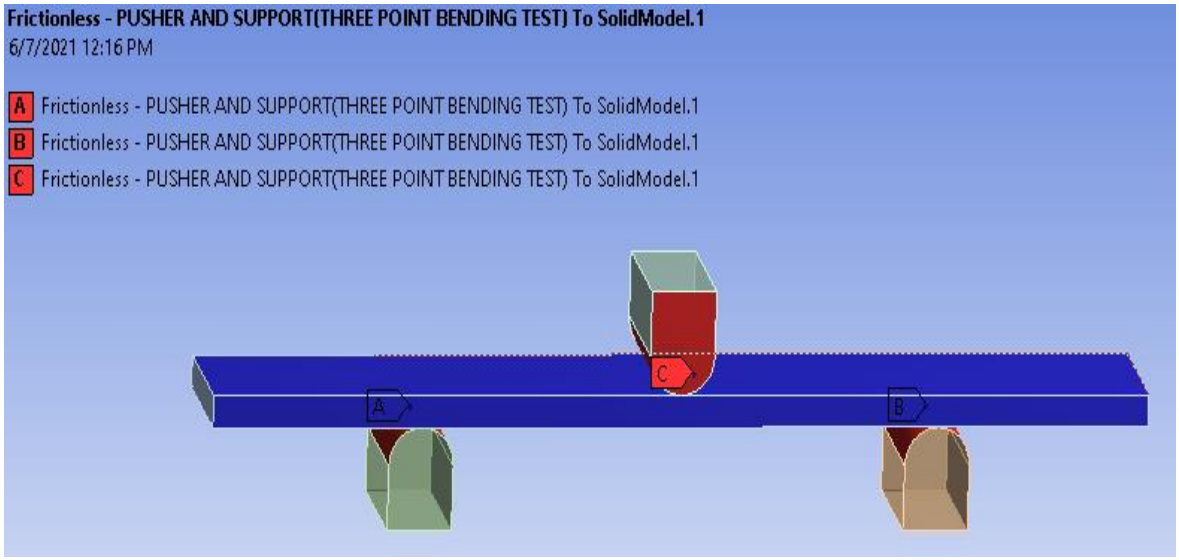

Figure 4. 13 Boundary conditions for flexural simulation

4.3.6. Applying Tsai-Wu criteria and stiffness degradation.

According to (Hahn HT, Tsai SW. 1974) delamination and matrix cracking in longitudinal (fiber direction) is due to damage induced by low velocity impact such as bending test. This damage reduce the structural strength and stiffness. The transverse young's modulus E22 and in plane shear modulus G12 of damaged plies is estimated to be degraded by the 10%of original value. The longitudinal elastic modulus E11 and in plane Poisson's ratio v12 remain unchanged. Considerably, the value of v21 is also reduced significantly near to zero.

4.4 Verification based on comparison with analytical solution

To check the validity of the FEA results for tensile and flexural simulation of composite for foot prosthetic it was necessary to compare it with an a theoretical laminate analysis as discussed in section 3.2. The MATLAB code constructed from this theory is used to construct a MATLAB to verify the FEA results.

4.5 FEA of Prosthetic foot Using ANSYS 19.2 workbench

In this simulation the performance of prosthetic foot made from the two material are analyzed. The model of prosthetic foot was taken from prosthetic and orthotic center in Ethiopia and this prosthetics are made from homo-polymer poly-propylene (HPP) material sheet (2000x2000x5mm) (SIMONA product) imported from Germany. The new composite material (third stacking configuration- SS-3) that yields high tensile and flexural strength is selected among the four stacking configurations for single blade prosthetic foot. The prosthetic foot modeled from this two material (i.e. HPP and new composite) are simulated here under the following design specification.

4.5.1 Design specification of prosthetic foot

Average weight of adult man (amputees) =62.0 kg [53]. Prosthetic foot can stand with 29% additional weight of user's. If the user's body weight is 62 kg, then the maximum load that can withstand the prosthetic foot is 62kg + 0.29x62kg=80kg. So that the static loading on ANSYS Software uses a force F =9.81x80= 784.8N, where g=9.81m/sec. Thickness of the blade for prosthetic foot made from HPP and composite are 5mm and 2.5mm respectively with in 32mm thick rigid keel. Three loading cases in figure 4.14 are applied with three phases in a walking cycle [54]:

- Initial foot contact (heel strike)-25% weight is supported=196.2N
- **Mid stance (limb support entire body)-support entire body=784.8N** and
- Propulsion (toe off), to enable the body weight to propel forwards,40% of weight is expected to be supported =313.92N

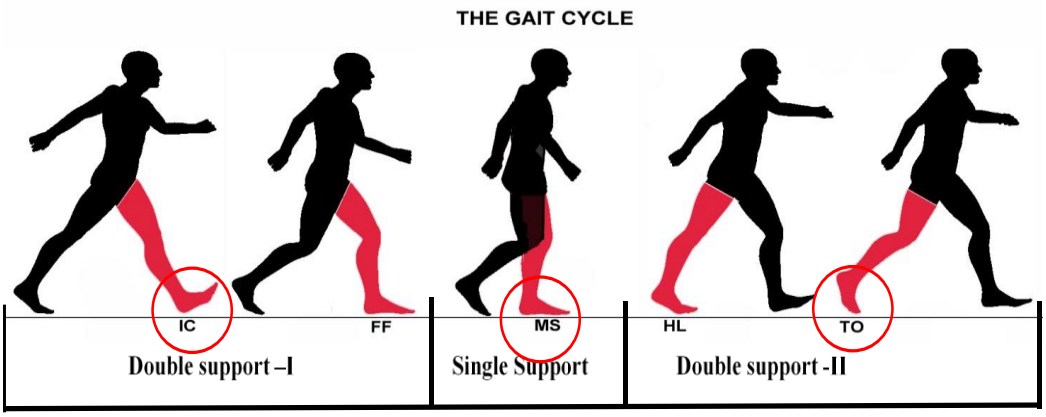

Figure 4. 14 The gait cycle (Foot-bionics, 2020)

Steps used in the solution procedure using ANSYS are the following:

- The geometry of the prosthetic foot to be analyzed is imported in an STEP format.
- The materials properties of the prosthetic foot are specified.
- Meshing of the three-dimensional prosthetic foot model is performed.
- The boundary conditions and external loads are applied.
- The solution is generated based on the input parameters.
- Stiffness, weight and cost analysis and calculation prosthetic foot models.

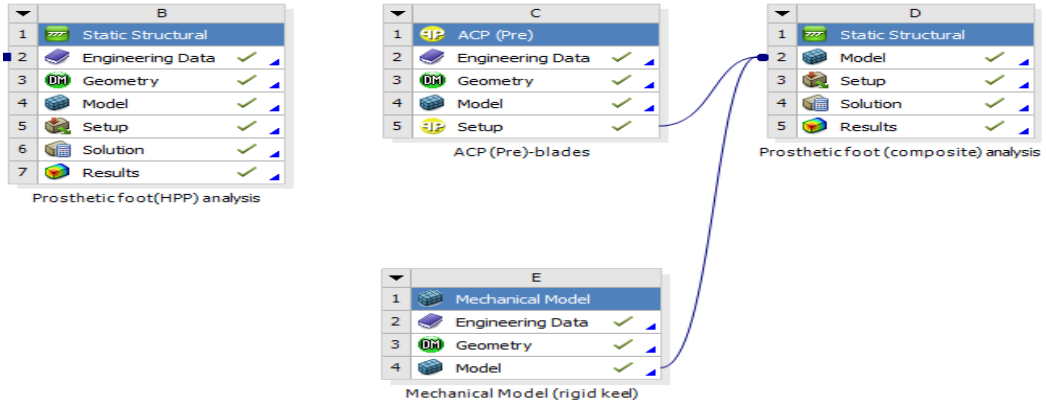

Figure 4. 15 ANSYS solution procedure for prosthetic foot analysis

4.5.2 Dimension and geometric modeling of prosthetic foot

The dimension of prosthetic foot for the adult man are obtained by direct measuring of prosthetic foot made in POC using caliper as shown in figure 4.16. The rigid keel and each blades made in the injection molding from HPP and assembled together and covered by rubber shell by high pressure in molding.

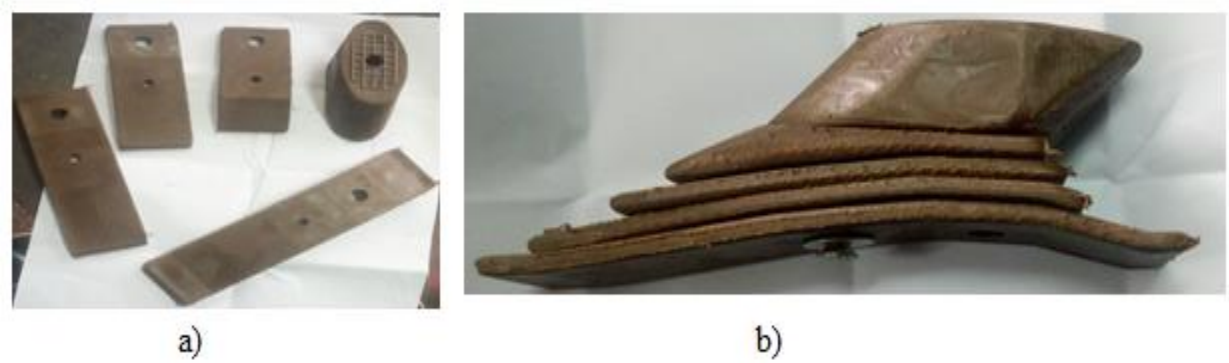

Figure 4. 16 a) blades and keel, b) Assembly of prosthetic foot (*Source: POC Ethiopia*)

The prosthetic has a total height of 57mm and length of 173mm as shown in appendix-4 and 4.17. The length of foot with the shell is 27cm. The detail drawing of single blade composite prosthetic foot and multi-blade HPP prosthetic foots are shown in figure 4.17.

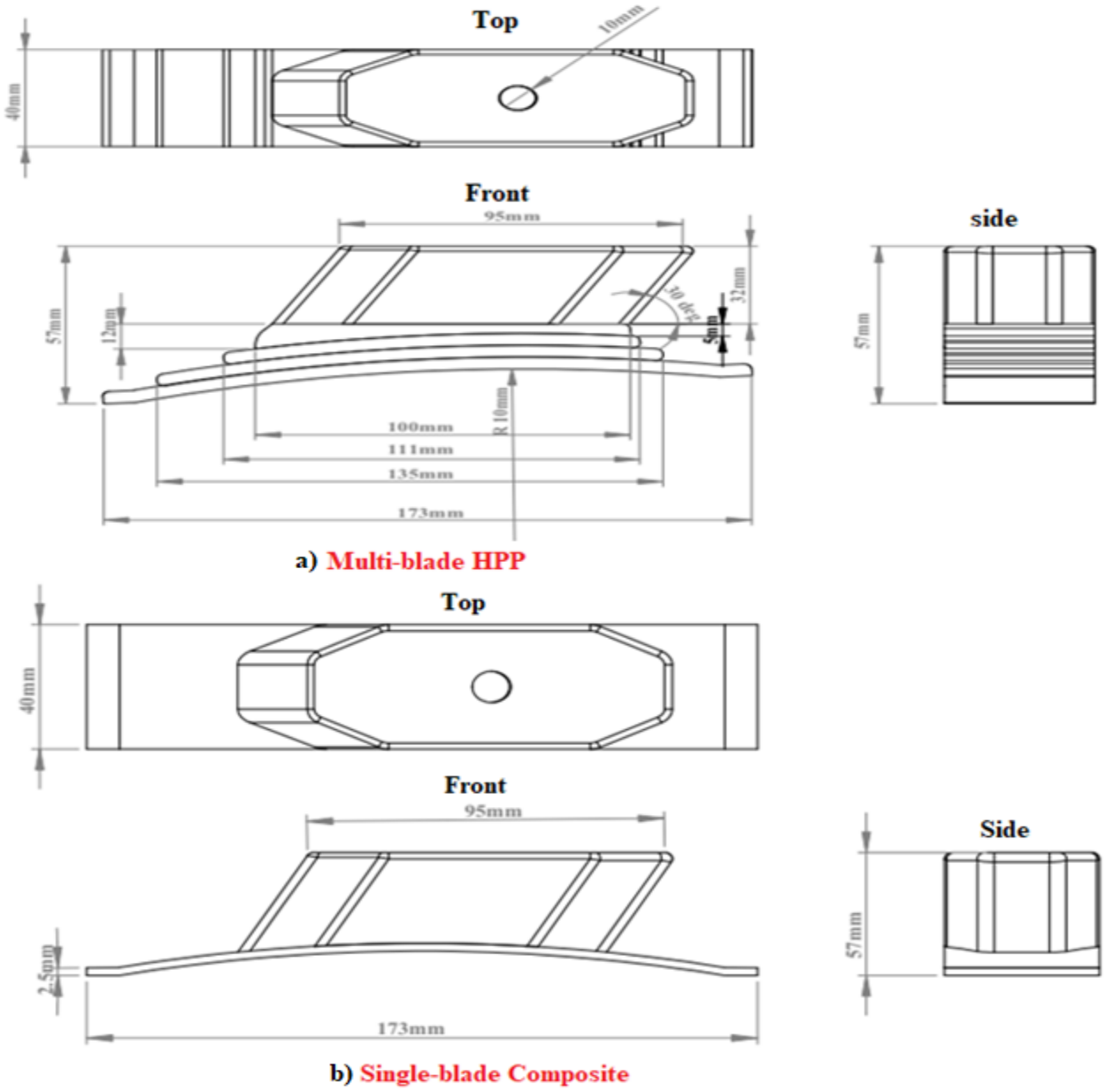

Figure 4. 17 The three basic views and dimension of prosthetic foot: a) HPP, b) Composite

Even though ANSYS has a capability of modeling objects; due to the complexity of the shape of the prosthetic foot blade and rigid keel, Solid Works have been used for modeling the three-dimensional model of the blade and keel. The blades and keels are assembled together as shown

in figure 4.18-4.19 and saved as STEP file to be imported to ANSYS 19.2 workbench. In the composite made prosthetic foot, the surface is generated from the imported geometry for blades by suppressing rigid keel and laminates are build up on this surface in ACP (pre). Solid model data of laminate blades is transferred to static structural for analysis.

Figure 4. 18 A 3D assembly model of prosthetic foot in SOLIDWORK: a) HPP, b) Composite

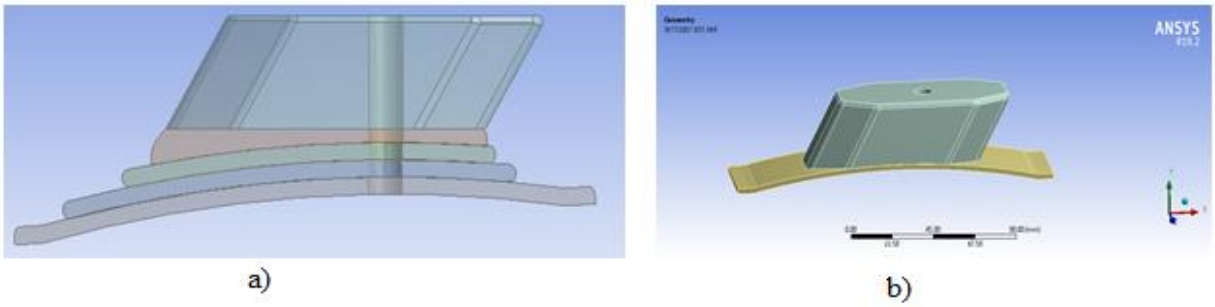

Figure 4. 19 The imported geometry in ANSYS workbench: a) HPP, b) Composite

4.5.3 Defining Material properties

Two materials are selected for prosthetic foot. One is HPP available in POC; its properties obtained from the SIMONA product data sheet as shown in figure 4.20 a) and the second material is a hybrid Glass-Carbon/epoxy composite (SS-3) characterized in this research. This properties used for finite element analyses and given in table 4.1 and figure 4.3. The Glass and carbon fibers are available in either woven and unwoven (unidirectional) as shown in figure 4.21 b) and c) below.

Figure 4. 20 Material used a) HPP b) E-glass and c) Carbon fiber [55]

Table 4. 1 Mechanical properties of HPP [56]

Properties	**Units**	**Value**
Density	g/cm^3	0.905
Tensile strength	MPa	37.3
Yield strength	MPa	27.2
Tensile modulus	GPa	1.4
Flexural strength	MPa	48.3
Flexural modulus	GPa	1.344
Impact strength (Izod)	J/m	48.06
Hardness	Rockwell	70
Poisson's ratio		0.36

The orthotropic property of E-glass and Carbon -Epoxy shown in figure 4.3; tensile and flexural properties of the hybrid composite are shown in table 5.5 and 5.7 respectively for SS-3. In ANSYS workbench of static structural analysis the first step is to define material properties in engineering data source. The material property of HPP added to engineering data library as shown in figure 4.21.

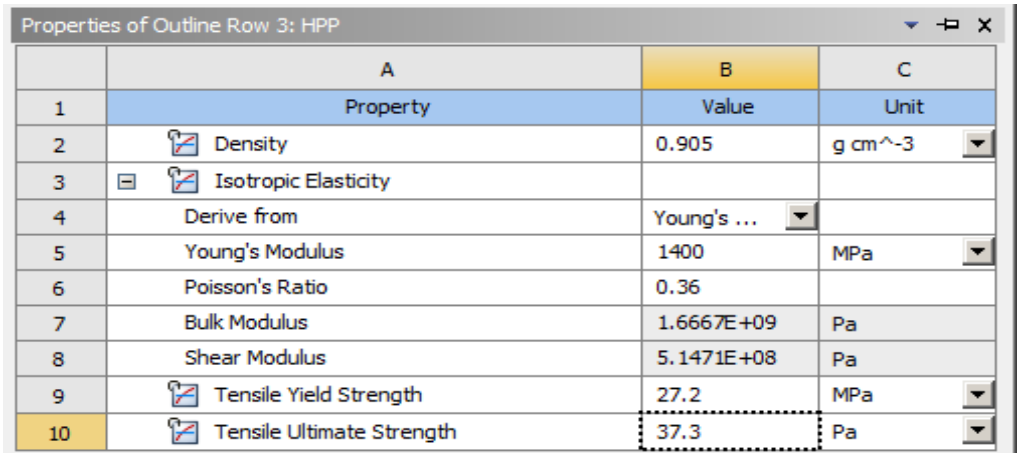

Figure 4. 21 Workbench material properties of HPP

4.5.4 Meshing of the 3D-prosthetic foot model

The mesh with the default settings is not adequate to get the accurate results for this analysis. In order to ensure accuracy of result, fine meshing and body sizing for required parts of the prosthetic

foot model is done with "Sizing" option in menu. The element size for the rigid keel and all blades is 1mm and 0.5mm respectively and the mesh is converged. Then the meshed model of the prosthetic foot shown in figure 4.22 has 210,935 nodes and 134,244 number of elements.

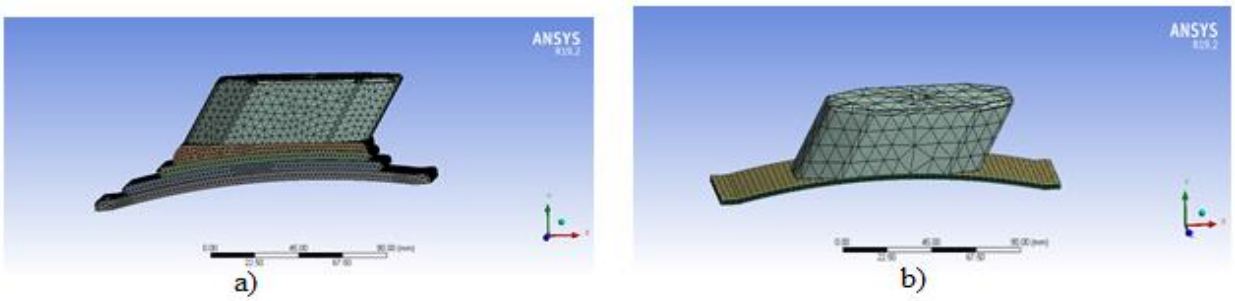

Figure 4. 22 Meshed model of prosthetic foot by body sizing: a) HPP, b) Composite

4.5.5 Boundary conditions and applied loads

The blades got a load from the ground and supported by rigid keels. The fixed support is applied on top faces of rigid keels. The applied loads due to the weight of the amputees depends three basic gait cycle. During the mid-stance, the entire weight (load) of amputees are supported by a single foot and this vertical loads distributed on two side of the blades. On the other hand, loads are distributed only on one side during heel strike and toe off. As the entire weight is supported during the mid-stance the analysis is done at this gait by fixing end side of the blade as shown in figure 4.23 below.

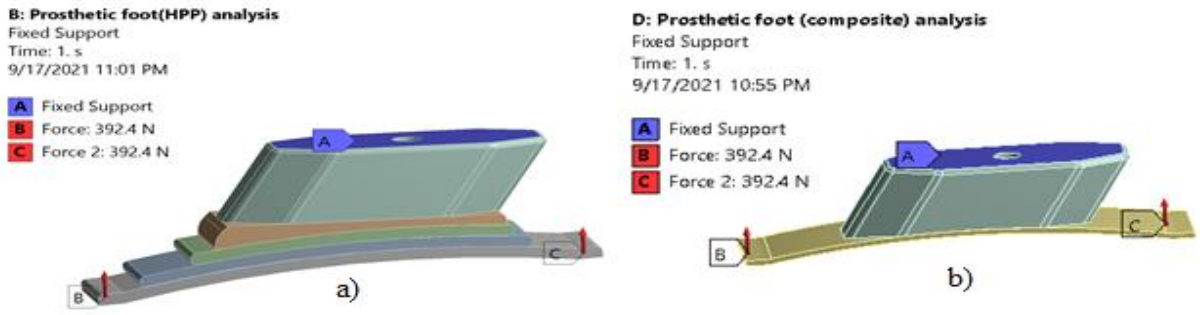

Figure 4. 23 Boundary and loading condition of prosthetic foot: a) HPP, b) Composite

After defining the boundary condition the solution in generated based on the input parameters. The results of this analysis shown and discussed in section 5.4 of fifth chapter.

4.5.6 Stiffness, weight, and cost analysis of prosthetic foot

The stiffness and weight of prostheses foot is another important parameter need to considered in design and modeling of foot. The selection of the best material for prosthetic product allows the minimization of overall manufacturing costs in addition to reducing the weight and providing comfort for amputees.

I. Stiffness calculations

The stiffness is proportional to the force and inverse with the deflection. The stiffness of the prosthetic foot model under loading is calculated according to the equation [57]

$$\text{Stiffness, k} = {}^{\text{F}}/_{\Delta \text{l}} - - - - - - - - 4.1$$

Where, F-applied load and Δl-is deflection (maximum deformation)

The same load is applied for both prosthetic foot which is 392.4N on end side of the blade figure 4.24.The formation due is obtained from the numerical analysis as shown in figure 5.14-5.15.

- Stiffness of current prosthetic foot made from HPP, $\frac{392.4\text{N}}{4.1194\text{mm}} = 95.26\text{N/m}$
- Stiffness of prosthetic foot made from composite, $\frac{392.4\text{N}}{3.3441\text{mm}} = 117.34\text{N/m}$

II. Weight Calculations

From the mass, density and volume relation the weight of the prosthetic foot can be calculated [58] as:

$$\text{Density, } \rho = \frac{\text{mass, m}}{\text{volume, V}} - - - - - - - - 4.2$$

$$\text{Weigth} = \text{mxg} \qquad \text{where m} = \rho\text{xV}$$

Therefore,

$$\text{Weigth} = \rho\text{xVxg} - - - - - - - - 4.3$$

a) Weight of current prosthetic foot made from HPP

Density of HPP = 0.905 gm/cm3 =905kg/m3and

Take acceleration due to gravity (g) = 9.81 m/s2

Now weight of the rigid keel = ρ× $V1 \times g$

The volume of the rigid keel,

$$\text{V1} = \text{L1} \times \text{t} \times \text{w} = 95\text{mm} \times 32\text{mm} \times 40\text{mm} = 121.6\text{x}10^{-6}\text{m}^3$$

where: L = length, t = thickness and w = width

The weight of rigid keel,

$$W_k = \frac{905kg}{m3} x121.6x10^{-6}m^3 \frac{x9.81m}{s2} = 1.08N$$

The weight of blades:

The thickness and width of each blades is 5mm and 40mm respectively.

The length of blades, first blade , l_1,second blade, l_2, third blade, $l_3$and fourth blade l_4 is 100mm,111mm,135mm and 173mm respectively.

- Volume of first blade $V_{b1} = l_1 xtxw = 20x10^{-6}m^3$
- Volume of second blade $V_{b2} = l_2 xtxw = 22.2x10^{-6}m^3$
- Volume of third blade $V_{b3} = l_3 xtxw = 27x10^{-6}m^3$
- Volume of fourth blade $V_{b4} = l_4 xtxw = 34.6x10^{-6}m^3$

Using equation 4.3 the weight of HPP blades are:

- Weight of first blade $W_{b1} = 0.178N$
- Weight of second blade $W_{b2} = 0.197N$
- Weight of third blade $W_{b3} = 0.240N$
- Weight of fourth blade $W_{b4} = 0.307N$

Therefore, the total weight, $W_{T,Hpp}$ of the current prosthetic foot using HPP becomes:

$$W_{T,HPP} = W_k + W_{b1} + W_{b2} + W_{b3} + W_{b4}$$

$$W_{T,HPP} = 1.08N + 0.178N + 0.197N + 0.240N + 0.307N$$

$$\mathbf{W_{T,HPP} = 2.002N}$$

b) Weight of prosthetic foot made from composite

Density of E-glass/epoxy and Carbon/epoxy lamina= 1970 kg/m3, 1518kg/m3 respectively. The length, L, of composite blade is 173mm with width, w, of 40mm. The total thickness of the laminate is 2.5mm with in six layer of lamina each with the thickness of 0.41666mm. From six lamina two of them is carbon/epoxy and four of them is E-glass/epoxy lamina. Therefore, the weight of blade is calculated for carbon/epoxy and E-glass/epoxy laminas to give the total weight of composite laminate blade. The weight of rigid keel is common for both foot as the keel is used mount prosthetic socket.

- Volume of two layers of carbon/epoxy lamina,

$$V_c = L \times t \times w = 173mmx(2x0.4166)mmx40mm = 5.767x10^{-6}m^3$$

$$where, t = thickness\ of\ two\ laminas\ of\ carbon - epoxy\ lamina$$

- Volume of four layers of E-glass/epoxy lamina,

$$V_c = L \times t \times w = 173mmx(4x0.4166)mmx40mm = 11.533x10^{-6}m^3$$

Weight of two carbon/epoxy layer in the laminate, W_c using equation 4.3:

$$W_c = \frac{1518kg}{m3} x5.767x10^{-6}m^3 \frac{x9.81m}{s2} = 0.0859N$$

Weight of four E-glass/epoxy layer in the laminate, w_g:

$$W_g = \frac{1970kg}{m3} x11.533x10^{-6}m^3 \frac{x9.81m}{s2} = 0.223N$$

Therefore, the total weight, $W_{T,C}$ of the composite prosthetic foot becomes:

$$W_{T,C} = W_k + W_c + W_g$$

$$W_{T,C} = 1.08N + 0.0859N + 0.223N$$

$$\mathbf{W_{T,c} = 1.389N}$$

The weight saved due to the single blade composite replaced multi blades of HPP prosthetic foot is calculated as:

Weight saved = 2.002N N – 1.389N = 0.613N

Weight saved in percentage= (0.613 ÷ 2.002) × 100=**30.62 %**

Therefore, the laminated hybrid glass-carbon/epoxy composite blade prosthetic foot is very light weight material than that of the current conventional HPP multi blade prosthetic foot in Prosthetic orthotic center.

III. Product cost estimation of prosthetic foot

The material, labor and machine/tool cost is important consideration in the design and production of prosthetic foot. The cost estimation of the prosthetic foot made from HPP and the hybrid composite calculated as:

- Material cost
- Manufacturing (machining/tooling) overhead cost
- Labor cost

a) Material Cost Estimation

- **HPP-material cost estimation for prosthetic foot**

The average price of HPP-(SIMONA SIMOLIFE pp-product number 010021846) product factory price from the real time price list is 3$/kg [59]. The current mass of prosthetic foot made from HPP is calculated from the total weight, $W_{T,HPP}$ as:

$$\text{Mass of HPP prosthetic foot, m} = \frac{W_{T,HPP}}{g} = \frac{2.002}{9.81} = 0.2041\text{kg}$$

Therefore, the cost HPP material used to manufacture a single foot is:

$$\text{Material cost for single foot} = 0.2041 * 3\$ = \mathbf{0.61\$/foot}$$

- **Composite-material cost estimation for prosthetic foot**

The cost of composite material is estimated according approach [60]. The price of E-glass fiber and carbon fiber from [61] is 1.8-1.9 $/kg and 15-20$/kg. The epoxy resin for fiber reinforcement is 1.75-2.34$/kg. The volume fraction of fiber is 55% as analyzed in chapter 3 and epoxy resin is 45%. This means, in a single lamina of fiber (glass or carbon)/epoxy composite 55% of is fiber and 45% is epoxy resign.

In two carbon/epoxy layer in the laminate, the weight of carbon fiber is =0.55x0.0859N=0.047N
In four E-glass/epoxy layer in the laminate, the weight of glass fiber is =0.55x0.223N=0.1227N
Weight of epoxy resign in two layer with carbon fiber=0.0859N-0.047N=0.0389N
Weight of epoxy resign in four layer of carbon fiber=0.223N-0.1227N=0.1003N
Total weight of epoxy resin=0.0389N+0.1003N=0.1392N

Using $mass, m = \frac{\text{Weight,W}}{\text{acceleration due to gravity,g}}$

- Mass of carbon fiber in the laminate$= \frac{0.047}{9.81} kg = 0.00479kg$
- Mass of glass fiber in the laminate$= \frac{0.1227}{9.81} kg = 0.0125kg$
- Mass of Epoxy resin in the laminate$= \frac{0.1392}{9.81} kg = 0.0142kg$
- Mass of rigid keel $= \frac{1.08}{9.81} kg = 0.1101kg$

Cost estimated for fibers and epoxy resin material to build a single prosthetic foot is calculated as:
Cost of carbon fiber material needed for single foot=0.00479kgx20$/kg=0.0958$
Cost of E-glass fiber material needed for single foot=0.0125kgx1.9$/kg=0.0238$

Cost of Epoxy resin material needed for single foot=0.0142kgx2.34$/kg=0.0332$

Cost of HPP rigid keel for single foot=0.1101kgx3$/kg=0.3303$

Total cost for fiber, epoxy and rigid keel material

= 0.0958$+0.0238$+0.0332$+0.3303$ =**0.48$/foot**

The material cost reduced due to the single blade composite replaced multi blades of HPP prosthetic foot is calculated as:

Reduced material cost = 0.61$ – 0.48$ = 0.13$ per single foot.

Cost reduction in percentage= (0.13 ÷ 0.61) × 100=**21.3 %**

Therefore, the laminated hybrid glass-carbon/epoxy composite blade prosthetic foot design require less material cost than that of the current conventional HPP multi blade prosthetic foot in Prosthetic orthotic center.

b) Machining/tooling cost of HPP and composite prosthetic foot

Machine costs are estimated as time-related costs, also often referred to as overhead costs [62]. Overhead includes time-related economic cost with an interest. The hourly cost of the different machine/tool used for composite manufacturing varies based on the capital cost of the equipment [60]. The total capital cost of the equipment is distributed into equivalent annual payments. The annual payment amount can be divided by the annual hours of operation to determine the hourly cost of a machine. In this thesis, estimate of machine/equipment cost for prosthetic foot is determined by considering each machine/tool operation hours. The total hours per year of machine usage is calculated using the value of machine operation hours per day. The total machine usage per year is calculated as [60]:

$$H = D \cdot E[H] - - - - - - - [4.4]$$

Where, H = Total yearly operation hours, D = Total operating days in a year.

The annual equivalent machine cost is calculated using the present worth of the equipment for a time-period and a fixed rate of interest (20%). The annual equivalent worth is calculated using equation [63].

$$A_i = \frac{p_i x R(1+R)^N}{(1+R)^N - 1} - - - - - - [4.5]$$

Ai = Annual equivalent cost for machine i, i = Index for equipment (i=1, 2, 3….), Pi = Present cost for machine I, R = Rate of interest, N = Time period for capital recovery. The next step is to calculate the hourly cost of all the machines using the annual equivalent machine cost. The hourly cost of machine i is calculated by:

$$C_{hi} = \frac{A_i}{H} - - - - - - - - - - [4.6]$$

Where, Chi = Hourly cost for equipment i, Ai = Annual payment for equipment i

The cost of operating each machine to make a part is calculated by multiplying the hourly operating cost with the actual operation hours to make a part as shown in equation 4.7.

$$c_{mi} = C_{hi} x A_{hi} - - - - - - - - [4.7]$$

Where, c_{mi} Operating cost of equipment i, A_{hi}= Actual operation hours for equipment i

Table 4. 2 Operating hour and days of a machine/tools.

Machine/tool	Machine/tool needed for	Capital cost ($)	Operating hr. /day	Operating day/year
Semi-automatic vertical molding Machine CICR	HPP prosthetic foot	2001.44$	5hr	240days
Plastic cutting saw (Size: approx. 22x1.5cm/8.6x0.6" Big Saw Length: approx. 25cm/9.8') [64]		8.5$	8hr	120days
Aluminum mold (4) [65]		200$	5hr	240days
Prosthetic Oven, SSI-PO-001		534.30$	6hr	220days
Safety gloves		2.5$ [66]	8hr	100days
Aluminum mold (1)		35$	8hr	240days

Fibers Scissor (2734-A)	Composite prosthetic foot	9.5$	8hr	300days
Hot blower vortex (DFH) for curing		21$	4hr	215days
Pressure roller (SSR)		3.3$	5hr	96days

The run time cost of the machine/tool is calculated using Equation 4.4-4.7 based on the capital cost, annual operating days and expected operating hr/day of the machine listed in Table 4.2 of machine /tool cost. The MATLAB code used for solving (Eq.4.4-4.7) the result is shown in appendix 9. The overall product costs estimated results for both model of prosthetic foot is shown in table 4.3.

c) Labor cost of HPP and composite prosthetic foot

The labor cost is estimated for the both prosthetic foot model based on time requirement for operation. The labor force costs up to 200 birr (4.26$)/day (8hr) in Ethiopia and it breakdown into time for each required operation as shown in table 4.3 for production of single prosthetic foot from HPP and composites.

Table 4. 3 Product cost (material, labor and machine/tool cost) of prosthetic foot

Cost type	Foot	Material type	Cost	Required amount(kg)	Cost/foot	Tax and shipping (20%)	Total cost/foot
Material cost	HPP	HPP	3$/kg	0.2041	0.61$	0.122$	0.73$
	Composite	E-glass fiber	1.9$/kg	0.0125	0.0238$	0.005$	0.58$
		Carbon fiber	20$/kg	0.0048	0.0958$	0.019$	
		Epoxy resin	2.34$/kg	0.0142	0.0332$	0.006$	
		HPP for rigid keel	3$/kg	0.1101	0.3303$	0.066$	

Labor cost		**Required operation**	**Labor time required (minutes)**	**Total time (minutes)**	**Labor cost/8hrs**		**Labor cost/foot**
	HPP	Cutting HPP	20	120 (2hr)	4.26$		1.06$
		Heating in oven machine	15				
		Mold adjustment	10				
		Injecting in to mold	35				
		Removing from the mold	30				
		Assembling together	10				
	Composite	Cutting fibers (in to required size)	15	110 (1hr50min)	4.26$		0.80$
		Mold preparation(cleaning and applying releasing agent)	10				
		Laying up (six layer)	30				
		Curing (with heat)	30				
		Removing from mold	10				
		Surface finishing	15				
Machine/tool cost		**Machine/tool**	**Run time**	**Hourly cost**	**Run cost/foot**	**Tax and shipping (20%)**	**Total cost**

	HPP	Semi-automatic vertical molding Machine CICR	35 min	0.463$/hr.	0.270$	0.054$	0.324$
		Prosthetic Oven, SSI-PO-001	15 min	0.135$/hr	0.034$	0.0068$	0.041$
		Aluminum mold (4)	10 min	0.0462$/hr	0.0077$	0.0015$	0.0092$
		Plastic cutting saw	20 min	0.0106$/hr	0.0035$	0.0007$	0.0042$
	Composite	Fibers Scissor (2734-A)	15min	0.0091$/hr	0.0023$	0.00046$	0.0027$
		Safety glove	1hr50min	0.0072$/hr	0.0131$	0.0026$	0.0157$
		Aluminum mold (1)	1hr10min	0.0418$/hr	0.0485$	0.0097$	0.0582$
		Hot blower vortex (DFH) for curing	30min	0.0560$/hr	0.0280$	0.0056$	0.0336$
		Pressure roller	30min	0.0157$/hr	0.0078$	0.00156$	0.0094$
*Total cost for HPP prosthetic foot=2.17$/foot or **101.91/foot** Ethiopian birr*							
*Total cost for single composite prosthetic foot=1.5$/foot or **70.5/foot** Ethiopian birr*							

As observed in table 4.3 above, manufacturing of prosthetic foot from HPP requires high material cost, labor cost and machine cost than composite prosthetic foot (made by hand layup techniques). The composite prosthetic foot 30.82% less production cost than HPP prosthetic foot.

CHAPTER-FIVE

RESULTS AND DISCUSSION

The simulations were undertaken totally on eight samples of composite for tensile and flexural property characterization. Each sample of composite made from six layer of laminas with thickness of 2.5mm for four stacking configuration for the application of prosthetic foot. The detail of simulation results are discussed in the following section.

5.1 Tensile Simulation results and Discussion

5.1.1 Effect of stacking sequence on order of ply failure

In this simulation, the six layers of composite lamina with four stacking sequence of was created composite specimen for tensile testing. The composite laminate is divided into three partition for analysis purpose. The top, middle and bottom ply respectively as shown in table 5.1-5.4.The strength ratio (SR) and failure index (FI) used to identify ply failure. The SR is the ratio of ultimate stress (load) to applied stress (load) and FI is vice versa. The FI$\geq$ 1 or SR$\leq$ 1 shows a failure. The ply failure load is obtained by multiplying applied load to SR.

Table 5. 1 FI and SR with applied load for SS-1

Ply no	***Partition***	***200N***		***1443.2N***		***1446.26N***		***1600N***		***1813.6N***	
		SR	***FI***	*SR*	***FI***	***SR***	***FI***	***SR***	***FI***	***SR***	***FI***
1(0)	*Top*	18.27	0.054735	2.5467	0.39266	2.5265	0.3958	1.1335	0.88221	0.94396	1.0594
2(90)		7.216	0.13939	1	1	0.99206	1.008	-	-	-	-
3(45)	*Middle*	8.35	0.11976	1.1639	0.85915	1.1547	0.86603	0.52451	1.9066	-	-
4(45)		8.0003	0.12499	1.1152	0.8967	1.1063	0.90387	0.53897	1.8554	-	-
5(90)	*Bottom*	7.2371	0.13818	1.0088	0.99127	1.0008	0.9992	-	-	-	-
6(0)		21.547	0.04641	3.0035	0.33294	2.9797	0.3356	1.6582	0.60305	0.52458	1.9063
Ply failure load		Initial		1st		2nd		3rd and 4th		5th and 6th	
Ply failure order				2		5		3 and 4		1 and 6	

In SS-1, initial load of 200N is applied to the right end side of composite to identify the first ply to be failed. At this load there is no failure in all plies and the minimum strength ratio 7.216 is observed on top portion of second layer (90^0 ply). This ply failed at the load 1443.2N, which obtained by multiplying applied load (200N) with SR (7.216) as shown in table 5.1. Additionally, this table shows failure load from first ply failure to ultimate failure with ply failure order depending up on SR and FI. The middle portion of 45^0 ply orientations are failed at of 1600N.

The zero degree ply orientation can carry largest axial load up to 1813.6N without any failure. The order ply failure are 90^0, 45^0 and 0^0 respectively.

Table 5. 2 FI and SR with applied load for SS-2

Ply no	***Partition***	***200N***		***1440.2N***		***1453.35N***		***1748.23N***		***2561.86N***	
		SR	***FI***	*SR*	***FI***	***SR***	***FI***	***SR***	***FI***	***SR***	***FI***
1(45)	*Top*	8.0215	0.12466	1.1139	0.89771	1.8578	0.53826	1.4654	0.6824	0.50294	1.9883
2(0)		20.199	0.049506	2.8051	0.35649	1.2029	0.8313	0.69181	1.4455	-	-
3(90)	*Middle*	7.2361	0.1382	1.0049	0.99515	0.76064	1.3147	-	-	-	-
4(90)		7.2008	0.13887	0.99997	1	-	-	-	-	-	-
5(0)	*Bottom*	22.015	0.045423	3.0572	0.32709	0.33191	3.0129	-	-	-	-
6(45)		7.2126	0.14099	0.98495	1.0153	-	-	-	-	-	-
Ply failure load		Initial		1^{st}		2^{nd} and 3^{rd}		4^{th} and 5^{th}		6^{th}	
Ply failure order				4 and 6		3 and 5		2		1	

In this stacking sequence (SS-2), the 45^0 orientation E-glass/epoxy lamina are laid at end sides of the composite. The 90^0 oriented lamina is stacked in middle portion of the composite and local stress distribution at the ultimate failure load as shown in figure 4.13.a) and b) respectively. The initial failure is occurred at fourth and sixth layer of the composite. In both stacking sequence of SS-1 and SS-2, the initial failure is observed in 90^0orientation, but in this stacking sequence the initial failure load is 1440.2N, i.e. it can handle more load without failure the first stacking sequence. The fourth (90^0) ply from middle portion and sixth (45^0) ply from the bottom portion are failed at the same failure load of 1440.2N. In the same way the third (90^0) ply from middle portion and sixth (0^0) ply from the bottom portion are flailed at the same failure load of 1453.35N.The detail of this discussion is shown in table 4.4. The 4^{th}, 6th, 3rd, 5th, 2nd and 1^{st} are the order of the failure respectively. The ultimate failure load and the tensile strength are 2561.86N and 1475.5MPa.

Table 5. 3 FI and SR with applied load for SS-3

Ply no	***Partition***	***200N***		***2401.6N***		***2471.01N***		***2554.53N***		***3154.57N***		***3592.74***	
		SR	***FI***	*SR*	***FI***	***SR***	***FI***	***SR***	***FI***	***SR***	***FI***	***SR***	***FI***
1(0C)	*Top*	28.24	0.0354	2.352	0.4251	2.248	0.444	1.23	0.8100	0.6680	1.4969	-	-
2(90)		13.91	0.0719	1.158	0.8635	1.866	0.535	1.91	0.5221	1.1389	0.8780	0.638	1.566
3(45)	*Middle*	12.00	0.0832	1	1	-	-	-	-	-	-	-	-
4(45)		12.35	0.0809	1.028	0.9719	0.639	1.562	-	-	-	-	-	-
5(90)	*Bottom*	14.14	0.0707	1.177	0.8491	0.659	1.516	-	-	-	-	-	-
6(0C)		30.29	0.0330	2.522	0.3964	1.033	0.967	0.60	1.6467	-	-	-	-
Ply failure load		Initial		**1^{st}**		**2^{nd} and 3^{rd}**		4^{th}		**5^{th}**		**6^{th}**	
Ply failure order				**3**		**4 and 5**		6		**1**		**2**	

The third stacking sequence (SS-3) modeled as the two layer of 0°E-glass/epoxy lamina at the end side of the composite laminate of SS-1 is replaced by 0°carbon-epoxy composite lamina. The two of them are carbon epoxy and the remaining four layers are E-glass epoxy composite lamina to become Glass/Carbon hybrid composite laminate. Due the carbon layer the 90° oriented ply is not failed under initial failure load unlike that of SS-1.The reason is that 90°orientation is near to the carbon layer and allow them to resist the initial failure load. The initial failure load and ultimate load is 2401.6N and 3592.74N respectively. The order of ply failures are shown in table 5.3 below. Additionally, keeping the high modulus Carbon fiber in outer layer and low modulus Glass fiber as inner layer, improved the dynamic stability of Glass/Carbon hybrid laminates as revealed by [67].In SS-4 The top and bottom surface of SS-2 laminated is replaced by carbon-epoxy lamina. This improves the yield strength from 148.35 to 331.37 MPa. Similarly, it improves the ultimate load carrying capacity and ultimate tensile strength 518.14 N and 390.4MPa. The ply failure orders are changed due the hybrid effect as shown in table 5.4. This prevents the bottom ply number 6(45°) to be failed at same load with 90° ply unlike SS-2.

Table 5. 4 FI and SR with applied load for SS-4

Ply no	***Partition***	***200N***		***1471.84N***		***1498.62N***		***1566.81N***		***1986.72N***		***3080.1N***	
		SR	***FI***	*SR*	***FI***	***SR***	***FI***	***SR***	***FI***	***SR***	***FI***	***SR***	***FI***
1(45C)	*Top*	14.468	0.06911	1.966	0.5086	0.8453	1.183	-	-	-	-	-	-
2(0)		28.418	0.03519	3.8616	0.2589	1.6192	0.6175	3.189	0.3135	1.5503	0.6450	0.638	1.566
3(90)	*Middle*	7.4931	0.01335	1.018	0.98212	0.9564	1.0456	-	-	-	-	-	-
4(90)		7.3592	0.13588	1	1	8.4728	0.1180	-	-	-	-	-	-
5(0)	*Bottom*	33.01	0.03029	4.4856	0.22294	2.3217	0.43072	1.268	0.78865	-	-	-	-
6(45C)		11.896	0.08406	1.616	0.61865	1.0455	0.9564	-	-	-	-	-	-
Ply failure load		Initial		1st		2nd and 3rd		4th		5th		6th	
Ply failure order				4		1 and 3		6		5		2	

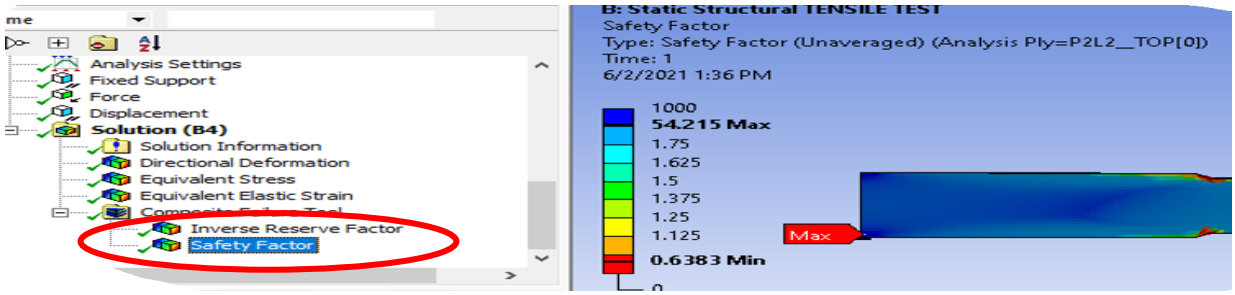

Figure 5. 1 Contour plots of ANSYS showing FI and SR

5.1.2Effect of stacking sequence on strength of E-glass/epoxy laminate

From the analysis of the two stacking sequence (SS-1 and SS-2) made from glass epoxy composite as shown in figure 5.2 and table 5.5 the first ply failure load of SS-1 is greater than SS-2 by 3N.This shows that the SS-1 carries higher load with-out any failure in the composite laminate than the SS-2. In the same manner, it has 4.1MPa more tensile strength than the second sequence at yield point. After the plies starts failure in the laminate its load carrying capacity and strength is much lower figure 5.3.

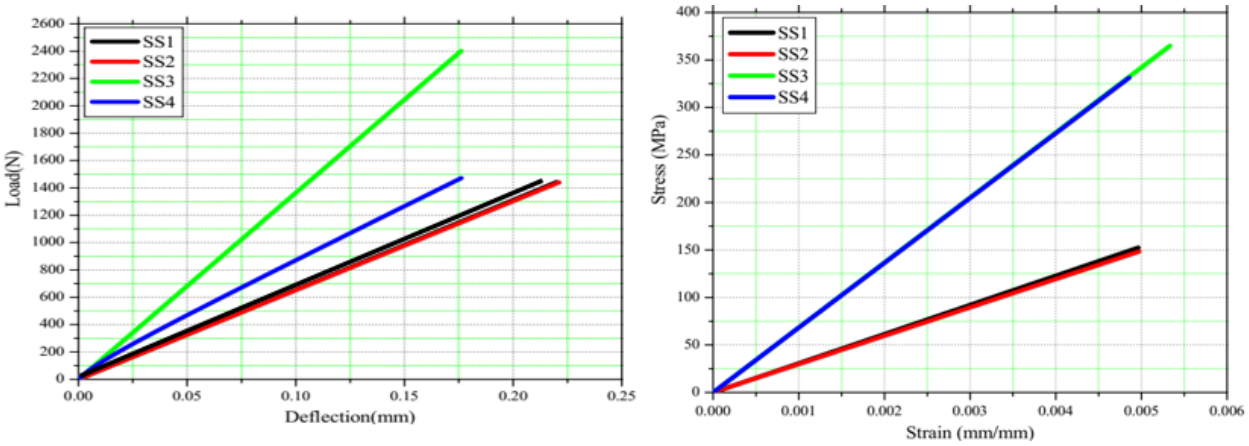

a) b)

Figure 5. 2 a) Load vs deflection, b) stress vs strain diagram of tensile simulation at FPF

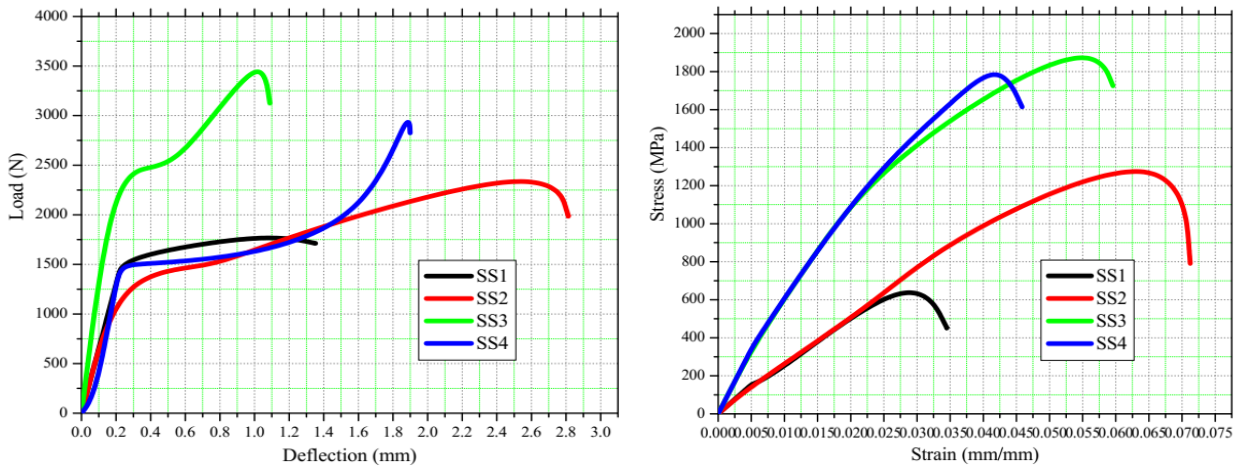

a) b)

Figure 5. 3 a) Load vs deflection, b) stress vs strain diagram of tensile simulation at LPF

5.1.3 Effect of stacking sequence on tensile strength of hybrid Glass carbon/epoxy laminate

The third and fourth stacking configuration (SS-3 and SS-4) are made from hybrid composite with addition of two layers of carbon. The FPF load obtained from the simulation are 2101.6 and 1471.8N respectively with their tensile strength of 364.9 and 331.37MPa for the respective stacking configurations. While the LPF load is 3592.74 and 3080.01N respectively with the ultimate tensile strength of 1935 and 1865.37MPa for respective configuration as shown in table 5.5. This result shows that the load carrying capacity and tensile strength of SS-3 are higher than SS-4 both at FPF and LPF figure 5.3-5.4. The tensile yield strength of SS-3 is increased by 33.53MPa compared to the SS-4 and similarly is ultimate strength is increased by 69.63MPa.unlike that of stacking configuration in SS-1 of glass/epoxy laminate,SS-3 of hybrid composite can carry more higher load after the initiation of the ply failure.

5.1.4 Comparisons between tensile strength of all stacking configuration

Among all stacking configuration the SS-3 has higher yield and ultimate strength compared to the others. While SS-2 and SS-1 smaller tensile yield and ultimate strength respectively as shown in bar chart of figure 5.5. The figure shows that Glass-Carbon/epoxy laminate yields higher tensile strength than pure E-glass/epoxy composite. The stacking configuration (SS-1and SS-3) made from $[0\ 90\ 45]_s$ results high tensile strength of the configuration (SS-2 and SS-4) made from $[45\ 0\ 90]_s$ as shown summary table 5.5.

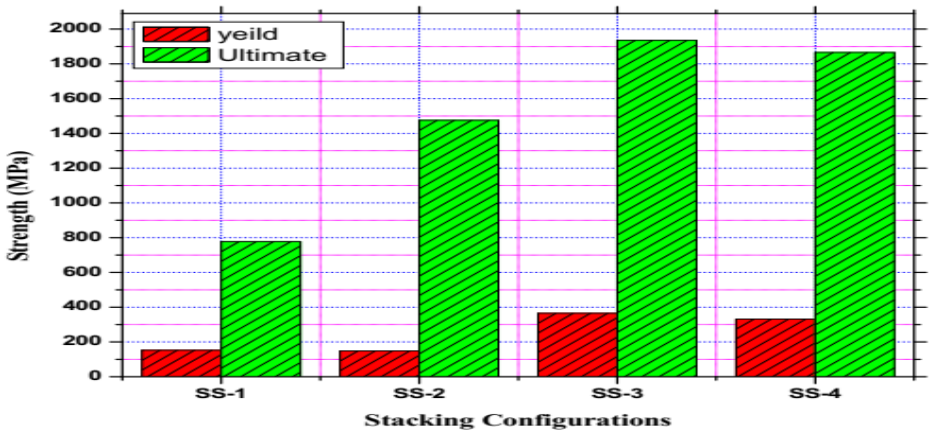

Figure 5. 4 Comparisons of yield (FPF) and ultimate (LPF) tensile strength of laminate

There is no difference in the shape of the stress-strain curve. All of them are exhibiting linear elastic behavior up to the instantaneous failure as shown in figure 5.3. While there is variation in shape of load vs deflection among the configuration. This shows that the failure load of plies in laminate of different stacking configuration vital role in determining final load vs deflection graph. Figure 5.5 is a contour a contour plot of equivalent stress in laminate of different configuration. This stress is equivalent to ultimate strength of at ultimate failure load laminate as the laminate can't resist load beyond this load.

The stress is maximum on fixed side of the testing specimen. The damage (failure) in the laminate starts at this stress and propagate to whole laminate as shown in figure 5.6. At the ultimate strength of laminate the whole part of become damaged and at this all plies in the laminate are damaged and unable to carry further load. The safety factor of laminate is much less than one as shown in the figure 5.6.

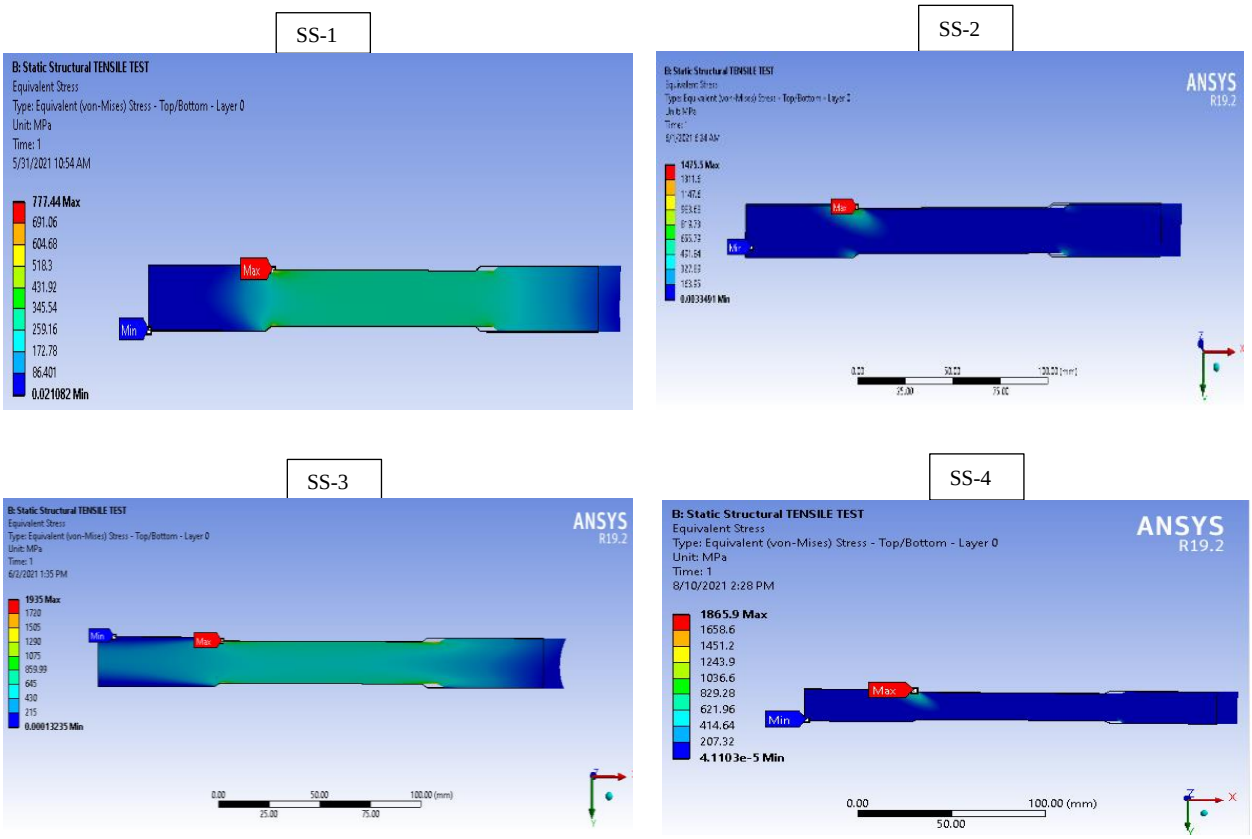

Figure 5. 5 Contour plots ANSYS ultimate tensile strength results stacking configurations.

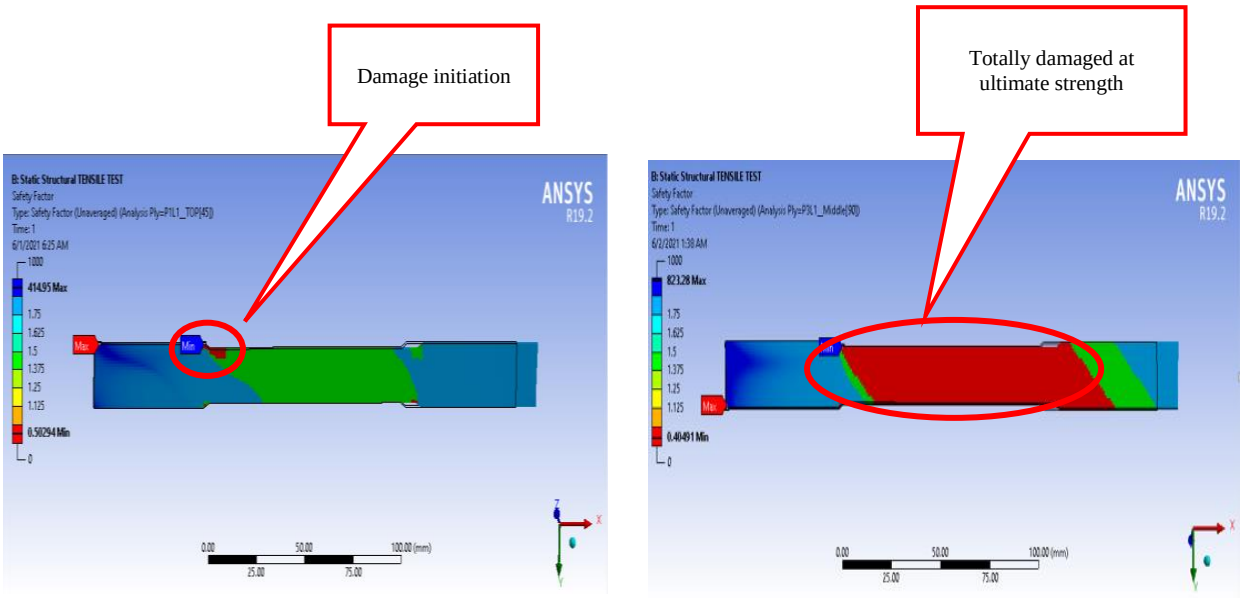

Figure 5. 6 Contour plot of ANSYS for damage of composite laminate

Table 5. 5 Summary of Tensile test simulation

Stacking sequences	Representation symbol	Failure load (N)		Strength (MPa)	
		FPF	**LPF**	**Yield, at FPF**	**ultimate ,at LFL**
[0 90 45 45 90 0]	**SS-1**	1443.2	1813.6	152.45	777.44
[45 0 90 90 0 45]	**SS-2**	1440.2	2561.86	148.35	1475.5
[0 c 90 45 45 90 0c]	**SS-3**	2401.6	3592.74	364.9	1935
[45 c 0 90 90 0 45c]	**SS-4**	1471.8	3080.01	331.37	1865.37

5.2 Flexural Simulation results and Discussion

The flexural simulation was set to run for the same thickness, number of layer and stacking configuration with the tensile simulation. The initial failure in the laminate is occurred at different amount of load depending on the configuration of the laminate as shown in table 5.7. Figure 5.7 shows that the failures are initiated in each ply at the mid-span where maximum equivalent stress is observed. The normal stress at ultimate failure load of the top and bottom ply is given in figure 5.8. The top ply is under compression and the bottom ply is under the tension. Since , the the

compressive stress on concave side of laminate is much higher than the tensile stress on convex side of the bottom laminate, the flexural strength is equivalent stress at ultimate failure load in compressive side (top) of the laminate.

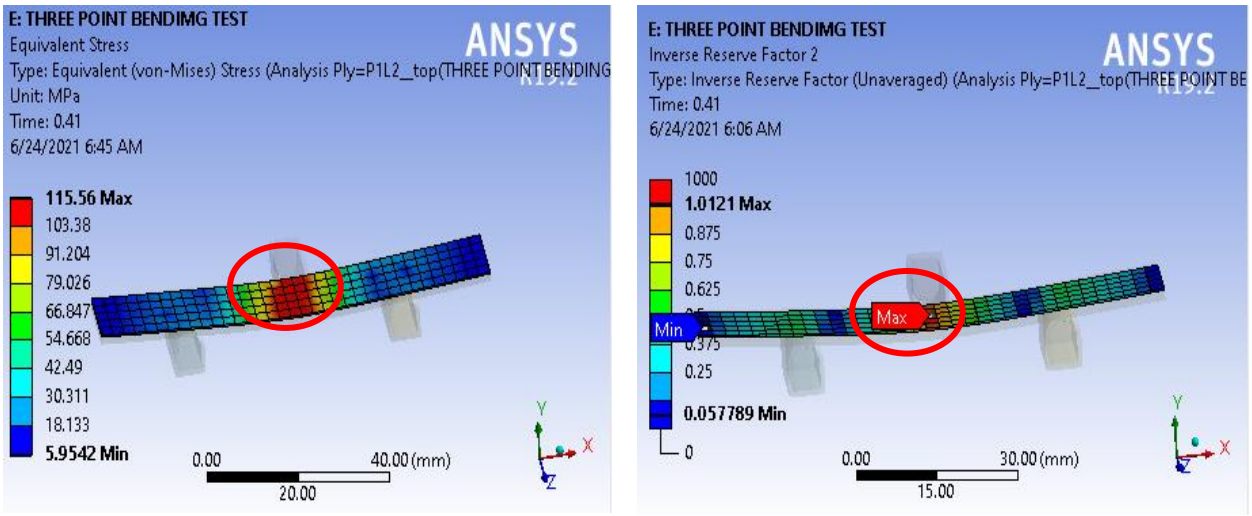

Figure 5. 7 Contour plot of equivalent stress (left) and FI (right) in a plies of a laminates.

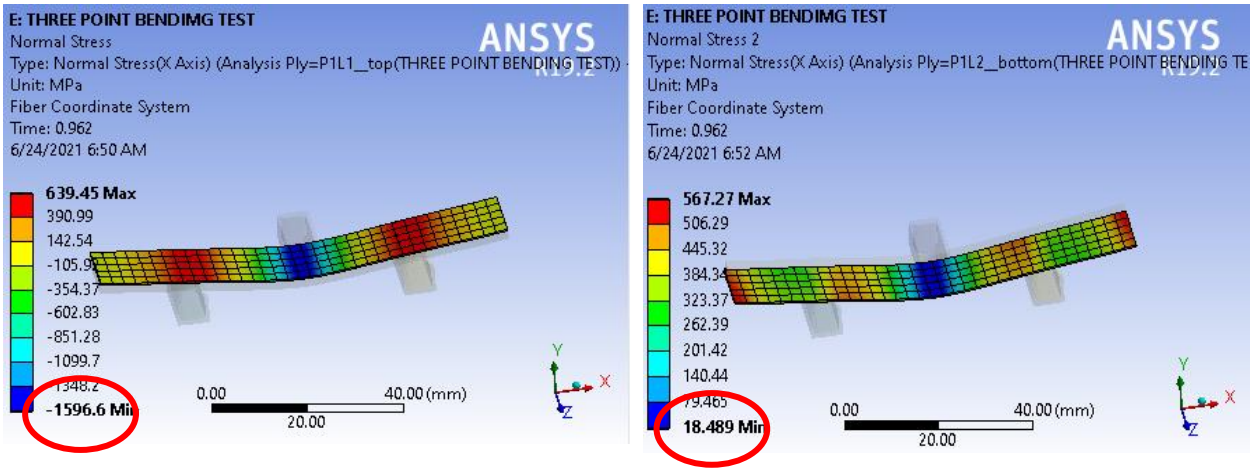

Figure 5. 8 Contour plot of normal stresses at top (left) and bottom (right) plies of a laminates.

5.2.1 Effect stacking configuration on order of plies failure in laminate

The plies failure order in the laminate is important in determining ultimate load capacity of laminate. This depends on position and orientation of lamina in the laminate. In a composite laminate made from pure glass/epoxy the failure in SS-2 laminates failure starts at load of 750.63N. While in SS-1 the failures starts at 882.28N. As shown in table 5.6, except for SS-4 failure in

laminate starts on plies in compressive side of flexural simulation. The hybrid of composite of SS-3 failure starts ply number 1 (0°_{C}) , but it resists larger load than other laminates up 912.15N.

Table 5. 6 Order of plies failure in flexural simulation

Stacking sequences	Representation Symbol	Order of plies failure
[0 90 45 45 90 0]	**SS-1**	2-5-1-3-4-6
[45 0 90 90 0 45]	**SS-2**	1-6-3-2-4-5
[0 c 90 45 45 90 0c]	**SS-3**	1-2-3-4-5-6
[45 c 0 90 90 0 45c]	**SS-4**	4-6-3-5-1-2

5.2.2 Effect of stacking sequence on flexural strength of E-glass/epoxy laminate

In case of the laminate made from pure Glass/epoxy composite the first stacking configutation (SS-1) has larger load carrying capacity and stronger than the SS-2. The SS-1 resists load up to 882.2N and stress up to 559.97MPa without any ply failure in the laminate as shown in table 5.7 While,SS-2 can resist only the load and stresses up 750.63N and 397.1MPa stress respectively.Similary, the first stacking sequence has 1351.4N and 850.82Mpa ultimate load and strength than SS-2. In stress vs strain and load vs deflection graph of figure 5.9-5.10 the black and red line shows the ralation among the first and second configration of Glass/epoxy laminate.

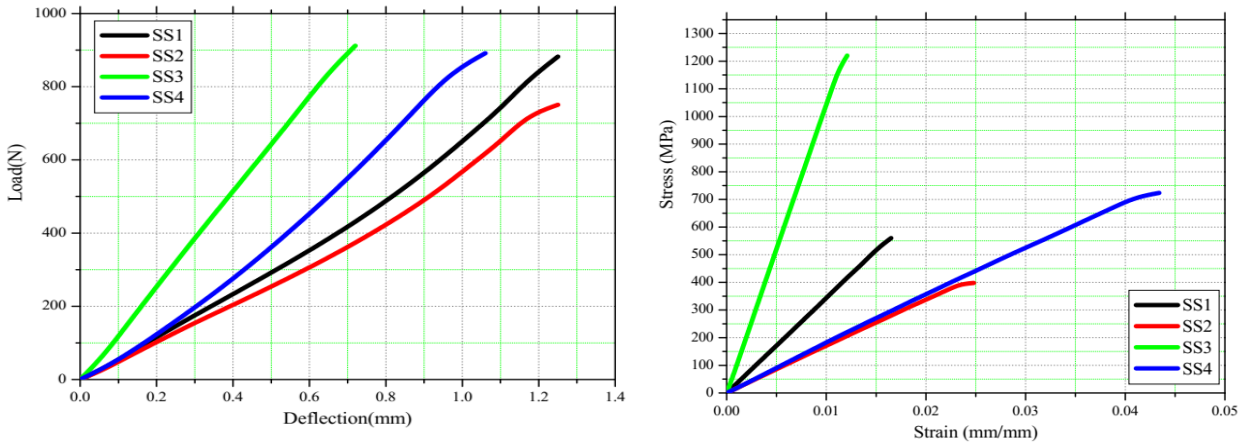

a) b)

Figure 5. 9 a) Load vs deflection, b) stress vs strain diagram of flexural simulation at FPF

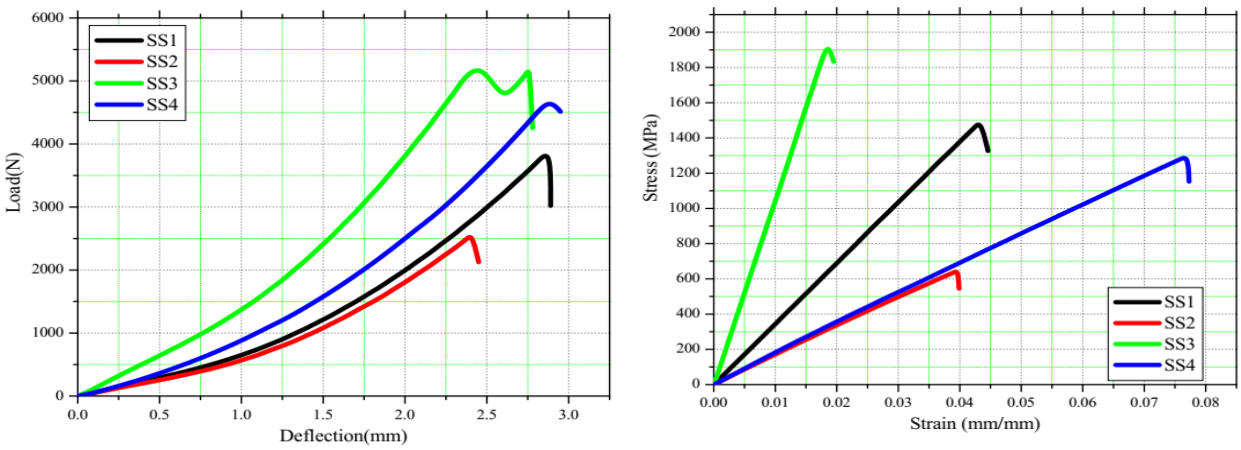

a) b)

Figure 5. 10 a) Load vs deflection, b) stress vs strain diagram of flexural simulation at LPF

5.2.3 Effect of stacking sequence on flexural strength of hybrid Glass-Carbon/epoxy

As presented in table 5.7 the stacking configuration has major factor in hybrid composites to determine flexural strength and load carrying capacity of laminate composites. The third sequence SS-3 resists 20.7N more load than the fourth configuration SS-4 without showing any ply failure in the laminate. Similarly, it has higher ultimate load and strength than all other stacking configuration. It's has 635.1MPa more ultimate strength than the fourth configuration. In figure 5.9-5.10, the green and the blue line shows the comparison among those hybrid composite laminates.

5.2.4 Comparisons between flexural properties of all stacking configuration

The third stacking configuration SS-3 of the hybrid composite laminate higher yield and ultimate strength than all configuration as shown on bar chart of figure 5.11. Compared to the other configuration the SS-2 lowest strength among all others. The ultimate strength of SS- 1 made from pure Glass/epoxy composite higher than that of SS-4 made from hybrid composite. There is no difference on shape of load –deflection curves expect for SS-4, in which near the ultimate failure there is increment and consequently decrement of load as presented in figure 5.10 above.

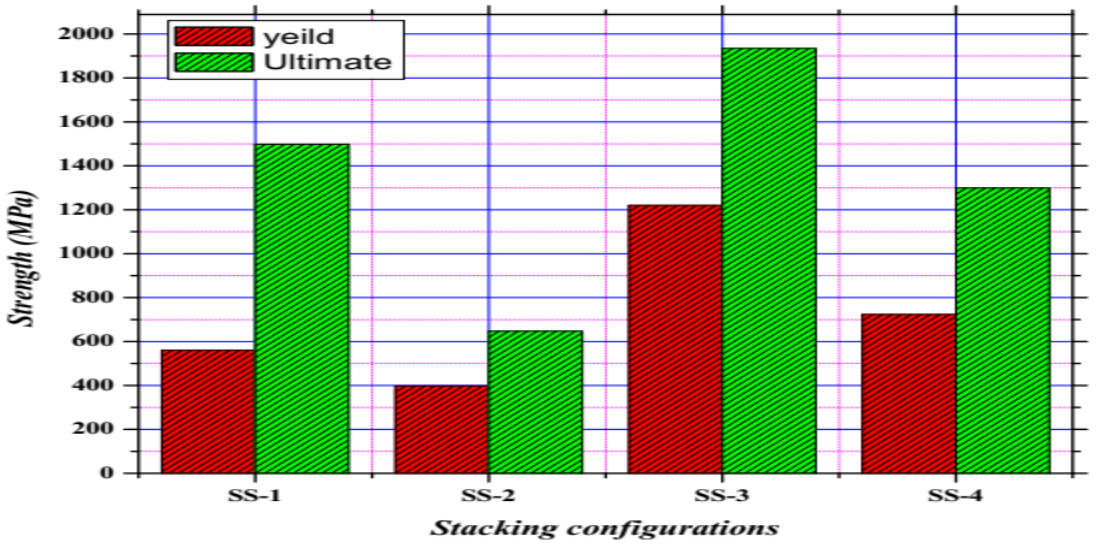

Figure 5. 11 Comparisons of yield (FPF) and ultimate (LPF) flexural strength of laminate

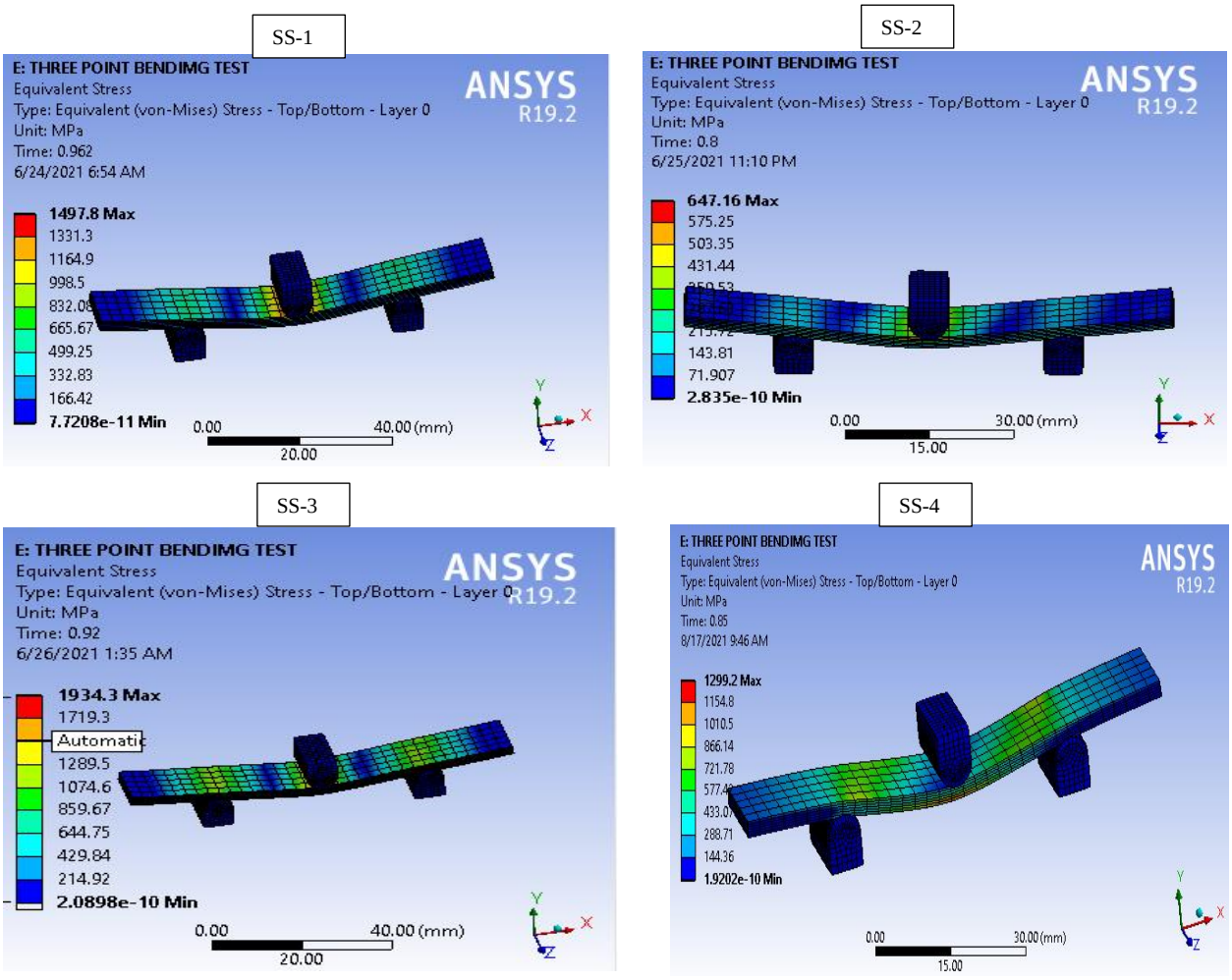

Figure 5. 12 Contour plots ANSYS ultimate flexural strength results stacking configurations.

Figure 5.12 above shows a contour a contour plot of equivalent stress in laminate of different configuration which is ultimate strength of at ultimate failure load laminate. A contour plot of figure 5.13 shows that at their respective ultimate failure load all plies in each laminate is damaged and unable to resist any additional load further. The red color on the sample shows the damage and the failure index is much higher than one.

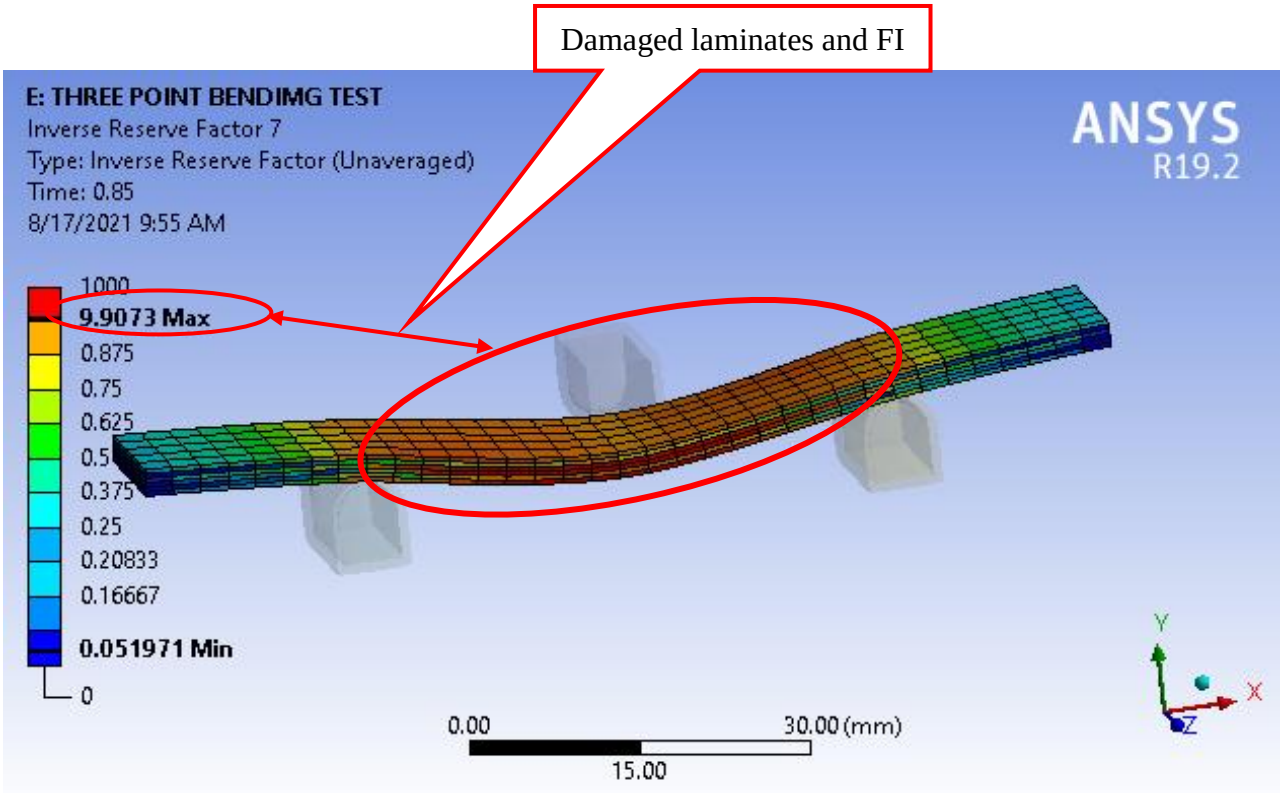

Figure 5. 13 Contour plot for damage of composite laminate under flexural simulation

Table 5. 7 Summary of flexural test simulation

Stacking sequences	Representation Symbol	Failure load (N)		Strength (MPa)	
		FPF	**LPF**	**Yield, at FPF**	**ultimate ,at LFL**
[0 90 45 45 90 0]	**SS-1**	882.28	3914	559.97	1497.98
[45 0 90 90 0 45]	**SS-2**	750.63	2562.6	397.71	647.16
[0 c 90 45 45 90 0c]	**SS-3**	912.15	5203.6	1220.1	1934.3
[45 c 0 90 90 0 45c]	**SS-4**	891.45	4715.3	723.4	1299.2

5.3 Theoretical Results and discussions for FEA verification

To verify the FEA solutions the theory discussed in chapter 3 of section 3.2 was applied to the geometry and loading conditions shown in Figure 4.1-4.2. (The Matlab script used to calculate the theoretical results was provided and can be found in Appendix 1).In this analysis the plies failure load results at FPF and LPF load is run in Matlab. The analysis result is shown in Table 5.8-5.9.

Table 5. 8 Matlab tensile failure load and ply failure order results in comparison with ANSYS

Stacking sequences	Representation Symbol	Failure loads (N)				Plies failure order	Error %	
		ANSYS Result		MATLAB Result		Matlab result		
		FPF	**LPF**	**FPF**	**LPF**		**FPF**	**LPF**
[0 90 45 45 90 0]	**SS-1**	1443.2	1813.6	1452.1	1821.6	2,5,3&4,5&6	1.3	1.5
[45 0 90 90 0 45]	**SS-2**	1440.2	2561.86	1450.3	2574.72	4,6,3&5,2,1	1.4	1.3
[0 c 90 45 45 90 0c]	**SS-3**	2401.6	3592.74	2410.5	3598.30	3,4&5,6,1,2	0.8	0.7
[45 c 0 90 90 0 45c]	**SS-4**	1471.8	3080.01	1481.9	3091.57	2,5,3&4,5&6	1.3	1.0

Table 5. 9 Matlab flexural failure load and ply failure order results comparison with ANSYS

Stacking sequences	*Representation Symbol*	*Failure loads (N)*				*Plies failure order*	*Error %*	
		ANSYS Result		*MATLAB Result*		*Matlab result*		
		FPF	***LPF***	***FPF***	***LPF***		***FPF***	***LPF***
[0 90 45 45 90 0]	**SS-1**	882.28	3914	904.56	3963.1	2,5,1,3,4,6	2.4	1.2
[45 0 90 90 0 45]	**SS-2**	750.63	2562.6	772.75	2615.5	1,6,3,2,4,5	2.8	2.0
[0 c 90 45 45 90 0c]	**SS-3**	912.15	5203.6	932.24	5250.14	1,2,3,4,5,6	2.1	0.9
[45 c 0 90 90 0 45c]	**SS-4**	891.45	4715.3	911.19	4762.18	4,6,3,5,1,2	2.2	1.0

There is small variation in matlab and finite element results. But, shows the same plies failure order in both tensile and flexural testing analysis. The matlab in tensile testing predicts the failure loads fairly accurately with Ansys results with error less than 2%. Similarly, the flexural testing analysis gives comparable results with error less than 3%. The factors that influence the variation in two result arises due to their analysis procedures. The matlab result is based on fully discount method in which the once the ply is failed its stiffness becomes zero, while the numerical analysis

is based on the progressive analysis that the stiffness of the failed ply becomes reduced to values other than zeros based stiffness degradation rule. In general, the matlab result validate in finite element results as the error small and acceptable.

5.4 Comparison of Composite and HPP made prosthetic foots model

The prosthetic foot made from HPP has less strength, less energy storage ability and lower safety factor compared to the prosthetic made from hybrid Glass-carbon/epoxy composite laminate under the same loading condition. This done by simulating the prosthetic foot model in ANSYS to calculate equivalent von-misses stress, total deformation, stiffness, strain energy and safety factor for showing how the blade interacted with the application of the loads and energy are stored in the blades. In HPP made prosthetic foot, four blades of HPP each with the thickness of 5mm is bonded together to build the prosthetic foot. While, this composite allows only single blade of the composite with the thickness of 2.5mm to be used. This allows the artificial foot to be less in weight and manufacturing cost in addition to providing more strength and comfort. The analysis results of this artificial foot are shown and discussed as follows.

5.4.1 Numerical results and Discussions

The simulation results of prosthetic foot model is shown in figure 5.14-5.15

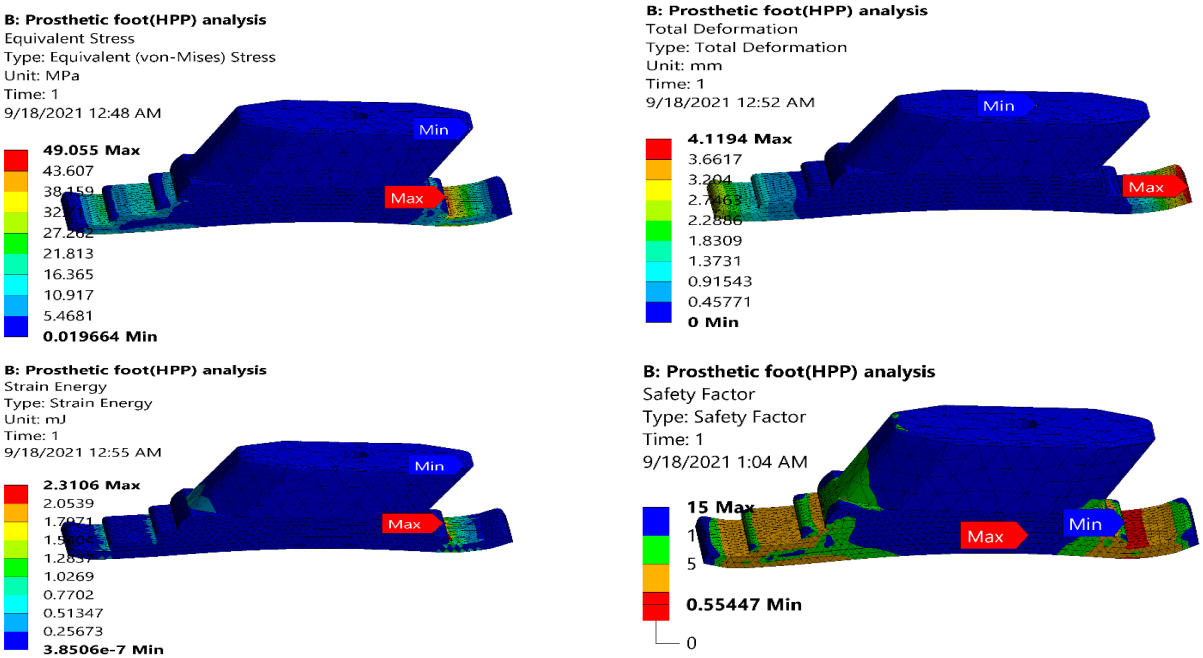

Figure 5. 14 HPP prosthetic foot stress, deformation, strain energy and factor of safety.

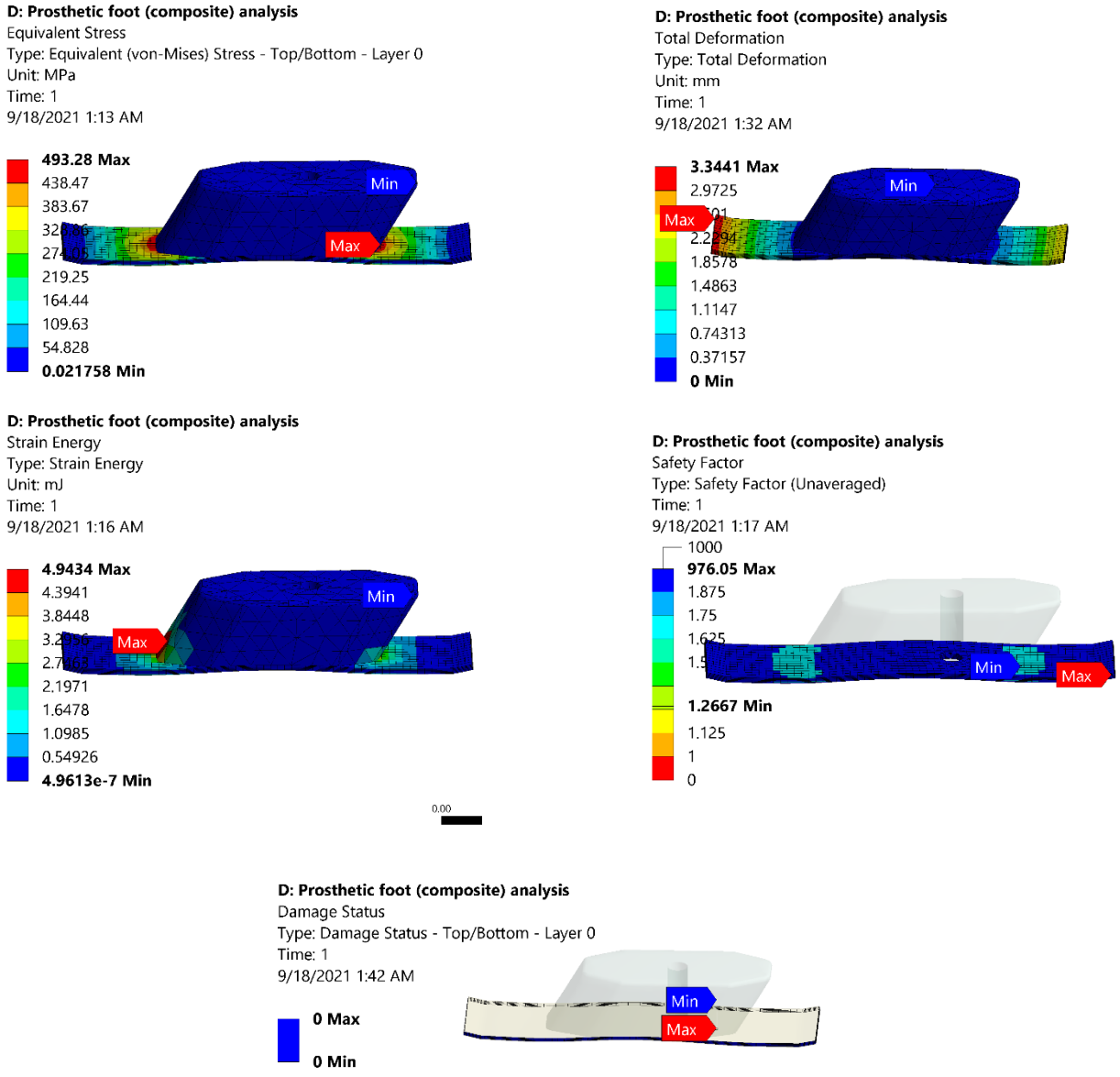

Figure 5. 15 Composite prosthetic foot stress, deformation, strain energy and factor of safety.

5.4.1.1 Equivalent stress (strength) Comparisons

From the analysis of the prosthetic foot model, the values of maximum equivalent stresses resulted in prosthetic foot model using HPP is 49.055MPa which is higher than its ultimate strength, 37MPa. This indicate the model is not operating under the material limits with in lower safety

factor. While, in composite model the equivalent stress is 493.28MPa which is lower than its ultimate strength shown in table 5.5.

5.4.1.2 Strain energy (Energy storage capacity) comparisons

Comparing the amount of energy absorption of the blade, the prosthetic foot model using composite blade absorbs more energy nearly 4.94MJ, but the HPP blade stores only 2.31MJ. This values of strain energy show that composite foot has higher ability to restore energy than HPP foot while walking. This allows the prosthetic foot comfortable for amputees and assist the forward propulsion of a body as the stored energy is released.

5.4.1.3 Deformation (Resistance to deflection) comparisons

The prosthetic foot model using composite and HPP blade deforms by the amount of 3.34mm and 4.12mm respectively as shown in figure 5.14-5.15. This shows that single blade composite deforms less under the same loading condition. This indicates that composite prosthetic blade has higher strength. Due to the higher strength of this composite, it is showed that less material (small thickness) of single blade composite can be used instead of large thickness multi blade foot to the allow the design for a reduction in weight and overall production cost.

5.4.1.4 Safety factor (safety of foot) comparisons

From the FEA analysis of safety factor values, it indicates that the single blade composite prosthetic foot model has higher safety factor value than the values obtained for the HPP blade. There is no damage in the composite laminates the blade under operating load as shown in figure 5.15 of damage status. Comparing the results, the safety factor is 0.55447 and 1.2667 for HPP and composite foot respectively. It indicates the HPP blade is operating under unsafe region as it's much lower than one. All results of simulation comparisons results is shown in figure 5.16 below. The performance of the prosthetic foot during the 'heel strike' and 'toe off' is shown in appendix 8 and it shows the composite prosthetic foot performance higher in each gait cycle.

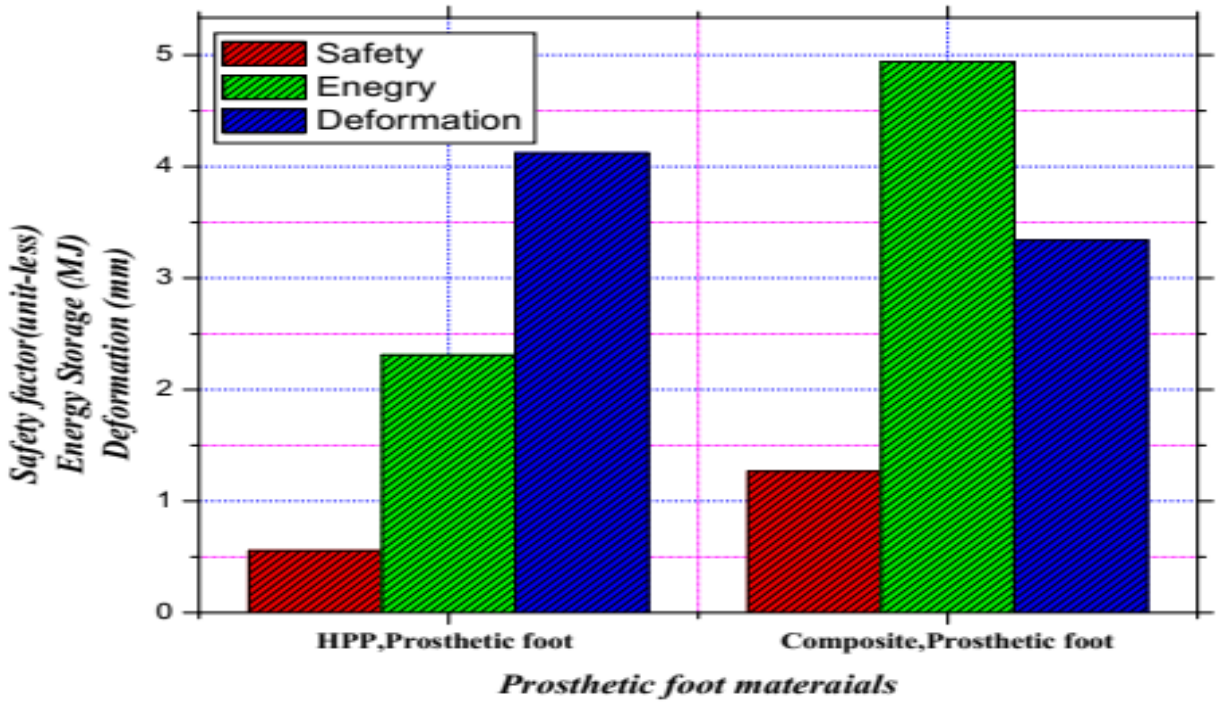

Figure 5. 16 Comparison of safety factor, deformation and energy storage of prosthetic foot,

5.4.2 Material Stiffness, weight and cost estimation comparisons

The stiffness, weight of prosthetic foot and material cost estimation for single prosthetic foot calculated in chapter four and discussed as follows.

5.4.2.1 Stiffness comparisons of prosthetic foot

The stiffness of material is important for the prosthetic foot to increase its weight carrying of amputees. Additionally, it allows the amputees to safely use the prosthetic foot as his/her body weight is increased. From the analysis of stiffness in chapter four of section 4.5.6, the stiffness of the prosthetic foot made from multi blade HPP and single blade composite is 95.26N/m and 117.34N/m respectively. This shows the stiffness of prosthetic foot is increased by 18.8% as the single blade of composite is replaced. This allows the prosthetic foot to serve the under safety region as weight of amputees may increase as human being is growing.

5.4.2.2 Weight Comparison of prosthetic foot

The weight of prosthetic foot is one of important consideration in design and modeling of prosthetic limbs. The weight of the current prosthetic foot model made from HPP and single blade

composite is 2.002N and 1.389N respectively. Due the replacement of multi blade HPP by single composite blade the thickness and number of blades is reduced from 5mm to 2.5mm and four blades to one blade respectively. In addition to this, the weight of prosthetic foot is saved by 30.62%. So, the laminated hybrid glass-carbon/epoxy composite blade prosthetic foot is very light weight material than that of the current conventional HPP multi blade prosthetic foot in Prosthetic orthotic center.

5.4.2.3 Product cost estimation comparisons for prosthetic foots

It's known that the carbon fiber is higher in its strength and cost than other synthetic fibers, while, E-glass fiber is cheaper and good in its strength. Considering this, only two layer carbon fiber/epoxy lamina is used in laminate; while, the four remaining layer is glass/epoxy layer. Even though the HPP is cheaper, due to four-blades of HPP each with 5mm laminated together to have strength for the prosthetic foot its cost is higher than composite made prosthetic foot. The cost of HPP material needed to produce single foot is estimated as 0.61$/foot without tax cost. The cost of composite material for producing single bladed prosthetic foot is estimated as 0.48$/foot. This shows 21.3% cost reduction due to the multi-blade foot is replaced by single bladed composite foot. Therefore, the laminated hybrid glass-carbon/epoxy composite blade prosthetic foot design require less material cost than that of the current conventional HPP multi blade prosthetic foot in Prosthetic orthotic center. The comparision among two materials in prosthetic foot in there stiffness,weight and cost are summarized in figure 5.17.

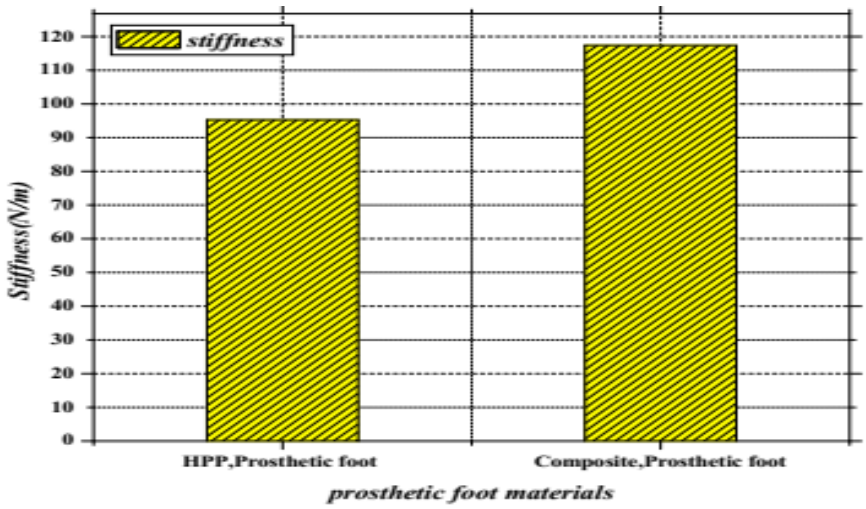

a)

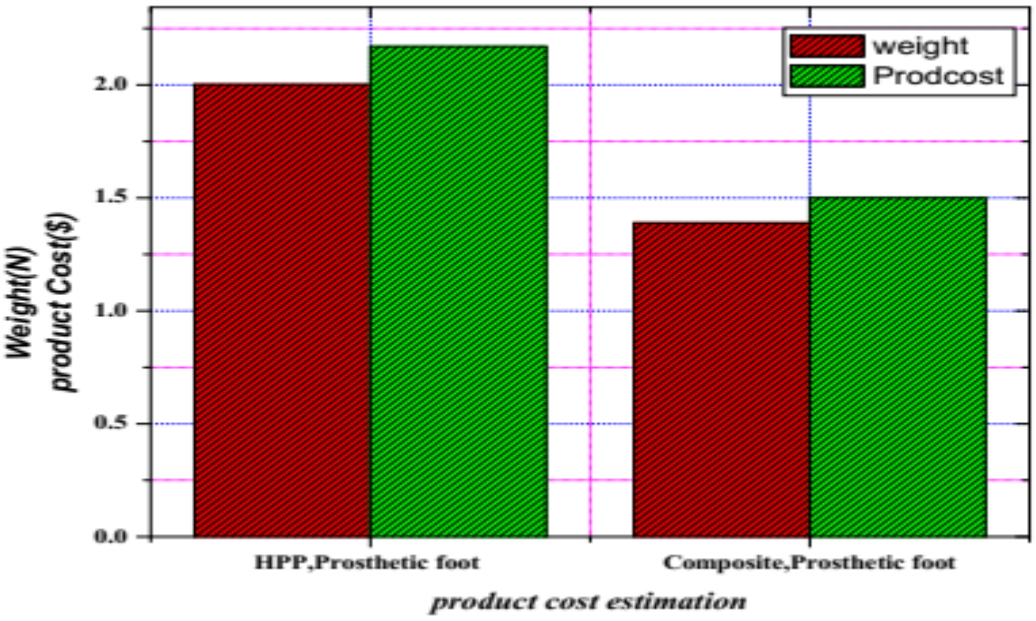

b)

Figure 5. 17 Comparison of a) stiffness, b) weight and cost estimation of prosthetic foot

Additionally, manufacturing of prosthetic foot from HPP requires high material cost, labor cost and machining cost than composite prosthetic foot. The production cost for single prosthetic foot from HPP is estimated as 101.91 Ethiopian birr while the composite prosthetic foot by hand layup techniques is estimated as 70.5 Ethiopian birr.

CHAPTER FIVE
CONCLUSION, RECOMMENDATION AND FUTURE WORK

Conclusion

As the development of composite material is in need to be the solution for HPP prosthetic foot problems, it's necessary characterize and select best configuration of composite laminate for this specific application with numerical method. In this thesis, the main objective is to characterize the tensile and flexural properties of the four stacking sequences of pure E-glass and hybrid (E-glass/carbon) epoxy composite proposed for prosthetic foot and selecting high strength configuration that yields higher performance prosthetic foot model than HPP model of prosthetic foot without experimental cost using powerful FEA software (ANSYS 19.2).This was started by applying micro-mechanics approach for determining the elastic and strength property of lamina, then applying progressive failure analysis based on Tsai-Wu failure theory in ANSYS 19.2 work bench and validating the numerical result with theoretical MATLAB solution with in terms of their ultimate failure load. The selected composite material (SS-3) was applied and simulated for the model of single blade of prosthetic foot that replaces the four blades of prosthetic foot model made from HPP in POC with higher performance, in terms of the its stiffness, strength, safety, weight, material cost and energy storage ability. From the result obtained the following is drawn.

- The ROM and Halpin-Tsai correctly predicts longitudinal and transversal properties of the lamina with an acceptable range of errors from (1.66%-3.04%) and (0.5%-3.02%) respectively compared to experimental result of [35].
- The strength of unidirectional lamina can be predicted by analytical model of [43] with an error less than 12.3% except for transversal compressive and shear strength lamina when compared with experimental results [35] of the same lamina.
- The plies failure order in the laminate is important in determining load carrying capacity of laminate and depends on stacking sequence of lamina in the laminate. In pure E-glass/epoxy composite under tensile loading changing stacking configuration from $[45/0/90]_s$ to $[0/90/45]_s$ increase FPF load from 1440.2N to 1443.2N. Similarly, in hybrid glass-carbon/epoxy composite changing the stacking sequence from $[45_c/90/45]_s$

to$[0_c/90/45]_s$ increases FPF load from 1471.84N to 2401.6N.Additionally, it has similar influence on flexural properties.

- The stacking sequence highly affects the ultimate tensile and flexural strength of laminate. In pure E-glass/epoxy and hybrid/epoxy laminate the ultimate tensile strength is increased from 777.44Mpa to1475.5Mpa and 1865Mpa to 1935Mpa respectively. Similarly, in flexural testing the ultimate flexural strength of hybrid composite is increased from 1299.2Mpa -1934.3Mpa due effect of stacking sequence.
- Among the all stacking configuration the SS-3 ($[0_c/90/45]_s$) results higher tensile and flexural strength and selected for prosthetic foot.
- The theoretical analysis of laminate accurately verify the numerical results. The ultimate failure loads of laminate in each stacking sequence verified the numerical results with an error less than 2% and 3% for tensile and flexural loading respectively.
- The single blade of composite with thickness of 2.5mm with higher performance replaces the four blades of HPP each with the thickness of 5mm is bonded together to build the prosthetic foot and allows the artificial foot to be less in weight and manufacturing cost in addition to providing more strength and comfort.
- The prosthetic foot model made from HPP has less strength and less resistance to deformation under the same loading condition. The model is not operating under the material stress limits. Its maximum equivalent stresses HPP is 49.055MPa which is higher than its ultimate strength, 37MPa. But, in composite model the equivalent stress is 493.28MPa which is lower than its ultimate strength. The deformation resistance of composite foot is increased by 18.9%. This indicates that composite prosthetic blade has higher strength. As a result less material (small thickness) can be used and allow the design for a reduction in weight and overall production cost.
- The composite prosthetic foot is comfortable for amputees and assist the forward propulsion of a body as the stored energy is released. It has higher ability to restore energy than HPP foot while walking. The energy storage capacity of the prosthetic blade is increased by 53.2%.
- The composite blade allows the safety factor to increase by 56.2% without showing any damage under operating load. Its stiffness is increased by 18.8% allows serve more

weighted amputees without permanent deformation that reduces energy storage capabilities.

- The laminated hybrid glass-carbon/epoxy composite blade prosthetic foot is very light weight material than that of the current HPP multi blade prosthetic foot in Prosthetic orthotic center. Due the replacement of multi blade HPP prosthetic foot design by single composite blade the weight of prosthetic foot is saved by 30.62% and allows material cost to be reduced by 21.3%.

Recommendation and future work

Finally, it is recommended that the hybrid glass-carbon/epoxy composite materials are suitable for prosthetic foot. It's suggested to be used by prosthetic producers. This material further recommended for POC of Ethiopia as it provides the solution for HPP made prosthetic foots. Several extensions on the current study could be performed. The prototype of prosthetic foot doesn't manufactured in this study. So I recommend further research study on porotype of the two models to be analyzed and compared for further verification and modification of the composite prosthetic foot. The experimental research can be performed on tensile and flexural characterization of selected composite for further verification of numerical and theoretical results. The numerical impact analysis of composite is expected for the future study by extracting important data of composite for numerical analysis by experimental investigation. Additionally, I recommend future study on the performance analysis of the two prosthetic foot model during the all gait cycle.

References

[1] H. Woldeyes, "Satisfaction of Lower Prosthesis Limb Users in Addis Ababa, Ethiopia," *Addis Ababa University,* pp. 1-2, 2016.

[2] M. Dessie, "Preventable amputations in Ethiopia," *East and Central African Journal of Surgery,* vol. 1, no. 9, 2004.

[3] Spoden, M., Nimptsch, U. and Mansky, T.,, " Amputation rates of the lower limb by amputation level–observational study using German national hospital discharge data from 2005 to 2015," *BMC health services research,* vol. 1, no. 19, pp. 1-9, 2019.

[4] H. Maddah, "Polypropylene as a promising plastic: A review," *Am. J. Polym. Sci,,* vol. 6, no. 1, pp. 1-11, 2016.

[5] North Sea-Plastics-Ltd, "North Sea Plastics Ltd," 2021. [Online]. Available: https://www.northseaplastics.com/products/homopolymer-polypropylene/. [Accessed 2021].

[6] Ottobock-Company, "catálogo-de-materiales-gb,ottobock materials, components and systems," Ottobocko-manufacturer, 2019.

[7] C. Groner, 2013. Available: Trends and techniques in materials, part I: O&P,https://lermagazine.com/article/trends-and-techniques-in-materials-part-i-op. [Accessed january 2013].

[8] D. A. Berry, "Composite-Materials for Orthotics And Prosthetics. Orthotics and Prosthetics, 40(4), 35-43," vol. 4, no. 40, pp. 35-43, 1987.

[9] Abood, S.H. and Faidh-Allah, M.H.,, "Analysis of prosthetic running blade of limb using different composite materials., 25(12), pp.15-25.," *Journal of Engineering,* vol. 25, no. 12, pp. 15-25, 2019.

[10] B. L. Klasson., "Carbon fiber and fibril lamination in prosthetics and orthotics; some basic theory and practical advice for the practitioner," *Prosthetics and Orthotics International,* Vols. 74-91, 1995.

[11] A. NamahHadi and J. Oleiwi., "Improve Flexural Strength of PMMA/SR Polymer Blend by Reinforcement with Carbon Fibers as Prosthetic Foot Polymer Material," *International Journal of Application or Innovation in Engineering & Management (IJAIEM),* vol. 4, no. 2, pp. ISSN 2319-4847, 2015.

[12] Jweeg, M. J., Alhumandy, A. A., & Hamzah, H. A., "Material Characterization and Stress Analysis of Openings in Syme's Prosthetics. , 17(04), 100-108.," *International Journal of Mechanical & Mechatronics Engineering IJMME-IJENS,* vol. 4, no. 17, pp. 100-108, 2017.

[13] Walke, K. M., & Pandure, P. S. , "(2017). Mechanical Properties of Materials Used for Prosthetic Foot: A Review.," *IOSR Journal of Mechanical and Civil Engineering (IOSR-JMCE),* pp. pp 61-65, 2017.

[14] Onal,L. and Adanur,.S., "Effect of stacking sequence on mechanical properties of glass-carbon hybrid composites before and after impact," *jounar of industrial textiles,* vol. 4, no. 31, pp. 255-271, 2002.

[15] Petru,M. and Novak,O., "FEM analysis of mechanical and stractural properties of long fiber-reinforced composites," *numerical analysis and solution techniques,* 2017.

[16] Autar-K.Kaw, Mechanics of Composite Materials, Second Ed. ed., US: Taylor & Francis Group: LLC, 2006.

[17] Clyne TW, Hull D., An introduction to composite materials, 3rd ed. ed., Cambridge : Cambridge University Press, 2019.

[18] Shahar FS, Hameed Sultan MT, Lee SH, Jawaid M, Md Shah AU, Safri SNA, Sivasankaran PN, "A review on the orthotics and prosthetics and the potential of kenaf composites as alternative materials for ankle-foot orthosis," *J Mech Behav Biomed Material,doi: 10.1016/j.jmbbm.2019.07.020.,* pp. 165-189, 2019.

[19] A. Jacob, "ACMA's composites 2004:The US composites industry. Reinforced Plastics," Elsevier, Florida, 2004.

[20] Rajak, D.K., Pagar, D.D., Kumar, R. and Pruncu, C.I, "Recent progress of reinforcement materials: A comprehensive overview of composite materials," *Journal of Materials Research and Technology,* vol. 8, no. 6, pp. 6354-6374, 2019.

[21] Gurit, "Guide to Composite," Gurit press, Uk, 2001.

[22] Bunsell AR, Renard J. , "Fundamentals of fiber reinforced composite materials," *CRC Press,* 2005.

[23] Compositeslab,"Compositeslab,"2016.Available:http://compositeslab.com/composites-manufacturingprocesses/. [Accessed 2016].

[24] Al-Khazraji, K., Kadhim, J., & Ahmed, P. S., "Tensile and fatigue characteristics of lower-limb prosthetic socket made from composite materials.," Istanbul,Turkey, 2012.

[25] Walke, K. M., & Pandure, P. S. , "Mechanical Properties of Materials Used for Prosthetic Foot: A Review., 61, 65.," *IOSR Journal of Mechanical and Civil Engineering (IOSR-JMCE),* Vols. 61,65, 2017.

[26] Mahmood, H., Vanzetti, L., Bersani, M., & Pegoretti, A., "Mechanical properties and strain monitoring of glass-epoxy composites with graphene-coated fibers," *Composites Part A: Applied Science and Manufacturing, 107,,* pp. 112-123, 2018.

[27] Abbas, S.M. and Kubba, A.I., " Fatigue Characteristics and Numerical Modelling Prosthetic for Chopart Amputation," *Modelling and Simulation in Engineering,2020,* 2020.

[28] Khare, J.M., Dahiya, S., Gangil, B. and Ranakoti, L., , "Influence of different resins on Physico-Mechanical properties of hybrid fiber reinforced polymer composites used in human prosthetics," *Materials Today: Proceedings,* vol. 38, pp. 345-349, 2021.

[29] Nurhaniza, M., Ariffin, M.K.A., Ali, A., Mustapha, F. and Noraini, A.W, "Finite element analysis of composites materials for aerospace applications. (Vol. 11, No. 1, p. 012010). IOP Pu," *In IOP conference series: materials science and engineering,* vol. 11, no. 1,p012010, 2010.

[30] Yogonanda. A, R. Vijayakumar, "Strength Prediction of Composite Laminate," *Nternational Journal of Engineering Research & Technology (IJERT),* Vol. 02, No. 08, 2013.

[31] C. Dong, "Flexural properties of symmetric carbon and glass fibre reinforced hybrid composite laminates. , 3,," *Composites Part C: Open Access p.100047.,* vol. 3, 2020.

[32] Ouarhim, W., Ait-Dahi, M., Bensalah, M. O., El Achaby, M., Rodrigue, D., Bouhfid, R., & Qaiss, A., "Characterization and numerical simulation of laminated glass fiber–polyester composites for a prosthetic running blade.," *Journal of Reinforced Plastics and Composites,* Vols. 3-4, no. 40, pp. 118-133, 2021.

[33] HCL-teams, 2020. [Online]. Available: https://slidetodoc.com/introduction-to-finite-element-analysis-1-introduction-to/. [Accessed 2020].

[34] U.S. Koruche, S.F.Patil,, "Application of Classical Lamination Theory and Analytical Modeling of laminates," *International Research Journal of Engineering and Technology (IRJET)* , vol. 02, no. 02 | May-2015, p. 1, 2015.

[35] Daniel, IM & Ishai, Engineering Mechanics of Composite Materials. Second edition, ,, New York.: Oxford University Press, 2006.

[36] M. Sudheer,Pradyoth K. R, S.Somayaji, "Analytical and Numerical Validation of Epoxy/Glass," *American Journal of Materials Science,* vol. 5, no. 3c, p. 1, 2015.

[37] R. M. JONES, Mechanics of composite materials, second edition ed., Philadelphia: Taylor & Francis, 1999.

[38] S. K. a. O.Soykasap, "On the Effective Tensile and Bending Properties of plane weave single glass/epoxy," Denver, Colorado, April 2011.

[39] P. Mallick, Fiber-reinforced composites : materials, manufacturing, and design, third edition ed., Dearborn, Michigan: CRC Press, 2007.

[40] Xin, H., Mosallam, A., Liu, Y., Veljkovic, M., & He, J., "Mechanical characterization of a unidirectional pultruded composite lamina," *University of California,* p. 27, 2019.

[41] R. Jones, Mechanics of Composite Materials, 2nd ed ed., New York: McGraw-Hill, 1975.

[42] Halpin, J. C., and Tsai, S. W., "Effects of Environmental Factors on Composite material," *AFML-TR,* pp. 67, pp. 423, 1969.

[43] E. J. Barbero, Introduction to Composite Materials Design, Second Edition ed., Taylor & Francis Group, LLC: CRC Press, 2011.

[44] Bright, R.J. and Sumathi, M., "Failure analysis of FRP composite laminates using progressive failure criteria.," *International Journal of Scientific & Engineering Research* , vol. 8, no. 6, p. 12, 2017.

[45] A. Das, "MATLAB Central File Exchange," 2021. [Online]. Available: https://www.mathworks.com/matlabcentral/fileexchange/54519-composite-laminate-failure), MATLAB Central File Exchange.. [Accessed 2021].

[46] ANSYS-Help, "ANSYS Help System version 19.2.," ANSYS., Canonsburg, PA, USA, 2019.

[47] ASTM-D3039, Standard Test Method for Tensile Properties of Polymer MatrixComposite Materials, 14(2): 99-109. ed., Philadelphia: Annual Book of ASTM Standards, American Society for Testing, 1995.

[48] Murugan, R., Narasimhan, R.L. and Harish, A , "Effect of Fiber Orientation on Effective Stacking Sequence of Glass/Carbon," Atlantis Press., February,2018.

[49] ANSYS-Inc., "ANSYS Composite PrepPost 17.0," ANSYS, Inc., 2015.

[50] Chen, D., Yan, R., Lu, X. and Li, M, "Progressive failure and ultimate strength analysis of sandwich composite hat-stringer-stiffened panels under transverse in-plane loading.," *Journal of Mechanics of Materials and Structures, 16(1), ,* vol. 16, no. 1, pp. pp.1-21., 2021.

[51] K. I. Tserpes, G. Labeas, P. Papanikos, et al., "Strength prediction of bolted joints in graphite/epoxy composite laminates," *Compos. B Eng. 33:7,* p. 521–529, 2002.

[52] Kozlov, M.V. and Sheshenin, S.V, "Modeling the progressive failure of laminated composites," in *Mechanics of Composite Materials*, vol. 51, springer, 2016, pp. pp.695-706.

[53] Stevens, Gretchen; Roberts, "The weight of nations: an estimation of adult human biomass, 12:439. 12 (1): 439," *BMC Public Health. ,* vol. 12, no. 1, p. 439, 2012.

[54] Bader, Rainer & Mau-Moeller, Anett., "The mental representation of the human gait in young and older adults.," *Frontiers in Psychology. 6. 943. 10.3389/fpsyg.2015.00943.,* 2015.

[55] Guritproduct,2019.Available:https://www.directindustry.com/prod/gurit/product37817-1403881.html.

[56] SIMONAProduct,2018.Available:https://www.simonaamerica.com/fileadmin/user_upload/USA/Downloads/SIMONA_PPH_Data_Sheet.pdf].

[57] Abood, S.H. and Faidh-Allah, M.H, " Analysis of prosthetic running blade of limb using different composite materials. , 25(12), pp.15-25.," *Journal of Engineering,* vol. 25, no. 12, pp. 15-25, 2019.

[58] M. A., "Design and Static Analysis of Carbon/Epoxy Composite Mono Leaf Spring for Light Vehicle Using FEM," *Addis Ababa university,* p. 66, 2017.

[59] SIMOLIFEPP,2020.Available:https://www.simona.de/index.php?id=206&L=1&productBase=Sheets.

[60] A. Joshi, "A Break-Down Model for Cost Estimation of Composites," in *Doctoral dissertation, Ohio University.*, Ohio, 2018.

[61] AlibabaTrading,2020.Available:https://www.alibaba.com/premium/fiberglass_price_per_kg.html?src=sem_ggl&from=sem_ggl&cmpgn=10516965275&adgrp=108101247510&fditm=&tgt=kwd358434804881&locintrst=&locphyscl=1005570&mtchtyp=e&ntwrk=g&device=c&dvcmdl=&creative=447940557546&plcmnt=&plcmntcat=.

[62] W. F. Lazarus, "Machinery cost estimation," university of minnesota, Minnesota, 2013.

[63] J. C. Hartman, "Engineering economy and the decision-making process.," in *Prentice Hall*, Pearson, 2007.

[64] Rehontec,"https://www.renhotecic.com/9-In-1-Magic-Handsaw-Set-DIY-HandBow Saws-Wood-Stone-Metal-Working-Cutting Tools?gclid=Cj0KCQjw8p2MBhCiARIsADDUFVH3IwpWZBpheRMIn5KtiX_g1Yy8uckOz1F0CWTzd5HKy7cmq_C1kGYaAuG_EALw_wcB," Renhotec, 2021. .

[65] "https://www.pet-mold.com/h-col-104.html," 2020. [Online].

[66] A.Goel, Economics of Composite MaterialManufacturingEquipment," Massachusetts Institute of Technology, 2000.

[67] R. Murugan, R. Ramesh and K. Padmanabhan, "Investigation of the mechanical behavior and vibration characteristics ofthin walled glass/carbon hybrid composite beams under a thin walled glass/carbon hybrid composite beams under a fixed BC," *Mechanics of Advanced Material nad structures*, vol. 23, no. 8, pp. 901-906, 2016.

[68] B. L. Klasson, "Carbon fiber and fibril lamination in prosthetics and orthotics; some basic theory and practical advice for the practitioner," *Prosthetics and Orthotics International,*, Vols. 74-91, 1995.

[69] Footbionics,2020.Available:https://www.footbionics.com/Patients/The+Gait+Cycle.html.

Appendix

Appendix-1

The material properties of E-glass fiber, carbon fiber, epoxy matrix and UD E-glass/epoxy lamina taken from [35]

TABLE A.2 Mechanical and Thermal Properties of Representative Fibers

Property	E-Glass	S-Glass	AS-4 Carbon	T-300 Carbon	IM7 Carbon	Boron	Kevlar 49 Aramid	Silicon Carbide (Nicalon)
Longitudinal modulus, E_{1f}, GPa (Msi)	73 (10.5)	86 (12.4)	235 (34)	230 (33)	290 (42)	395 (57)	131 (19)	172 (25)
Transverse modulus, E_{2f}, GPa (Msi)	73 (10.5)	86 (12.4)	15 (2.2)	15 (2.2)	21 (3)	395 (57)	7 (1.0)	172 (25)
Axial shear modulus, G_{12f}, GPa (Msi)	30 (4.3)	35 (5.0)	27 (4.0)	27 (4.0)	14 (2)	165 (24)	21 (3.1)	73 (10.6)
Transverse shear modulus, G_{23f}, GPa (Msi)	30 (4.3)	35 (5.0)	7 (1.0)	7 (1.0)	—	—	—	—
Poisson's ratio, ν_{12f}	0.23	0.23	0.20	0.20	0.20	0.13	0.33	0.20
Longitudinal tensile strength, F_{1f}, MPa (ksi)	3450 (500)	4500 (650)	3700 (535)	3100 (450)	5170 (750)	3450 (500)	3800 (550)	2070 (300)
Longitudinal coefficient of thermal expansion, α_{1f}, 10^{-6}/°C (10^{-6}/°F)	5.0 (2.8)	5.6 (3.1)	−0.5 (−0.3)	−0.7 (−0.4)	−0.2 (−0.1)	16 (8.9)	−2 (−1.1)	3.2 (1.8)
Transverse coefficient of thermal expansion, α_{2f}, 10^{-6}/°C (10^{-6}/°F)	5.0 (2.8)	5.6 (3.1)	15 (8.3)	12 (6.7)	10 (5.6)	16 (8.9)	60 (33)	3.2 (1.8)

TABLE A.3 Properties of Typical Polymer Matrix Materials

Property	Epoxy (3501-6)	Epoxy (977-3)	Epoxy (HY6010/ HT917/DY070)	Polyesters	Vinylester (Derakane)	Polyimides	Poly-ether-ether-ketone (PEEK)
Density, ρ, g/cm³ (lb/in³)	1.27 (0.046)	1.28 (0.046)	1.17 (0.043)	1.1–1.5 (0.040–0.054)	1.15 (0.042)	1.4–1.9 (0.050–0.069)	1.32 (0.049)
Young's modulus, E_m, GPa (Msi)	4.3 (0.62)	3.7 (0.54)	3.4 (0.49)	3.2–3.5 (0.46–0.51)	3–4 (0.43–0.58)	3.1–4.9 (0.45–0.71)	3.7 (0.53)
Shear modulus, G_m, GPa (Msi)	1.60 (0.24)	1.37 (0.20)	1.26 (0.18)	0.7–2.0 (0.10–0.30)	1.1–1.5 (0.16–0.21)		
Poisson's ratio, ν_m	0.35	0.35	0.36	0.35	0.35		
Tensile strength, F_{tu}, MPa (ksi)	69 (10)	90 (13)	80 (11.6)	40–90 (5.8–13.0)	65–90 (9.4–13.0)	70–120 (10.1–17.4)	96 (14)
Compressive strength, F_{cu}, MPa (ksi)	200 (30)	175 (25)	104 (15.1)	90–250 (13–35)	127 (18.4)		
Shear strength, F_{su}, MPa (ksi)	100 (15)	52 (7.5)	40 (5.8)	45 (6.5)	53 (29)		
Coefficient of thermal expansion, α_m, 10^{-6}/°C (10^{-6}/°F)	45 (25)	—	62 (3.4)	60–200 (33–110)	100–150 (212–514)	90 (50)	
Glass transition temperature, T_g, °C (°F)	200 (390)	200 (390)	152 (305)	50–110 (120–230)	—	280–320 (540–610)	143 (290)
Maximum use temperature, T_{max}, °C (°F)	150 (300)	177 (350)	—	—	—	300–370 (570–700)	250 (480)
Ultimate tensile strain, ε_m^u, (%)	2–5	—	—	2–5	1–5	1.5–3.0	

TABLE A.6 Properties of Typical Unidirectional and Fabric Composite Materials (Three-Dimensional)

	E-Glass/Epoxy		Kevlar 49/Epoxy		Carbon/Epoxy	
Property	Unidirectional	Fabric (M10E/ 3783)	Unidirectional	Fabric (K120/ M10.2)	Unidirectional (AS4/ 3501-6)	Woven Fabric (AGP370-5H/ 3501-6S)
Fiber volume ratio, V_f	0.55	0.50	0.60	—	0.63	0.62
Density, ρ, g/cm³ (lb/in³)	1.97 (0.071)	1.90 (0.068)	1.38 (0.050)	—	1.60 (0.058)	1.60 (0.058)
Longitudinal modulus, E_1, GPa (Msi)	41 (6.00)	24.5 (3.55)	80 (11.6)	29 (4.2)	147 (21.3)	77 (11.2)
Transverse in-plane modulus, E_2, GPa (Msi)	10.4 (1.50)	23.8 (3.45)	5.5 (0.80)	29 (4.2)	10.3 (1.50)	75 (10.9)
Transverse out-of-plane modulus, E_3, GPa (Msi)	10.4 (1.50)	11.6 (1.68)	5.5 (0.80)	—	10.3 (1.50)	13.8 (2.0)
In-plane shear modulus, G_{12}, GPa (Msi)	4.3 (0.62)	4.7 (0.68)	2.2 (0.31)	18 (2.6)	7.0 (1.00)	6.5 (0.94)
Out-of-plane shear modulus, G_{23}, GPa (Msi)	3.5 (0.50)	3.6 (0.52)	1.8 (0.26)	—	3.7 (0.54)	4.1 (0.59)
Out-of-plane shear modulus, G_{13}, GPa (Msi)	4.3 (0.62)	2.6 (0.38)	2.2 (0.31)	—	7.0 (1.00)	5.1 (0.74)
Major in-plane Poisson's ratio, ν_{12}	0.28	0.11	0.34	0.05	0.27	0.06
Out-of-plane Poisson's ratio, ν_{23}	0.50	0.20	0.40	—	0.54	0.37
Out-of-plane Poisson's ratio, ν_{13}	0.28	0.15	0.34	0.05	0.27	0.50
Longitudinal tensile strength, F_{1t}, MPa (ksi)	1140 (165)	433 (62.8)	1400 (205)	369 (53.5)	2280 (330)	963 (140)
Transverse tensile strength, F_{2t}, MPa (ksi)	39 (5.7)	386 (55.9)	30 (4.2)	369 (53.5)	57 (8.3)	856 (124)
Out-of-plane tensile strength, F_{3t}, MPa (ksi)	39 (5.7)	27 (3.9)	30 (4.2)	—	57 (8.3)	60 (8.7)
Longitudinal compressive strength, F_{1c}, MPa (ksi)	620 (90)	377 (54.6)	335 (49)	129 (18.7)	1725 (250)	900 (130)
Transverse compressive strength, F_{2c}, MPa (ksi)	128 (18.6)	335 (48.6)	158 (22.9)	129 (18.7)	228 (33)	900 (130)
Out-of-plane compressive strength, F_{3c}, MPa (ksi)	128 (18.6)	237 (34.4)	158 (22.9)	—	228 (33)	813 (118)
In-plane shear strength, F_6, MPa (ksi)	89 (12.9)	84 (12.2)	49 (7.1)	113 (16.4)	76 (11.0)	71 (10.3)
Out-of-plane shear strength, F_4, MPa (ksi)	—	44 (6.3)	—	33 (4.8)	—	65 (9.5)
Out-of-plane shear strength, F_5, MPa (ksi)	—	41 (5.9)	37 (5.4)	33 (4.8)	—	75 (10.8)
Longitudinal thermal expansion coefficient, α_1, 10^{-6}/°C (10^{-6}/°F)	7.0 (3.9)	—	−2.0 (−1.1)	—	−0.9 (−0.5)	3.4 (1.9)
Transverse thermal expansion coefficient, α_2, 10^{-6}/°C (10^{-6}/°F)	26 (14.4)	—	60 (33)	—	27 (15)	3.7 (2.1)
Out-of-plane thermal expansion coefficient, α_3, 10^{-6}/°C (10^{-6}/°F)	26 (14.4)	—	60 (33)	—	27 (15)	52 (29)
Longitudinal moisture expansion coefficient, β_1	0	—	0	—	0.01	0.05
Transverse moisture expansion coefficient, β_2	0.2	—	0.3	—	0.20	0.05
Out-of-plane moisture expansion coefficient, β_3	0.2	—	0.3	—	0.20	0.27

Appendix-2

%Program Code Written By Galana Abay Kebede (AAiT)

```
%STEP-1:Orientation of lamina,lamina thickness and number of ply in laminate
theta=[0;90;45;45;90;0];%orientation of each ply
ply_thickness=0.41666;%thickness of single ply
number_of_plys=length(theta);%number of ply
ply_thickness=ply_thickness*ones(number_of_plys,1);%ply thickness if varying according to orientation
%STEP-2:Define material properties
E_1=41e9;
E_2=10.4e9;
G_12=4.3e9;
v_12=0.28;
v_21=E_2*v_12/E_1;
%STEP-3:Define load and moment applied (Tensile loading, Nx and flexural loading, MX )
N=[1000;1000;0];%in Newton/Meter
M=[0;0;0];
%STEP-4:Find the value of the stiffness matrix [Q]
Q11=E_1/(1-v_12*v_21);
Q22=E_2/(1-v_12*v_21);
Q12=v_12*E_2/(1-v_12*v_21);
Q66=G_12;
Q=[Q11,Q12,0;Q12,Q22,0;0,0,Q66];
%STEP-5:Define total thichness,size of ABD matrix and location ply
%surfaces(top and bottom)
h=sum(ply_thickness);%total thickness of laminate
A=zeros(3,3);%size of A matrix
B=zeros(3,3);%size of B matrix
D=zeros(3,3);%size of D matrix
z(1,:)=-h/2;%z1
for i=2:4 %Z2-Zn, where n is number of surface for each ply
```

```
z(i,:)=z(i-1)+ply_thickness(i-1);
end
%STEP-6:Find transformed reduced stiffness matrix Q_ for each ply and
%re-define stiffness matrix [Q] in terms of a,b,c and d for simplification
a=181.81e9;%a=Q11
b=2.897e9;%b=Q12
c=10.35e9;%c=Q22
d=7.17e9;%d=Q66
for i=(1:number_of_plys)
   m=cosd(theta(i));
   n=sind(theta(i));
Q_11=(a*m^4)+(c*n^4)+(2*(n^2)*(m^2))*(b+2*d);%Q=(Q_11 ) ?
Q_12=((a+c-(4*d))*(n^2)*(m^2))+b*((m^4)+(n^4));%R=(Q_12 ) ?
Q_16=(((a-b-(2*d))*(m^3)*n)-((c-b-(2*d))*(n^3)*m));%S=(Q_16 ) ?
Q_22=(a*n^4)+(c*m^4)+(2*(n^2)*(m^2))*(b+2*d);%T=(Q_22 ) ?
Q_26=(((a-b-(2*d))*(n^3)*m)-((c-b-(2*d))*(m^3)*n));%U=(Q_26 ) ?
Q_66=((a+c-(2*d)-(2*b))*(n^2)*(m^2))+d*((m^4)+(n^4));%V=(Q_66 )
Q_(:,:,i)=[Q_11,Q_12,Q_16;Q_12,Q_22,Q_26;Q_16,Q_26,Q_66];
A=A+Q_(:,:,i)*ply_thickness(i);
B=B+Q_(:,:,i)*(ply_thickness(i)*(z(i)+(ply_thickness(i)/2)));
D=D+Q_(:,:,i).*((ply_thickness(i)+z(i))^3-((z(i))^3))/3;
end
%STEP-7:Solve the six simultaneous equations to find the mid-plane strains and
%curvatures.
C=[A,B;B,D];%matrix made from matrix ABD
F=C\[N;M];%F=midplane starin and curvature or F=C\[N;M]=inv(C)*[N;M]
midstarin=F(1:3);
curvatures=F(4:6);
%STEP-8:Find the global strains in each ply(ex,ey,rxy)
for i=1:number_of_plys
   globalstraintop(:,:,i)=(midstarin +z(i,:).*curvatures);%global strain at top of 0,60,-60
```

```
   globalstrainbottom(:,:,i)=(midstarin +z(i+1,:).*curvatures);%global strain at bottom of 0,60,-60
end
%STEP-9:Find the global stresses using the stress-strain equation.
for i=(1:number_of_plys)%z1-z4
   globalstresstop(:,:,i)=Q_(:,:,i)*globalstraintop(:,:,i);%global stress at top of 0,90,45,45,90,0
   globalstressbottom(:,:,i)=Q_(:,:,i)*globalstrainbottom(:,:,i);
end
%STEP-10:Find the local strains and stress using the transformation equation.
R=[1,0,0;0,1,0;0,0,2];
for i=(1:number_of_plys)
   m=cosd(theta);
   n=sind(theta);
   T(:,:,i)=[m(i)^2,n(i)^2,2*m(i)*n(i);n(i)^2,m(i)^2,-2*m(i)*n(i);-m(i)*n(i),n(i)*m(i),m(i)^2-
n(i)^2];
   localstraintop(:,:,i)=R*T(:,:,i)*inv(R)*globalstraintop(:,:,i);%local strain at top of
0,90,45,45,90,0
   localstrainbottom(:,:,i)=R*T(:,:,i)*inv(R)*globalstrainbottom(:,:,i);%local strain at bottom of
0,90,45,45,90,0
end
for i=(1:number_of_plys)
   m=cosd(theta);
   n=sind(theta);
   T(:,:,i)=[m(i)^2,n(i)^2,2*m(i)*n(i);n(i)^2,m(i)^2,-2*m(i)*n(i);-m(i)*n(i),n(i)*m(i),m(i)^2-
n(i)^2];
   localstresstop(:,:,i)=T(:,:,i)* globalstresstop(:,:,i);%local stress at top of 0,60,-60
   localstressbottom(:,:,i)=T(:,:,i)* globalstressbottom(:,:,i);%local stress at top of 0,60,-60
end
%STEP-11:solve global and local for strain and stress at the middle of each
%ply
h=sum(ply_thickness);
Amid=zeros(3,3);
```

```
Bmid=zeros(3,3);
Dmid=zeros(3,3);
zmid(1,:)=(-h/2)+ply_thickness(1)/2;
for j=2:number_of_plys
zmid(j,:)=zmid(j-1)+ply_thickness(j-1)/2+ply_thickness(j)/2;
end
%STEP-11 (a):Find the value of the transformed reduced stiffness matrix [Q] for each
%ply
for j=(1:number_of_plys)
   mmid=cosd(theta(j));
   nmid=sind(theta(j));
Q_11mid=(a*mmid^4)+(c*nmid^4)+(2*(nmid^2)*(mmid^2))*(b+2*d);%Q=(Q_11 ) ?
Q_12mid=((a+c-(4*d))*(nmid^2)*(mmid^2))+b*((mmid^4)+(nmid^4));%R=(Q_12 ) ?
Q_16mid=(((a-b-(2*d))*(mmid^3)*nmid)-((c-b-(2*d))*(nmid^3)*mmid));%S=(Q_16 ) ?
Q_22mid=(a*nmid^4)+(c*mmid^4)+(2*(nmid^2)*(mmid^2))*(b+2*d);%T=(Q_22 ) ?
Q_26mid=(((a-b-(2*d))*(nmid^3)*mmid)-((c-b-(2*d))*(mmid^3)*nmid));%U=(Q_26 ) ?
Q_66mid=((a+c-(2*d)-(2*b))*(nmid^2)*(mmid^2))+d*((mmid^4)+(nmid^4));%V=(Q_66 )
Q_mid(:,:,j)=[Q_11mid,Q_12mid,Q_16mid;Q_12mid,Q_22mid,Q_26mid;Q_16mid,Q_26mid,Q
_66mid];
Amid=Amid+Q_mid(:,:,j)*ply_thickness(j);
Bmid=Bmid+Q_mid(:,:,j)*(ply_thickness(j)*zmid(j));
Dmid=Dmid+Q_mid(:,:,j)*(ply_thickness(j)*zmid(j)^2+ply_thickness(j)^3/12);
end
%STEP-11 (b):Solve the six simultaneous equations to find the mid-plane strains and
%curvatures.
Cmid=[Amid,Bmid;Bmid,Dmid];%matrix made from matrix ABD
Fmid=Cmid\[N;M];%F=midplane starin and curvature or F=C\[N;M]=inv(C)*[N;M]
midstarinmid=Fmid(1:3);
curvaturesmid=Fmid(4:6);
%STEP-11 (c):Find the global strains in each ply(ex,ey,rxy)
for j=1:number_of_plys
```

```
   globalstrainmiddle(:,:,j)=(midstarinmid +zmid(j,:).*curvaturesmid);%global strain at top of
0,90,45,45,90,0
end
%STEP-11 (d):Find the global stresses using the stress?strain equation.
for j=(1:number_of_plys)%z1-z4
   globalstressmiddle(:,:,j)=Q_mid(:,:,j)*globalstrainmiddle(:,:,j);%global stress at top of
0,90,45,45,90,0
end
%STEP-11 (e):Find the local strains using the transformation equation.
R=[1,0,0;0,1,0;0,0,2];
for j=(1:number_of_plys)
   mmid=cosd(theta);
   nmid=sind(theta);
   Tmid(:,:,j)=[mmid(j)^2,nmid(j)^2,2*mmid(j)*nmid(j);nmid(j)^2,mmid(j)^2,-
2*mmid(j)*nmid(j);-mmid(j)*nmid(j),nmid(j)*mmid(j),mmid(j)^2-nmid(j)^2];
   localstrainmiddle(:,:,j)=R*Tmid(:,:,j)*inv(R)*globalstrainmiddle(:,:,j);%local strain at top of
0,60,-60
end
for j=(1:number_of_plys)
    mmid=cosd(theta);
    nmid=sind(theta);
   Tmid(:,:,j)=[mmid(j)^2,nmid(j)^2,2*mmid(j)*nmid(j);nmid(j)^2,mmid(j)^2,-
2*mmid(j)*nmid(j);-mmid(j)*nmid(j),nmid(j)*mmid(j),mmid(j)^2-nmid(j)^2];
   localstressmiddle(:,:,j)=Tmid(:,:,j)*globalstressmiddle(:,:,j);%local stress at top of
0,90,45,45,90,0
end
% STEP-12:The portion of the load Nx taken by each ply,product of the stress at the middle of
% each ply and the thickness of the ply.
for j=(1:number_of_plys)
   loadtakenbyeachply(1,:,j)=globalstressmiddle(1,:,j).*ply_thickness;
end
```

Appendix-3

```
% Depending on stress analysis failure it identifies whether plies fail or not under a applied load.
t=input('enter thickness matrix ');
ang=input('enter angle matrix');
q0=input('enter q0 matrix');
n=input('enter loading matrix');
sigmalu=input('enter longitudinal tensile limit');
sigmaluc=input('enter longitudinal compressive limit');
sigmatu=input('enter transverse tensile limit');
sigmatuc=input('enter transverse compressive limit');
taultu=input('enter shear limit');
count=0;
s=size(t);
el=s(1,2);
u1=((3*q0(1,1)+3*q0(2,2)+2*q0(1,2)+4*q0(3,3))/8);
u2=((q0(1,1)-q0(2,2))/2);
u3=((q0(1,1)+q0(2,2)-2*q0(1,2)-4*q0(3,3))/8);
u4=((q0(1,1)+q0(2,2)+6*q0(1,2)-4*q0(3,3))/8);
u5=((q0(1,1)+q0(2,2)-2*q0(1,2)+4*q0(3,3))/8);
for i=1:el
   c=i+1;
   q0(1,1,c)=u1+u2*cos(2*ang(1,i))+u3*cos(4*ang(1,i));
   q0(1,2,c)=u4-u3*cos(4*(ang(1,i)));
   q0(1,3,c)=.5*u2*sin(2*(ang(1,i)))+u3*sin(4*(ang(1,i)));
   q0(2,1,c)=q0(1,2,c);
   q0(2,2,c)=u1-u2*cos(2*(ang(1,i)))+u3*cos(4*(ang(1,i)));
   q0(2,3,c)=.5*u2*sin(2*(ang(1,i)))-u3*sin(4*(ang(1,i)));
   q0(3,1,c)=q0(1,3,c);
   q0(3,2,c)=q0(2,3,c);
   q0(3,3,c)=u5-u3*cos(4*(ang(1,i)));
```

```
end
   sum=0;
   for i=1:el
      sum=sum+t(1,i);
   end
   strt=-sum/2;
   tmat(1,1)=strt;
   for i=1:el
      c=i+1;
      tmat(1,c)=tmat(1,c-1)+t(i);
   end
   a=[0 0 0
      0 0 0
      0 0 0];
   b=[0 0 0
      0 0 0
      0 0 0];
   d=[0 0 0
      0 0 0
      0 0 0];
   for i=1:el
      cf=i+1;
      a=a+q0(:,:,cf)*(tmat(1,i+1)-tmat(1,i));
   end
    for i=1:el
      cf=i+1;
      b=b+q0(:,:,cf)*(tmat(1,i+1)^2-tmat(1,i)^2);
    end
    b=b*.5;
    for i=1:el
      cf=i+1;
```

```
   d=d+q0(:,:,cf)*(tmat(1,i+1)^3-tmat(1,i)^3);
 end
d=d/3;
stif=[0 0 0 0 0 0
    0 0 0 0 0 0
    0 0 0 0 0 0
    0 0 0 0 0 0
    0 0 0 0 0 0
    0 0 0 0 0 0];
for i=1:3
    for j=1:3
        stif(i,j)=a(i,j);
    end
end
for i=1:3
    for j=4:6
        stif(i,j)=b(i,j-3);
    end
end
for i=4:6
    for j=1:3
        stif(i,j)=b(i-3,j);
    end
end
for i=4:6
    for j=4:6
        stif(i,j)=d(i-3,j-3);
    end
end
com=inv(stif);
strn=com*n;
```

```
ep=[0
   0
   0];
kap=[0
   0
   0];

ep(1,1)=strn(1,1);
ep(2,1)=strn(2,1);
ep(3,1)=strn(3,1);
kap(1,1)=strn(4,1);
kap(2,1)=strn(5,1);
kap(3,1)=strn(6,1);
trans=[0 0 0
   0 0 0
   0 0 0];
for i=1:el
   c=i+1;
   an=ang(1,i);
   trans(1,1)=(cos(an)^2);
   trans(1,2)=(sin(an)^2);
   trans(1,3)=2*(sin(an)*cos(an));
   trans(2,1)=(sin(an)^2);
   trans(2,2)=(cos(an)^2);
   trans(2,3)=-2*(sin(an)*cos(an));
   trans(3,1)=-(sin(an)*cos(an));
   trans(3,2)=(sin(an)*cos(an));
   trans(3,3)=(cos(an)^2)-(sin(an)^2);
   strain1=ep+kap*tmat(1,i);
   stress1=q0(:,:,c)*strain1;
   stress12=trans*stress1;
```

```
if stress12(1,1)>=0
   if stress12(2,1)>=0
      cond1=((stress12(1,1))/sigmalu)^2-
(stress12(1,1)*stress12(2,1)/(sigmalu^2))+(stress12(2,1)/sigmatu)^2+(stress12(3,1)/taultu)^2;
   else
      cond1=((stress12(1,1))/sigmalu)^2-
(stress12(1,1)*abs(stress12(2,1))/(sigmalu*sigmaluc))+(stress12(2,1)/sigmatuc)^2+(stress12(3,1)
/taultu)^2;
   end
else
   if stress12(2,1)>=0
      cond1=((stress12(1,1))/sigmaluc)^2-
(abs(stress12(1,1))*stress12(2,1)/(sigmaluc*sigmalu))+(stress12(2,1)/sigmatu)^2+(stress12(3,1)/
taultu)^2;
   else
      cond1=((stress12(1,1))/sigmaluc)^2-
(abs(stress12(1,1))*abs(stress12(2,1))/(sigmaluc^2))+(stress12(2,1)/sigmatuc)^2+(stress12(3,1)/t
aultu)^2;
   end
end
strain2=ep+kap*tmat(1,i+1);
stress2=q0(:,:,c)*strain2;
stress12=trans*stress2;
if stress12(1,1)>=0
   if stress12(2,1)>=0
      cond2=((stress12(1,1))/sigmalu)^2-
(stress12(1,1)*stress12(2,1)/(sigmalu^2))+(stress12(2,1)/sigmatu)^2+(stress12(3,1)/taultu)^2;
   else
      cond2=((stress12(1,1))/sigmalu)^2-
(stress12(1,1)*abs(stress12(2,1))/(sigmalu*sigmaluc))+(stress12(2,1)/sigmatuc)^2+(stress12(3,1)
/taultu)^2;
```

```
            end
        else
            if stress12(2,1)>=0
                cond2=((stress12(1,1))/sigmaluc)^2-
(abs(stress12(1,1))*stress12(2,1)/(sigmaluc*sigmalu))+(stress12(2,1)/sigmatu)^2+(stress12(3,1)/
taultu)^2;
            else
                cond2=((stress12(1,1))/sigmaluc)^2-
(abs(stress12(1,1))*abs(stress12(2,1))/(sigmaluc^2))+(stress12(2,1)/sigmatuc)^2+(stress12(3,1)/t
aultu)^2;
            end
        end

        if cond1<=1 && cond2<=1
            fprintf('this lamina is safe\n');
            count=count+1;
        else
            fprintf('this lamina is not safe\n');
        end
    end
    if count==el
        fprintf('laminate is safe\n');
    else
        fprintf('laminate is unsafe\n');
    end
```

Appendix-4

Data collected at POC through visual observation and interview

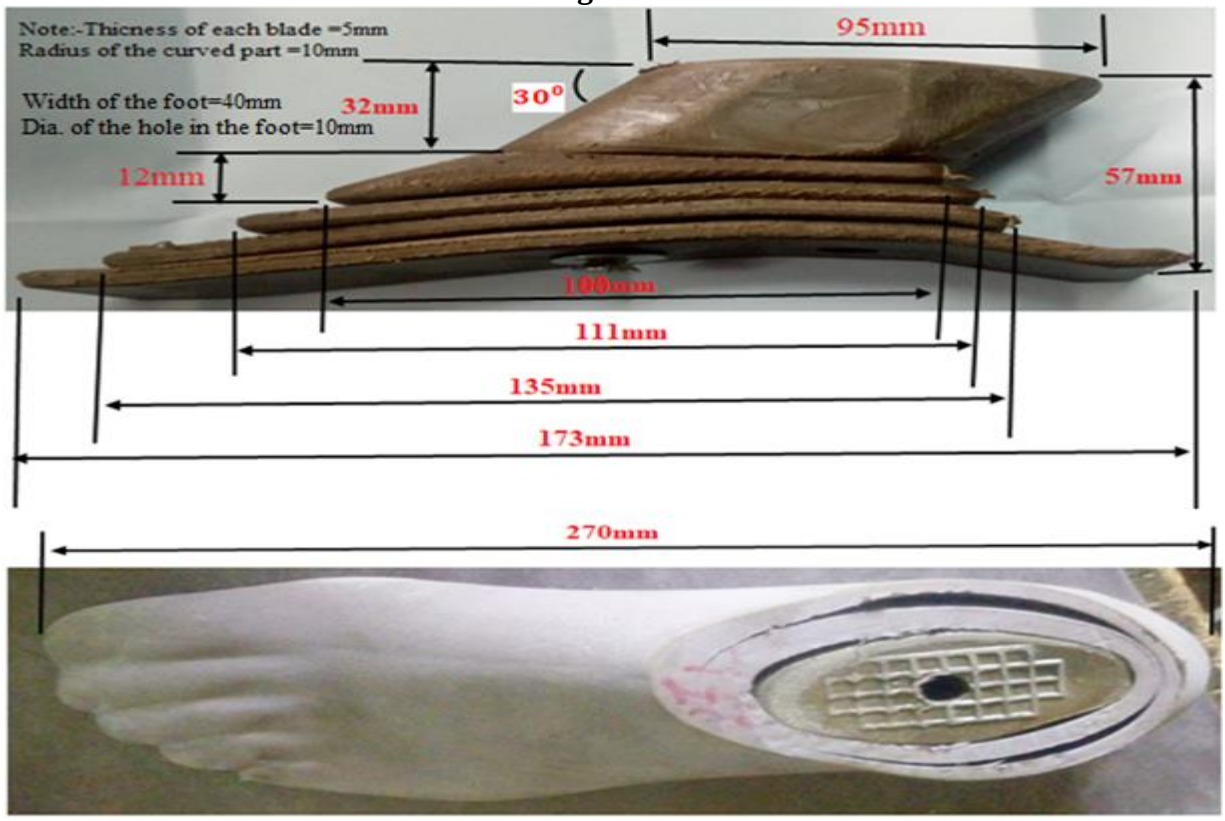

The dimension of prosthetic foot by direct measurement at POC



Interview with POC technician, prosthetic foot blades and injection molding machines

Appendix-5

At the initial load of 1443.2N the stress, strain and deformation are shown in figure below. The failure index of second layer laminate (90^0) are also shown in this figure.

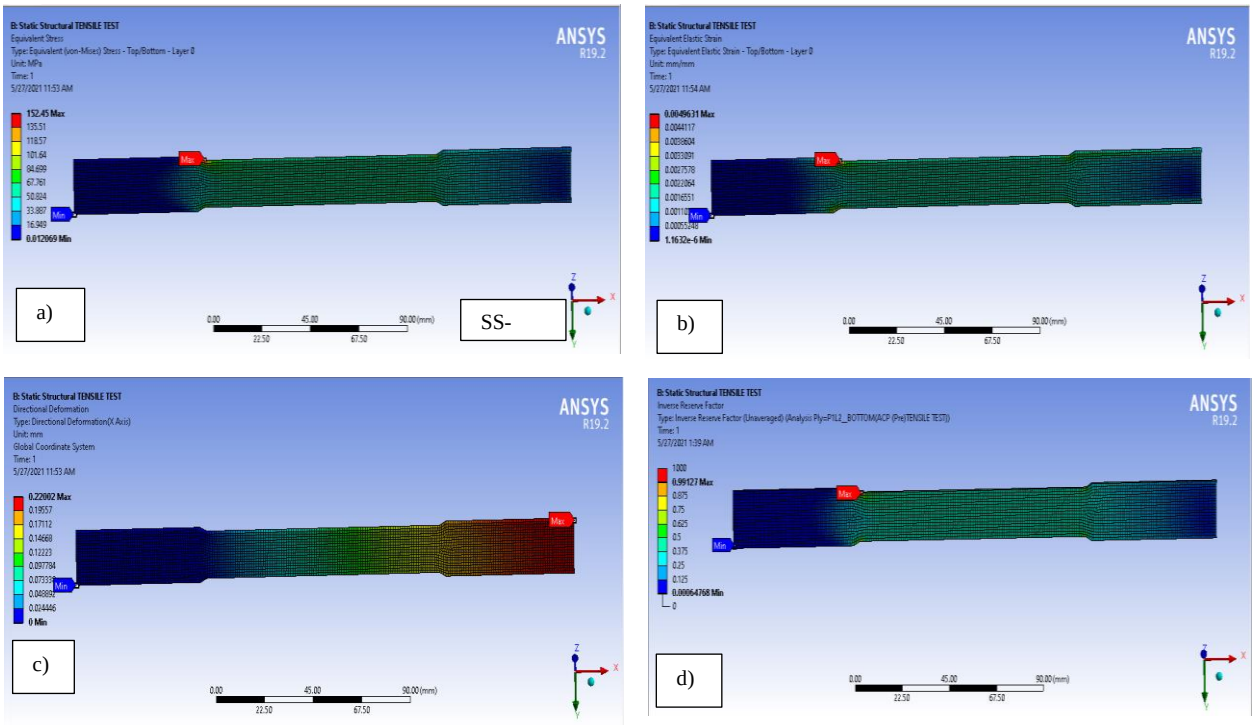

a)Stress, b)Strain c)deformation of composite and d) FI of second layer at 1443.2N

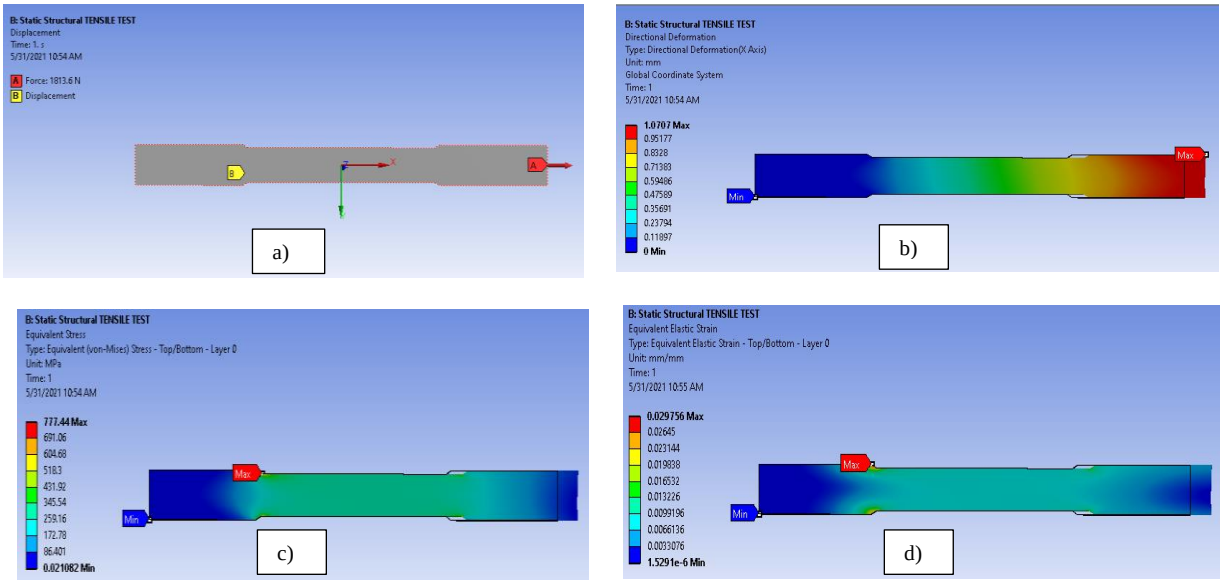

a) Ultimate failure load, b) deformation c) tensile strength and d) Strain at 1813.6N

Appendix-6

Summary of load, deflection, stress, and strain results tensile simulation SS-1 to SS-4 respectively

Force(N)1		**Displacement (mm)**	**Stress (MPa)**	**Strain (mm/mm)**
200	Initial applied load	0.030669	21.25	0.00069182
1443.2	First ply failure load	0.22002	152.45	0.0049631
1446.26	Second ply failure load	0.22178	153.67	0.0050028
1600	Third and fourth ply failure load	0.30584	209.76	0.0088371
1813.6	Fifth and six ply failure load	1.0707	777.44	0.029756
1711.98	Failure beyond last ply failure	1.3524	451.45	0.034521

Force (N)2		**Displacement (mm)**	**Stress (MPa)**	**Strain (mm/mm)**
200	Initial applied load	0.030704	20.602	0.00069053
1440.2	First ply and second failure load	0.2211	148.35	0.0049725
1453.35	third and fourth ply failure load	0.75472	596.33	0.02421
1748.23	Fifth ply failure load	1.1076	940.29	0.03522
2561.86	last ply failure load	2.7129	1475.5	0.069713
1985.25	Failure beyond last ply failure	2.8135	791.11	0.071245

Force(N)3		**Displacement(mm)**	**Stress(Mpa)**	**Strain(mm/mm)**
200	Initial applied load	0.014663	30.394	0.00044421
2401.6	First ply load	0.17608	364.97	0.005334
2471.01	second and third ply failure load	0.39917	785.34	0.013478
2554.53	Fourth ply failure load	0.56405	1257.1	0.02304
3154.57	Fifth ply failure load	0.82773	1768	0.044088
3592.74	last ply failure	1.0497	1935	0.057129
3125.12	Failure beyond last ply failure	1.0887	1725	0.059584

Force(N)4		Displacement(mm)	Stress(Mpa)	Strain(mm/mm)
200	Initial applied load	0.08874	45.027	0.00066011
1471.8	First ply load	0.21249	331.37	0.0048579
1498.62	second and third ply failure load	0.24573	394.16	0.0058145
1566.81	Fourth ply failure load	0.99936	1205.5	0.021645
1986.72	FIFTH ply failure load	1.6563	1626.3	0.034813
3080.01	last ply failure	1.891	1865.37	0.042475
2825.13	Failure beyond last ply failure	1.899	1614.25	0.04586

Appendix-7

Mesh convergence analysis results

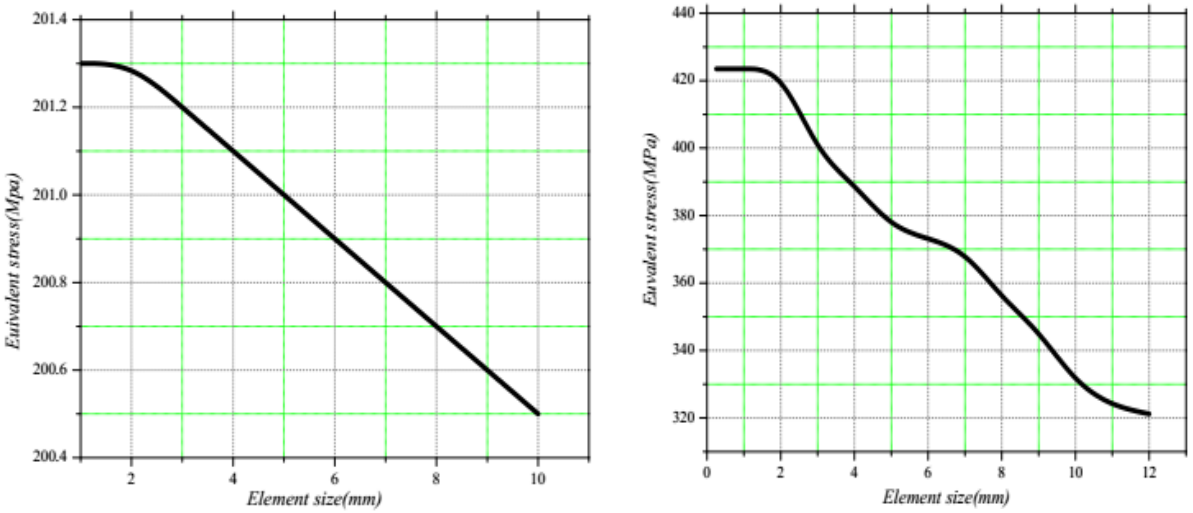

Mesh convergence analysis of tensile (left) and flexural (right) testing specimen model

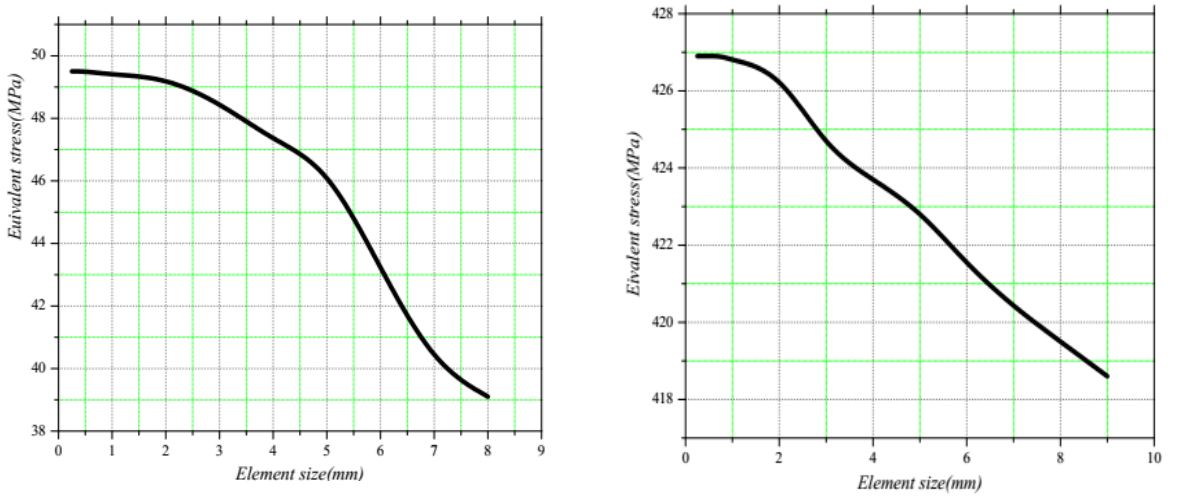

Mesh convergence analysis of HPP (left) and composite (right) prosthetic foot

Appendix-8

The simulation results of prosthetic foot model at the '**Heel strike**' with load of 196.2N

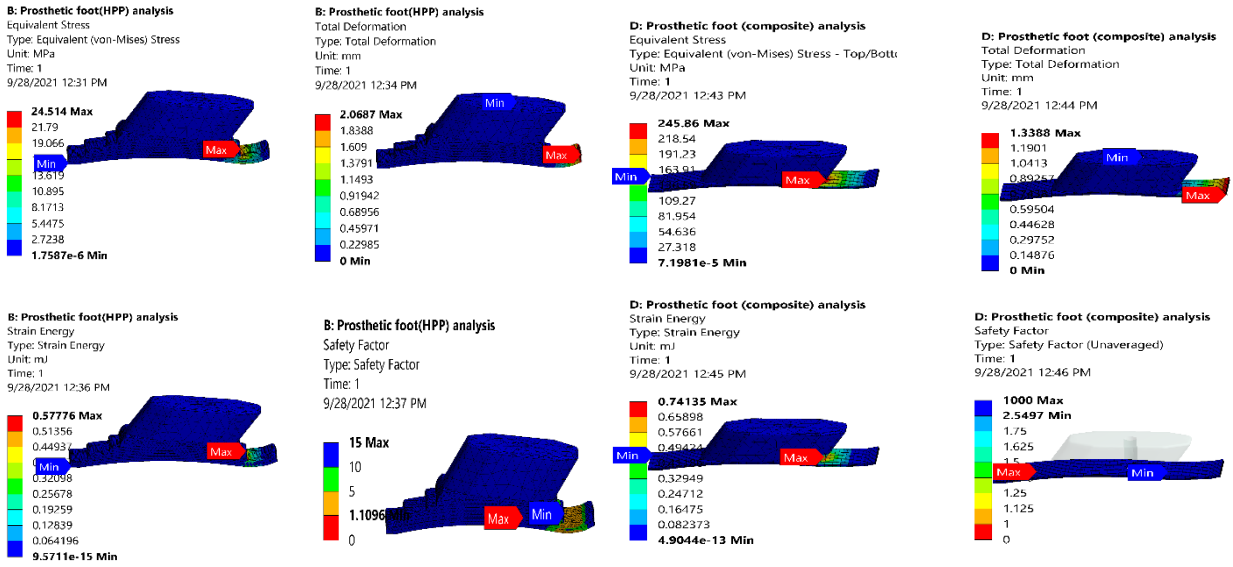

Prosthetic foot stress, deformation, strain energy and factor of safety.

The simulation results of prosthetic foot model at the '**Toe off**' with load of 313.92N

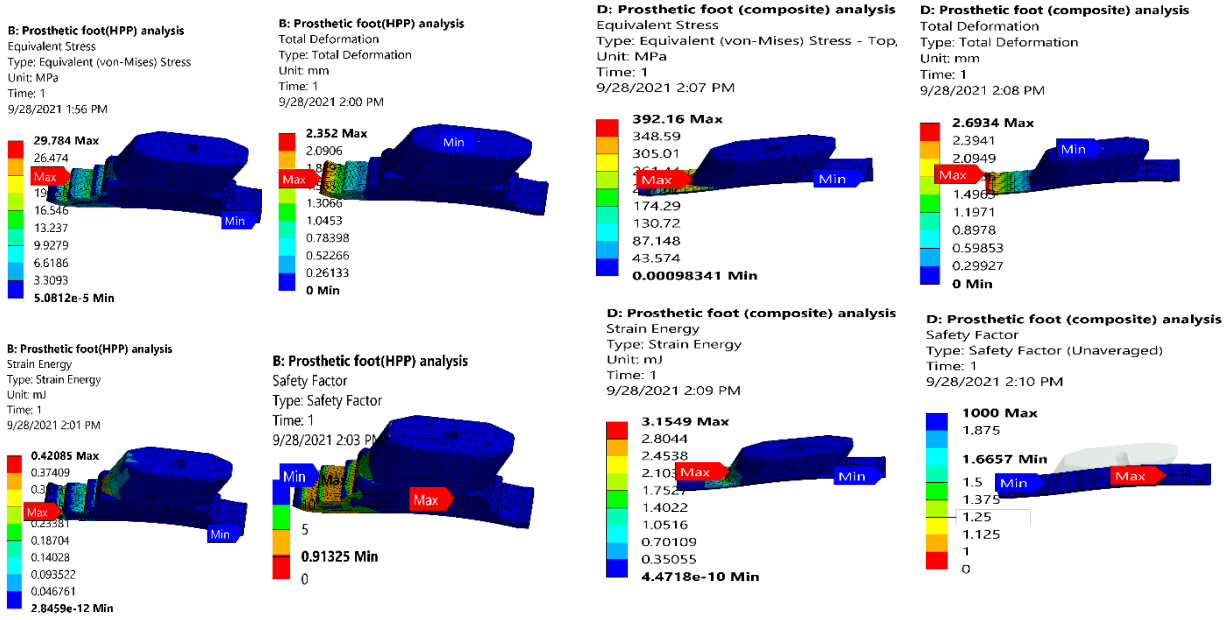

Prosthetic foot stress, deformation, strain energy and factor of safety.

Appendix-9

% Machine/tool cost break down analysis of prosthetic foot

```
a=6;%operating hr/day, a-is changed for each machine or tool

d=220;%Operating day per year,d-is changed for each machine/tool

e=0.25;%actual operating hr, e-is changed for each machine/tool

h=d*a;%machine usage hr/year

p=534.30;%capital cost, p-is changed for each machine/tool

r=0.2;%fixed interest rate

n=5;%time period for capital recovery, n-is changed for each machine/tool

b=(p*r*(1+r)^n)/(((1+r)^n)-1);%annual equivalent machine cost

c=b/h;%The hourly cost of machine

f=c*e;%Operating cost of equipment/machine
```